the LIMADOU experiment on the CSES satellite

Roberto Iuppa
roberto.iuppa@unitn.it

February 13-14 2020

With great contribution from S. Beolè, S. . Coli, F.M. Follega, G. Gebbia, E. Ricci, P. Zuuccon and the LIMADOU collaboration

Topics

particle detection in space

- objectives
- constraints
- methods

the Limadou experiment on board the CSES satellite

- HEPD-01 description
- event reconstruction
- preliminary results

space weather and Earth remote sensing

- trapped particles
- particle bursts

the HEPD-02 tracker

- needs
- concept
- spatialize a new technology: how to

Roberto Iuppa

Topics

particle detection in space

- objectives
- constraints
- methods

space weather and Earth remote sensing

- trapped particles
- particle bursts

lecture 1

Roberto Iuppa

Topics

lecture 2

the Limadou experiment on board the CSES satellite

- HEPD-01 description
- event reconstruction
- preliminary results

the HEPD-02 tracker

- needs
- concept
- spatialize a new technology: how to

Roberto Iuppa

The LIMADOU collaboration today

agenzia spaziale italiana

INFN
Istituto Nazionale di Fisica Nucleare

INAF ISTITUTO NAZIONALE DI ASTROFISICA

iaps

IFAC

ISTITUTO NAZIONALE DI GEOFISICA E VULCANOLOGIA

Università di Roma Tor Vergata

UNIVERSITAS STUDIORUM ATHESINA

SIGIL. VNIVERS. AVGVSTAE TAVRINORVM

ALMA MATER STUDIORUM UNIVERSITÀ DI BOLOGNA A.D. 1088

UNINETTUNO

What is the meaning of Limadou?

Matteo Ricci

From Wikipedia, the free encyclopedia

For other people named Matteo Ricci, see Matteo Ricci (disambiguation).

Matteo Ricci (Italian pronunciation: [matˈtɛːo ˈrittʃi]; Latin: *Mattheus Riccius Maceratensis*; 6 October 1552 – 11 May 1610), was an Italian Jesuit priest and one of the founding figures of the Jesuit China missions. His 1602 map of the world in Chinese characters introduced the findings of European exploration to East Asia. He is considered a Servant of God by the Roman Catholic Church.

Ricci arrived at the Portuguese settlement of Macau in 1582 where he began his missionary work in China. He became the first European to enter the Forbidden City of Beijing in 1601 when invited by the Wanli Emperor, who sought his services in matters such as court astronomy and calendrical science. He converted several prominent Chinese officials to Catholicism, such as Xu Guangqi, who aided in translating *Euclid's Elements* into Chinese as well as the Confucian classics into Latin for the first time.

Contents [hide]

His name in mandarin:
Lì Mǎdòu

Servant of God
Matteo Ricci

A 1610 Chinese portrait of Ricci

Title	Superior General of the China mission
Personal	
Born	6 October 1552 Macerata, Papal States
Died	11 May 1610 (aged 57) Beijing, Ming Empire
Resting place	Zhalan cemetery, Beijing
Religion	Roman Catholic
Ethnicity	Italian

Early life [edit]

Ricci was born 6 October 1552, in Macerata, part of the Papal States, and today a city in the Italian region of Marche. He made his

Roberto Iuppa

Chinese Seismo-Electromagnetic Satellite (CSES)

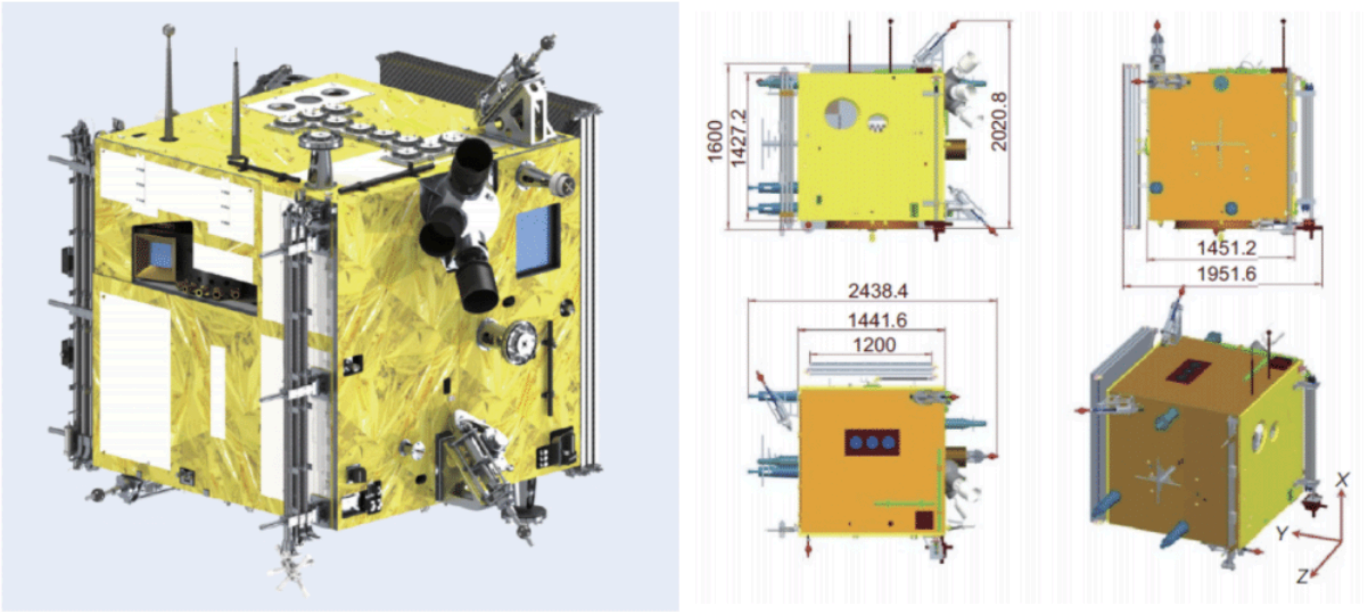

Figure 1: **Layout of the CSES satellite:** the main body has size 145 cm (Y) × 144 cm (Z) × 143 cm (X), which increases after the deployment of the solar panel and booms.

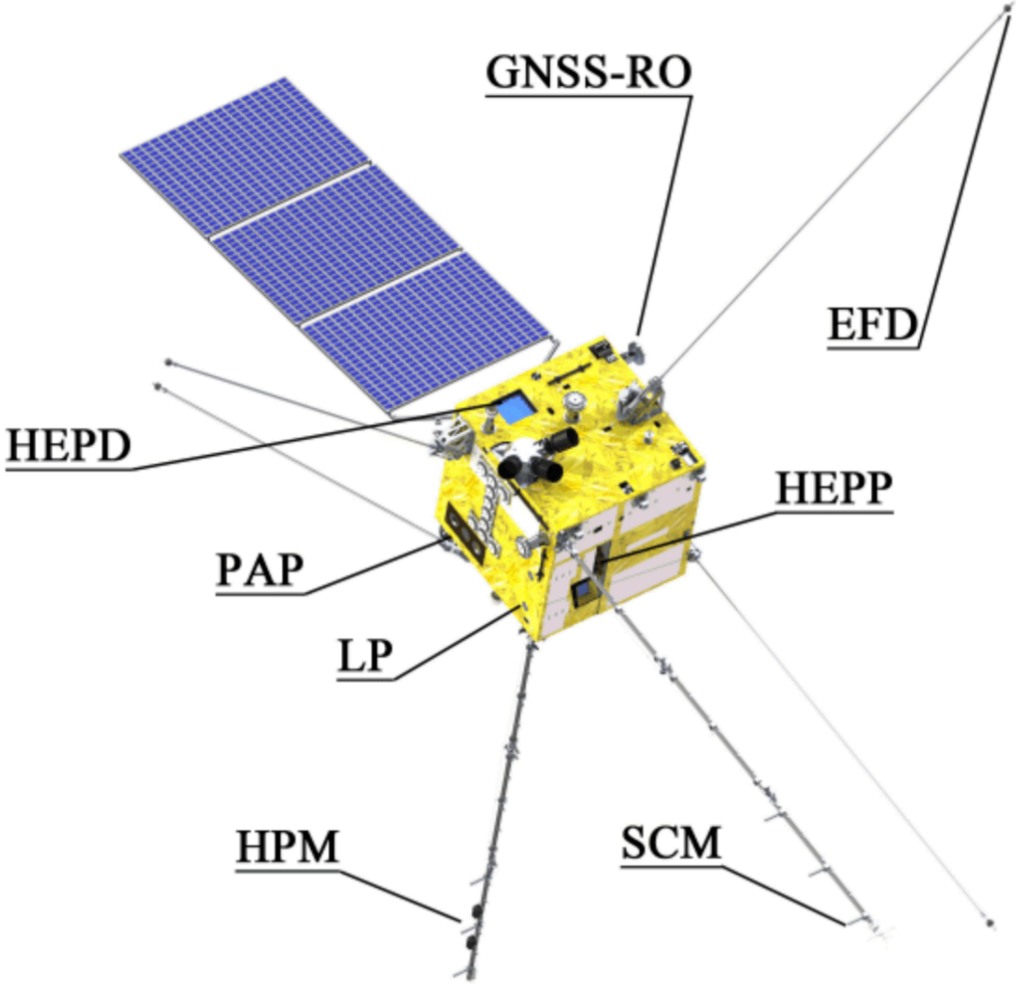

The High Energy Particle Detector (HEPD)

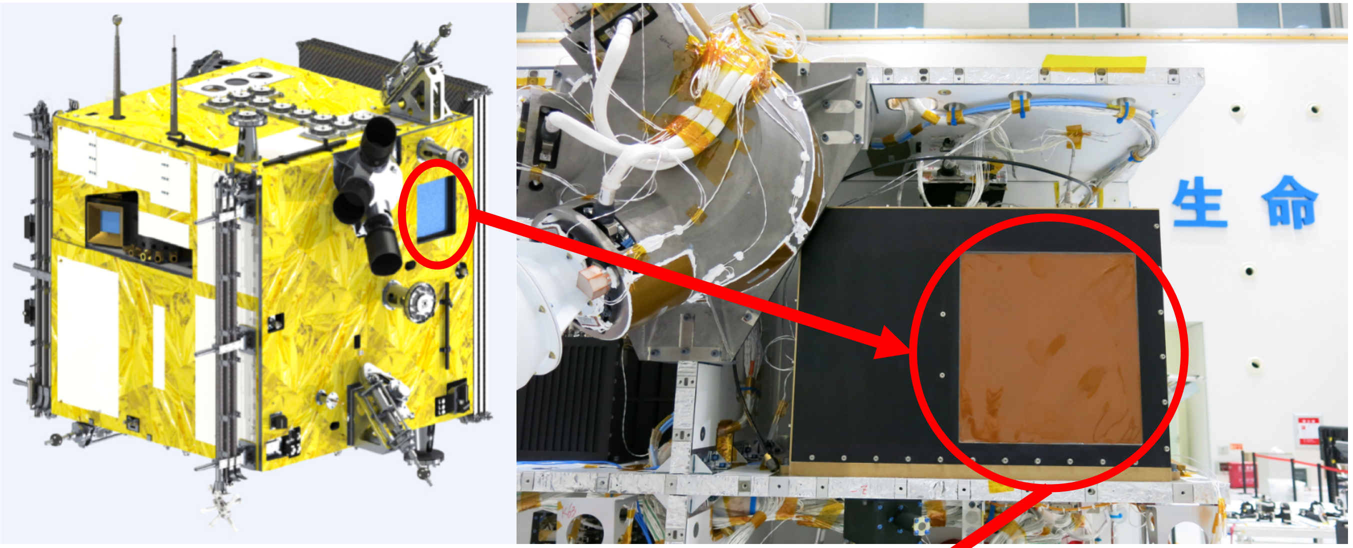

- **Energy range**
  - **Electron: 3-100 MeV**
  - **Proton: 30-200 MeV**
- **Angular resolution<8º@ 5 MeV**
- **Energy resolution<10% @ 5 MeV**
- **Particle Identification>90%**
- **Maximum Omni-directional Flux:10^7 $cm^{-2}s^{-1}sr^{-1}$** (accepted by trigger before prescaling)
- Operating temperature: -10 ºC ~ + 35 ºC
- Mass (including electronics) ≤ 44 kg (budget ≤ 45 kg)
- Power Consumption ≤ 27 W (Power budget ≤ 43 W)
- Scientific Data Bus: RS-422
- Data Handling Bus: CAN 2.0
- Operation mode: Event by Event
- **Life span: ≥ 5 Years**

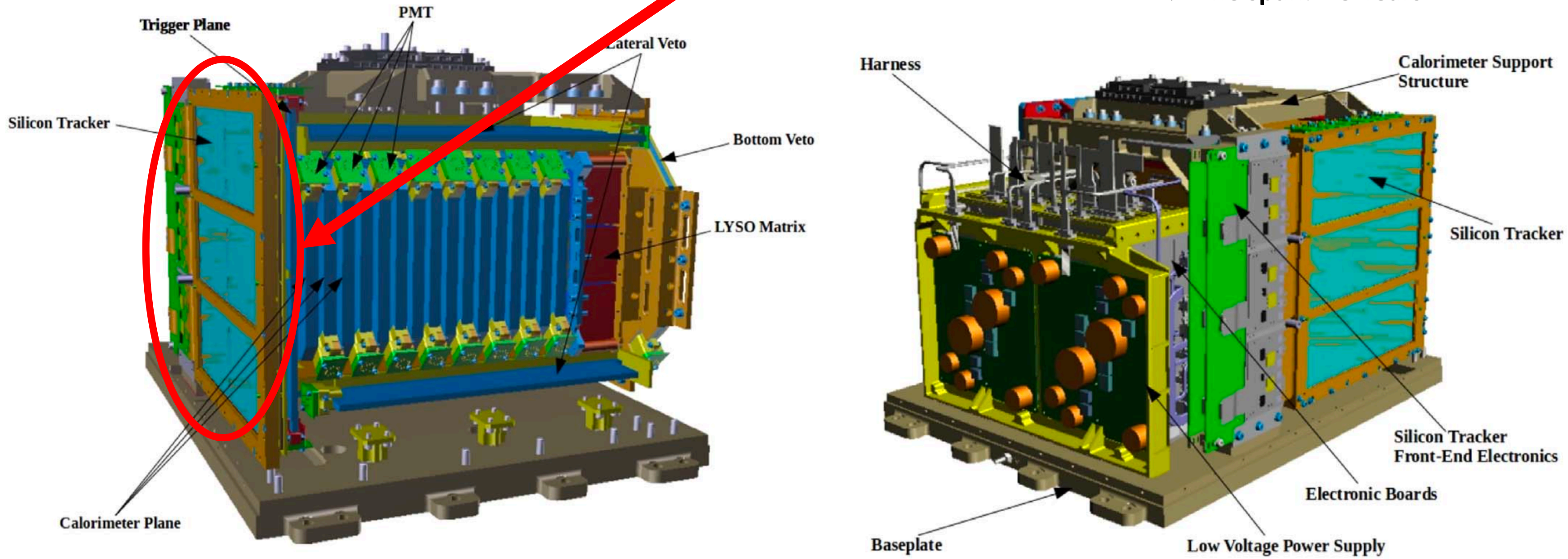

Figure 6. Schematic views of the HEPD electronics box and detecting units.

Roberto Iuppa

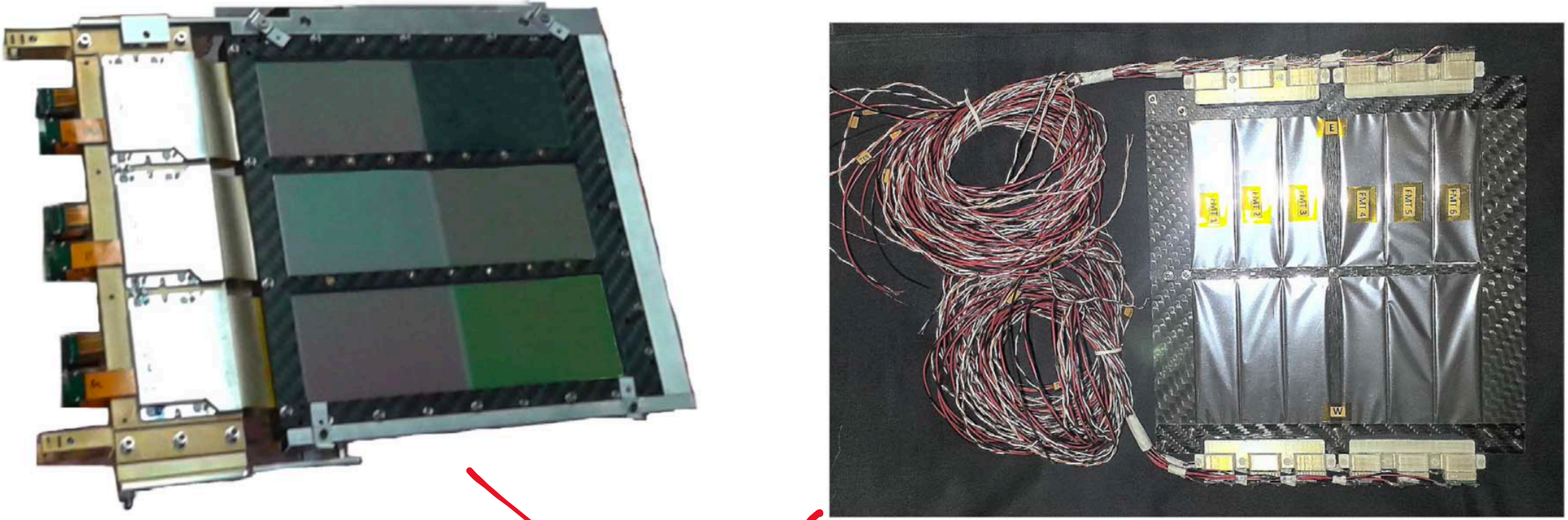

Figure 17. Left: assembled plane of silicon detecting units. Right: picture of the segmented trigger plane.

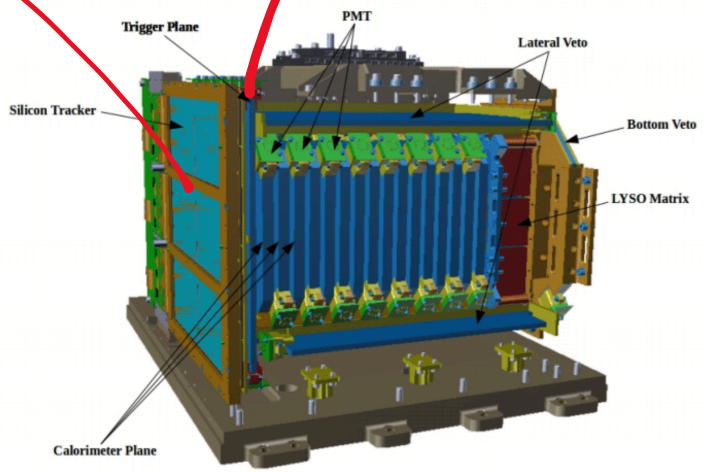

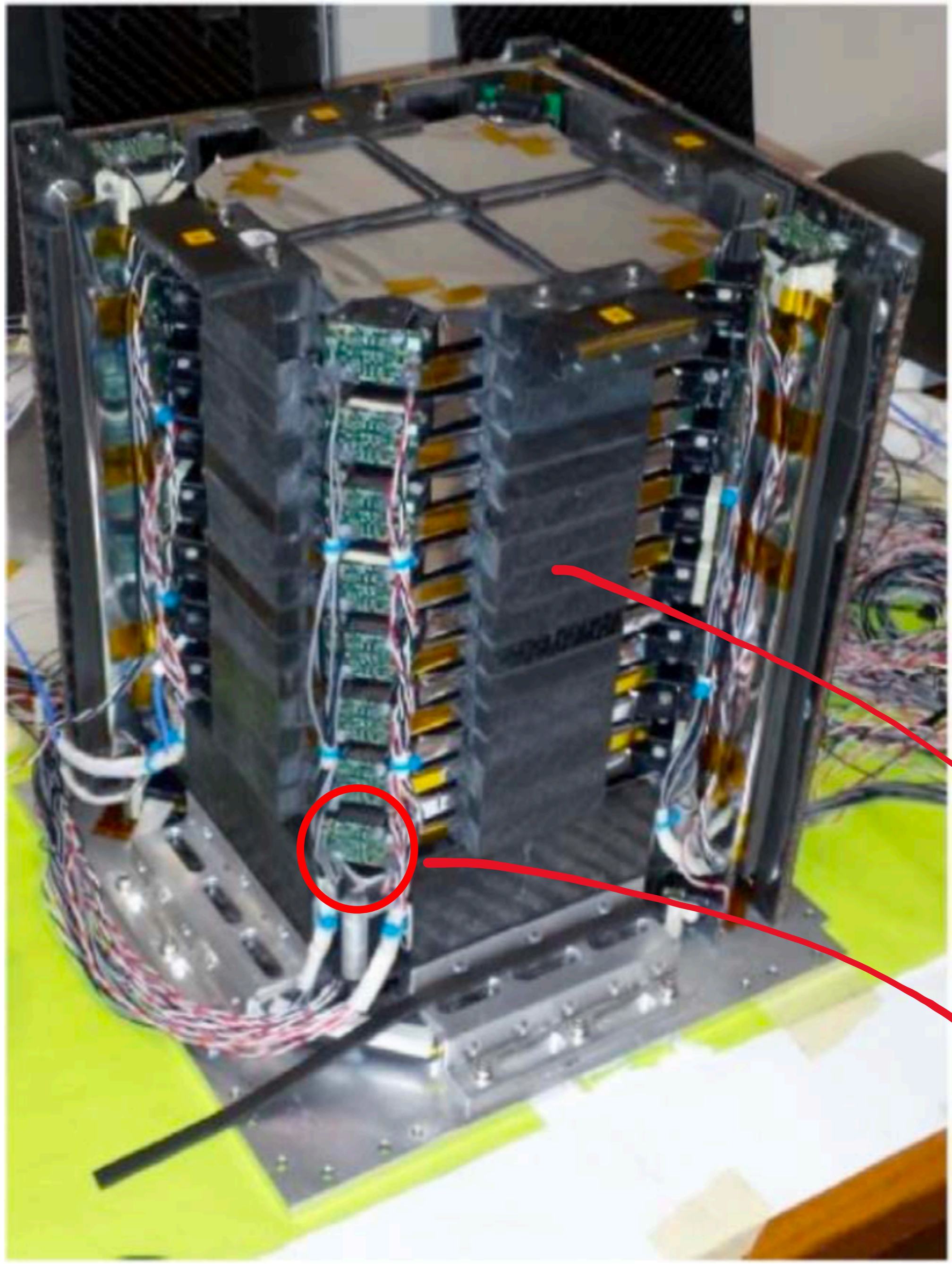

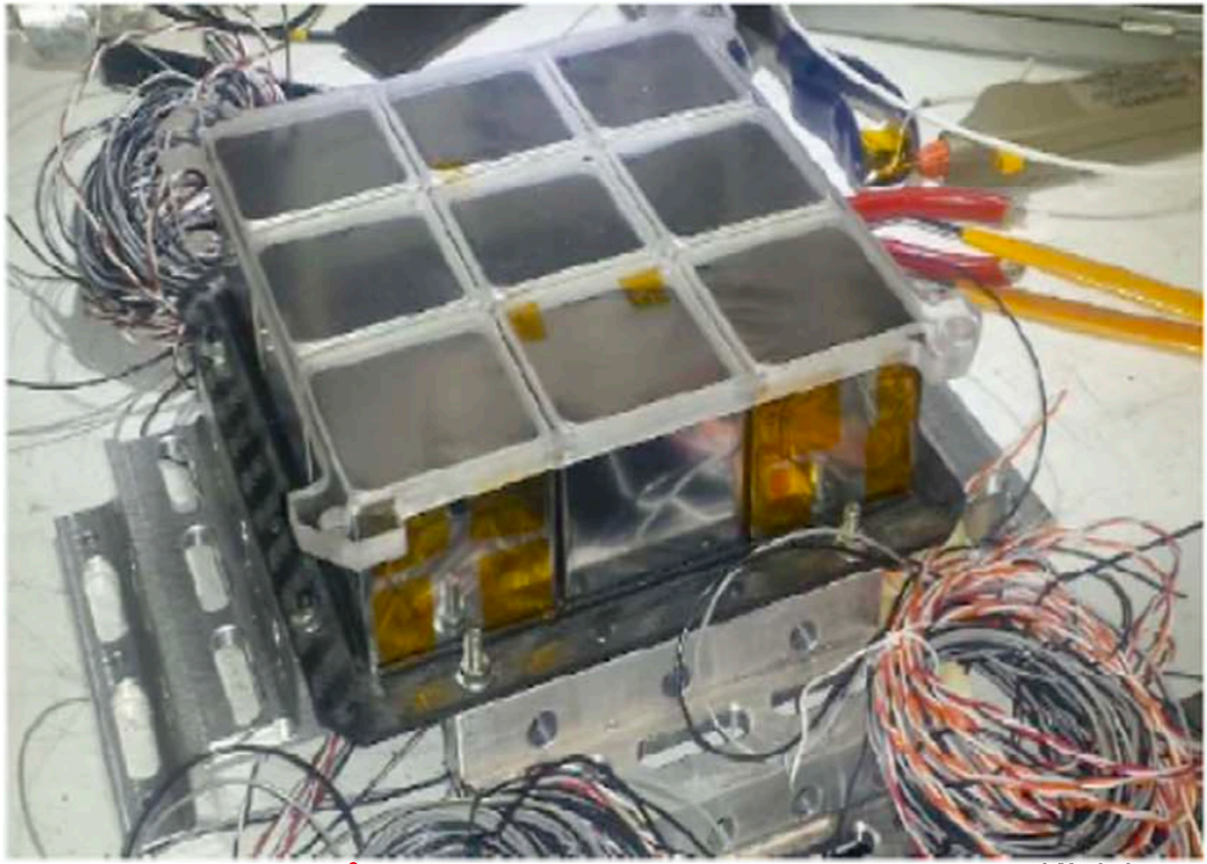

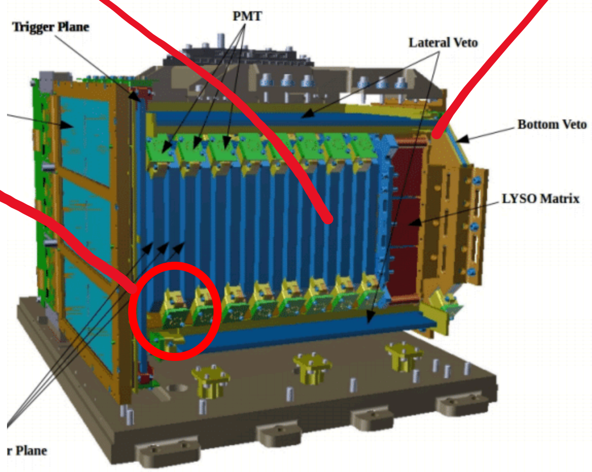

DU Experiment on
SES Satellite

Hamamatsu R9880U-210

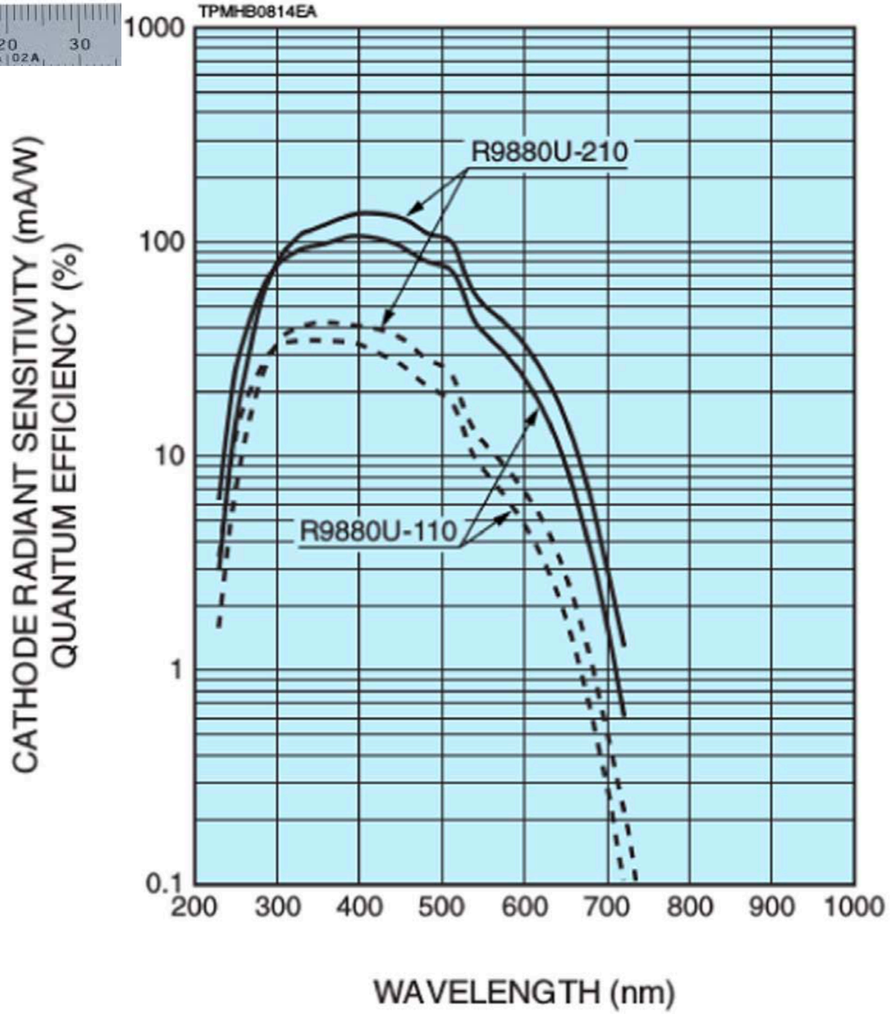

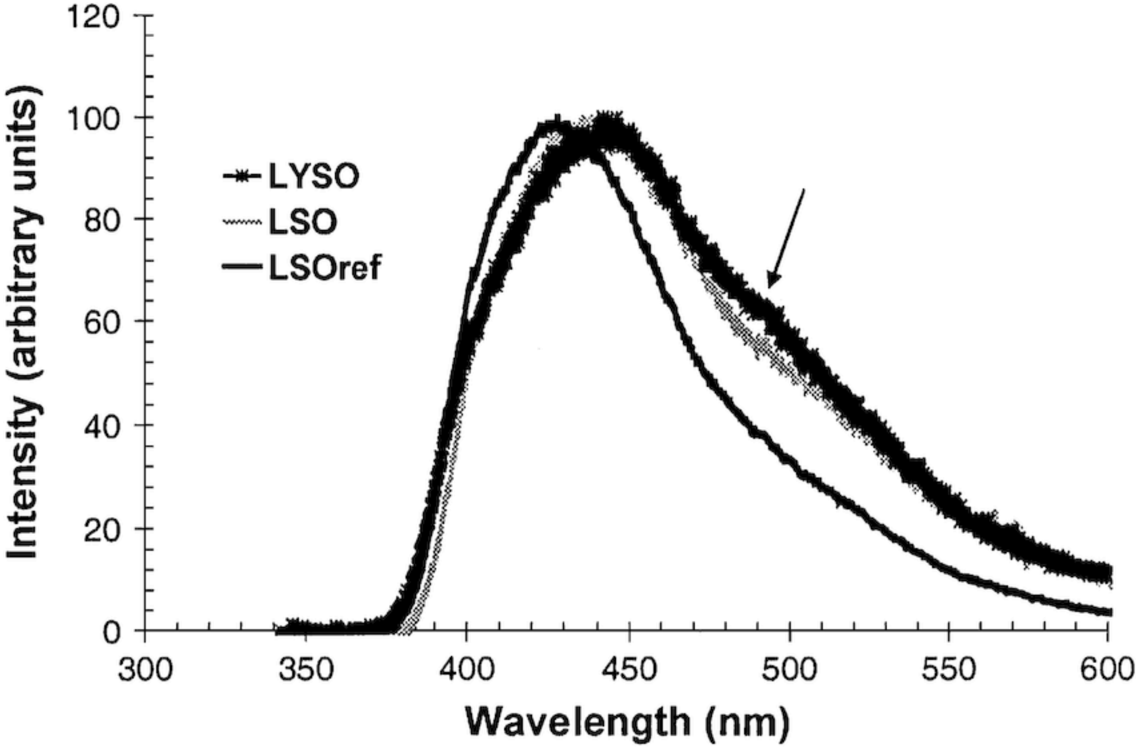

EJ-200 EMISSION SPECTRUM

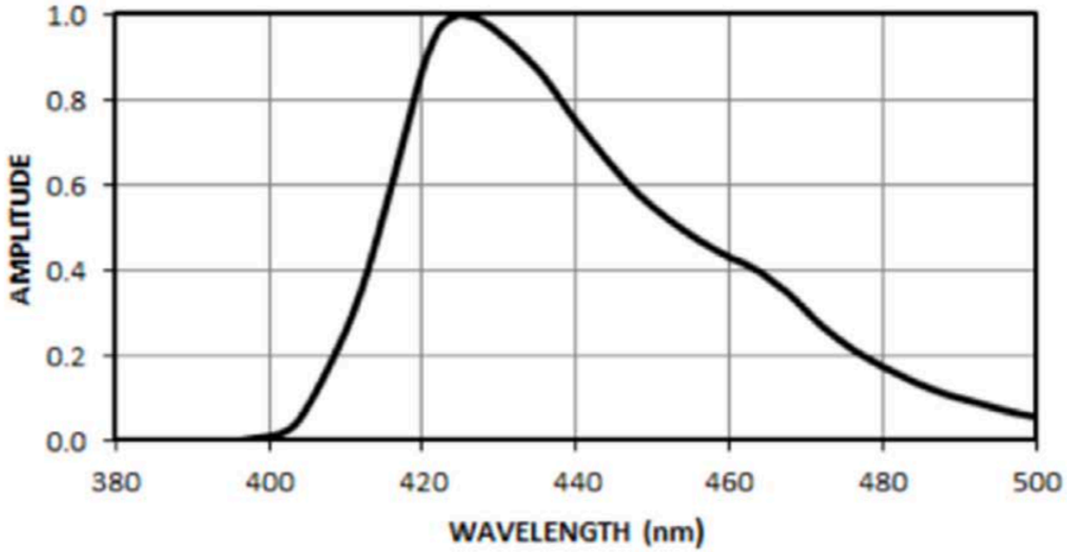

Roberto Iuppa

HEPD electronics and power supply

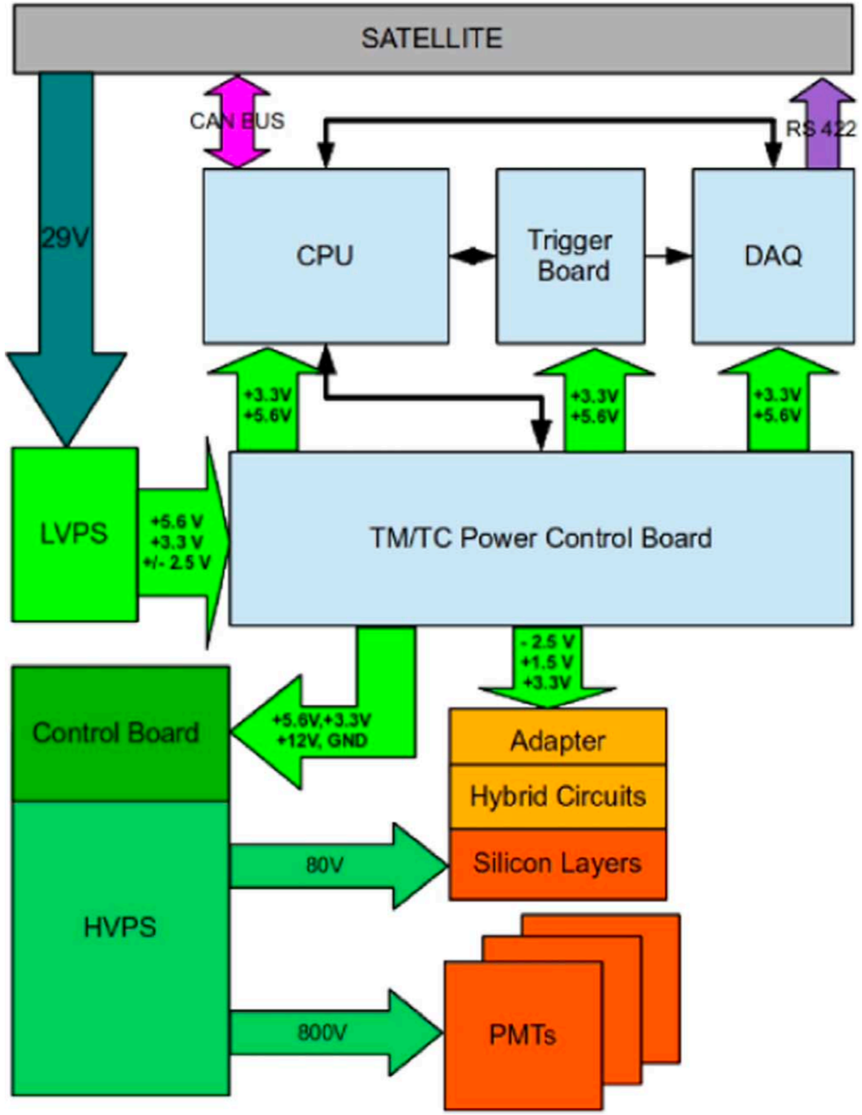

Figure 21. General scheme of HEPD electronics and power supply subsystems. Communication and power lines between the boards and toward the satellite are shown as well.

Roberto Iuppa

What does an event look like?

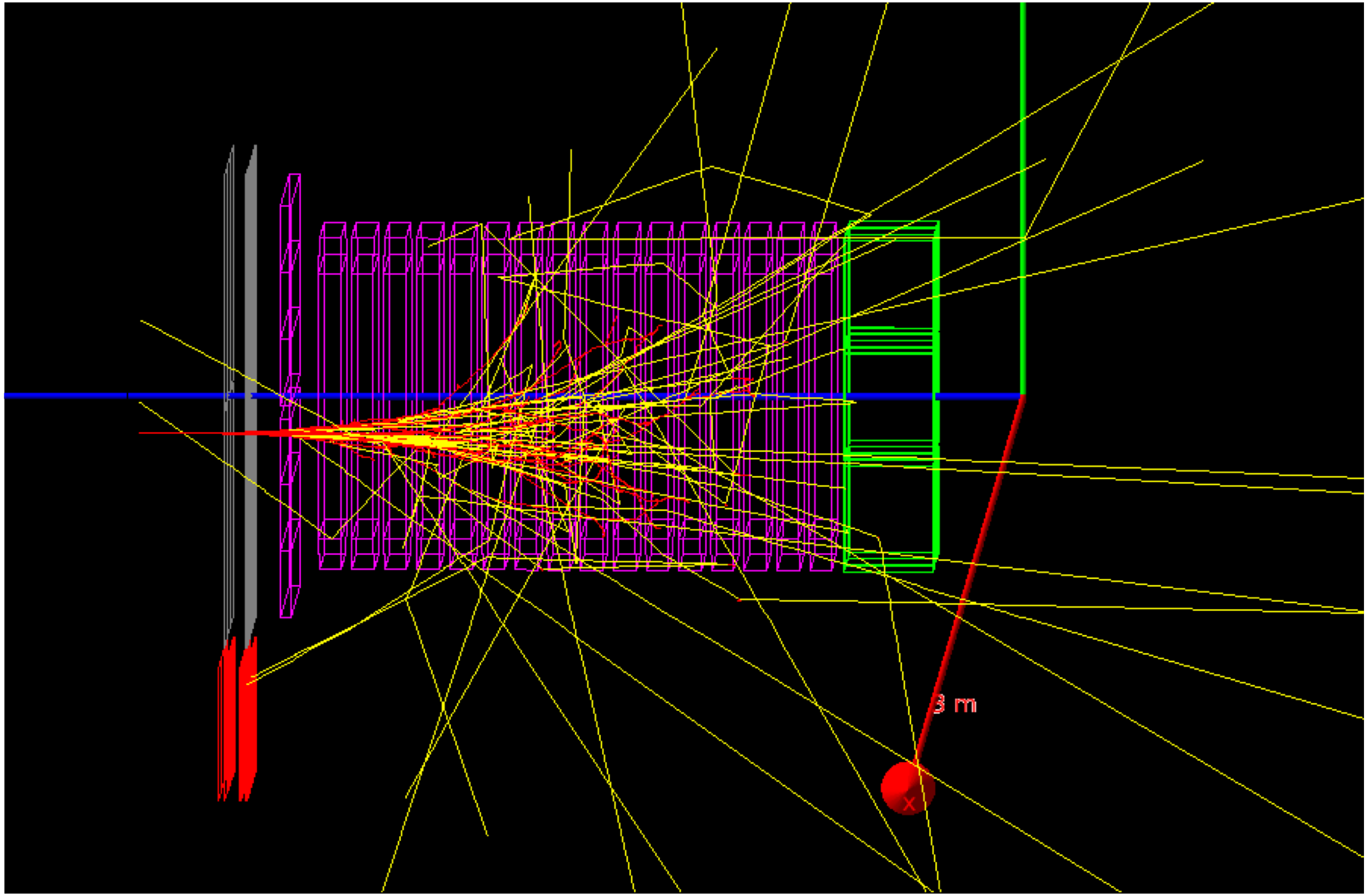

GEANT4 simulation of a 25 MeV electron entering the HEPD from the left. Red tracks represent electrons, yellow tracks photons. Gray planes make the silikon tracker, whereas purple blocks are scintillators. Green cubes on the right are LYSO crystals to contain higher energy particles.

Pre-flight characterization and calibration

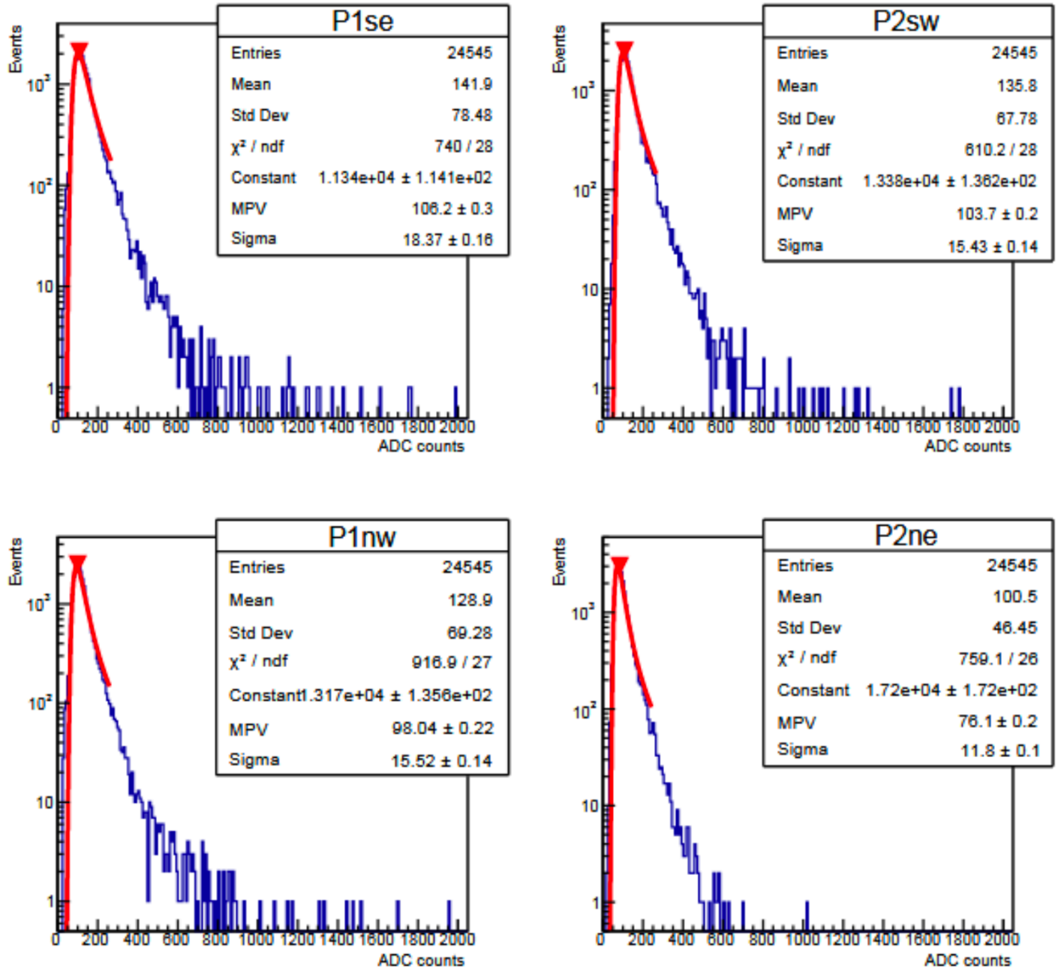

Figure 5: **A sample of muon signal distributions for HEPD PMTs (the four ones lying in the first two calorimeter planes)**: for any PMT of the apparatus, the most probable value (MPV) from Landau fit was used to retrieve the corresponding equalization factor. The "se" label stands for south-est, "sw" for south-west, "ne" for north-est, and "nw" for north-west. All labels are related to the positions of the PMTs.

Roberto Iuppa

Beam test facilities: BTF (Frascati)/APSS (Trento)

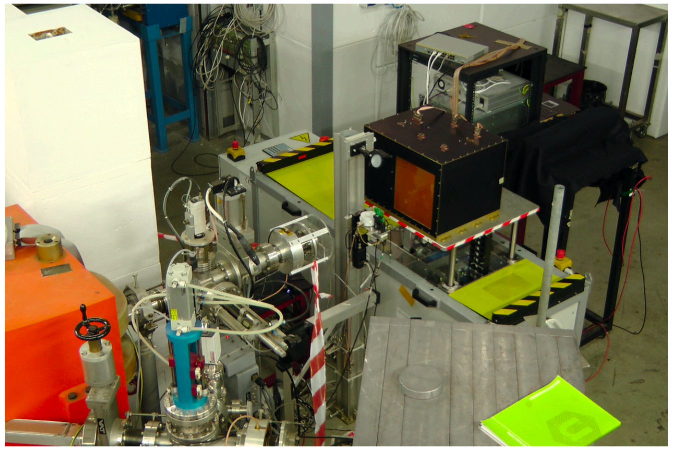

Figure 6: **HEPD setup at BTF:** HEPD - the black box with the orange window in correspondence to the active detector - placed on the movable platform in front of the beam is connected to the EGSE; the Medipix and calorimeter provided by BTF staff for beam monitoring are visible on the front and back side of HEPD, respectively.

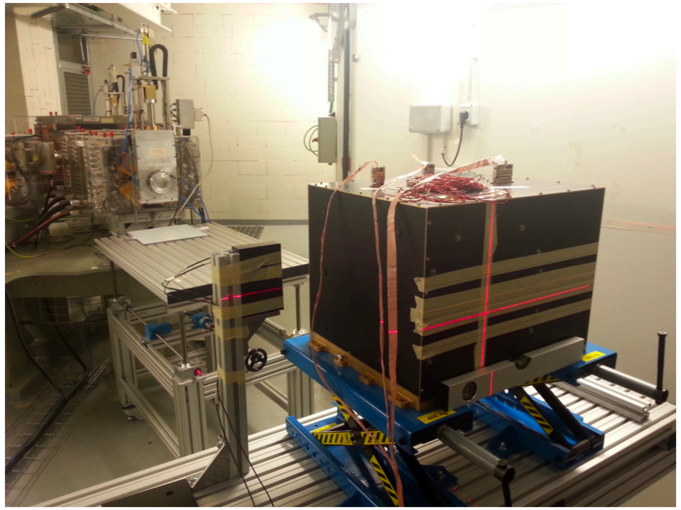

Figure 7: **HEPD setup at the Trento Proton-Therapy Center:** HEPD was placed on a movable platform with the incident beam located at the center of HEPD window by laser pointing.

Roberto Iuppa

MC setup developed for each beam test

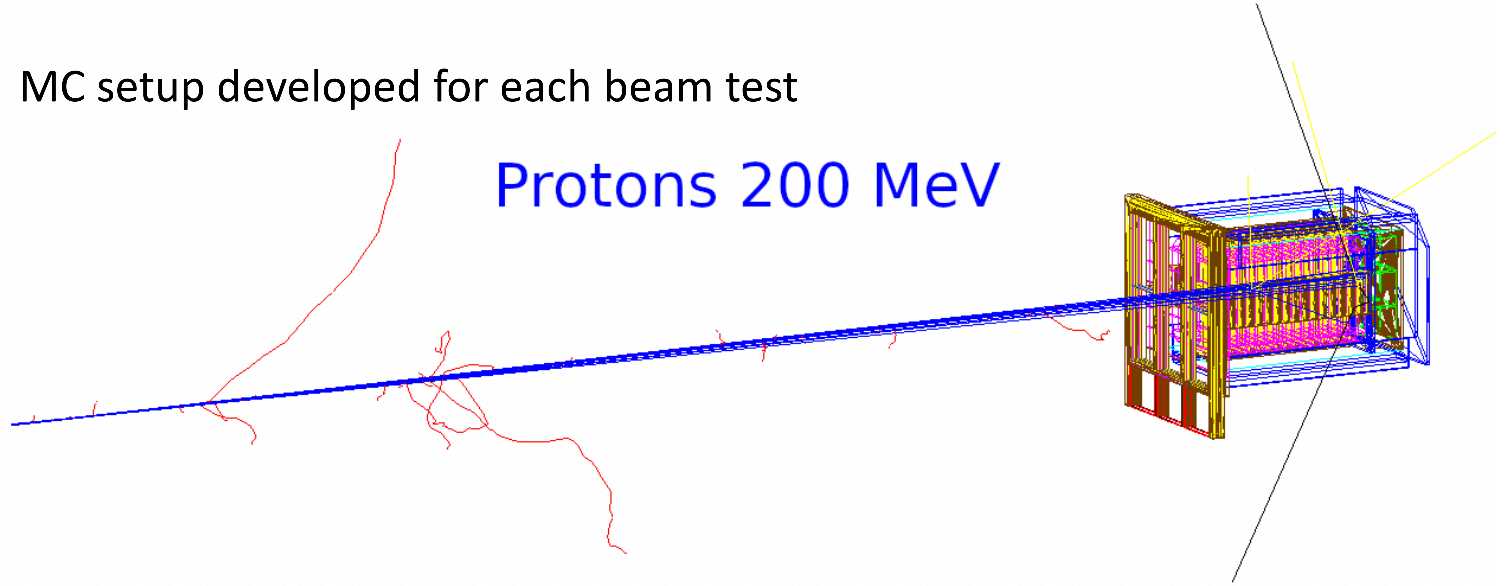

PMTs ADC-photoelectrons calibration curves

Roberto Iuppa

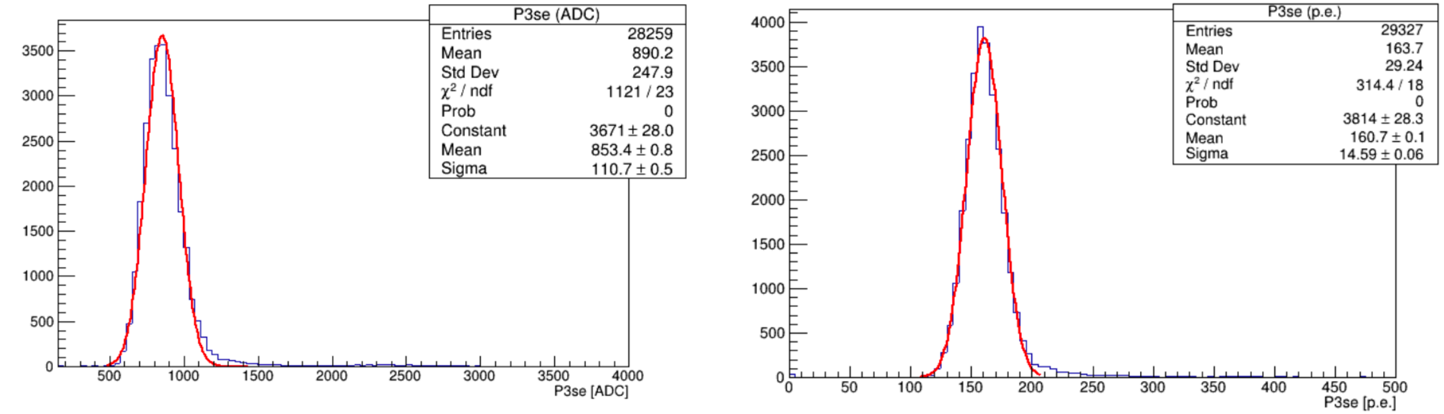

Figure 10: **Distributions from a 100 MeV proton run for the south east PMT of the third calorimeter plane (P3se):** the ADC signal distribution for P3se from the beam test data (left) and the photo-electron distribution in P3se from the Monte Carlo simulation (right).

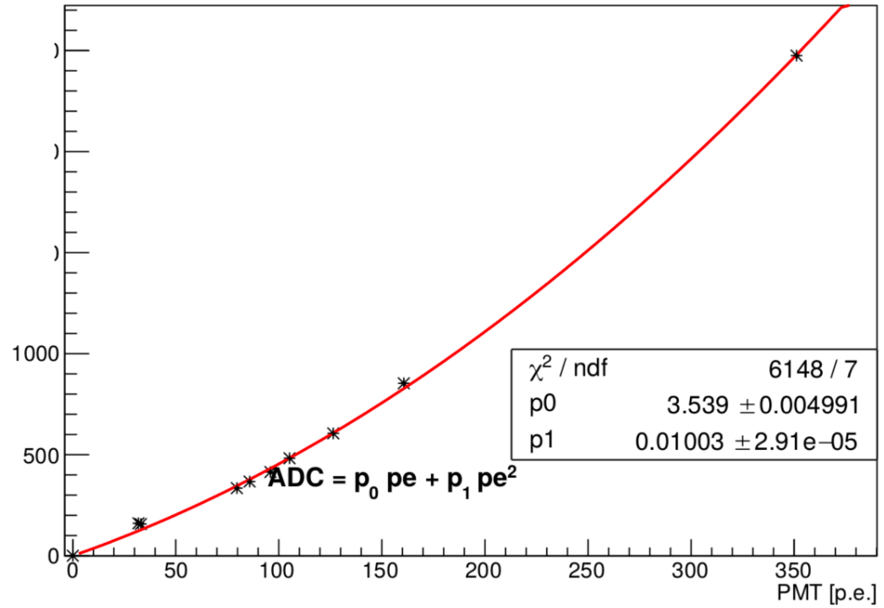

Figure 11: **Conversion curve from photo-electrons into ADC counts for the P3se PMT:** the black asterix points correspond to a cosmic muon run, a 30 MeV electron run and seven proton runs (70, 100, 125, 154, 174, 202 and 228 MeV).

Validation of calibration curves

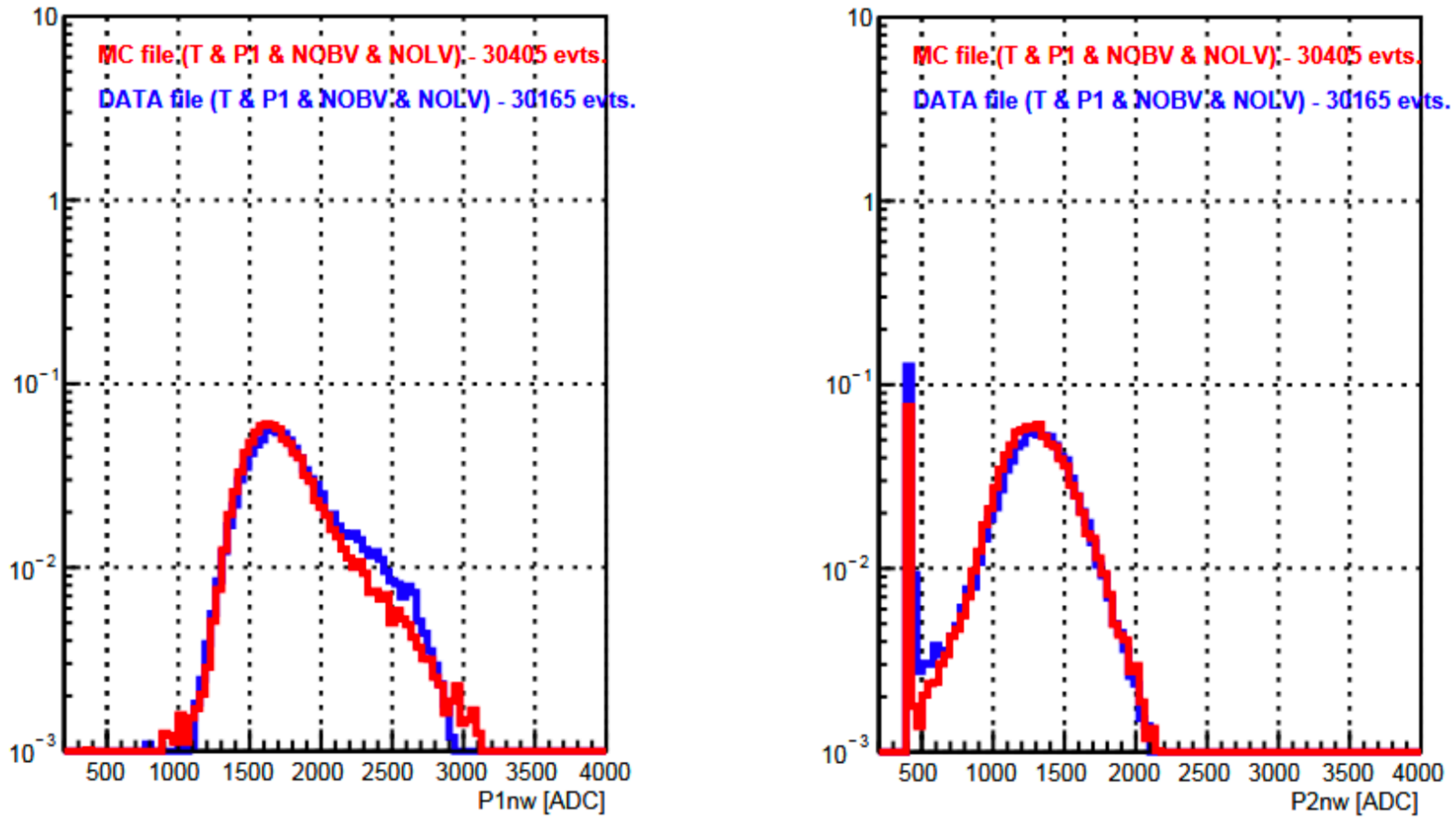

Figure 12: **ADC signal distributions from proton beam test data (blue curve) and digitized Monte Carlo simulation (red curve):** the two distributions for the P1nw (left) and P2nw (right) PMTs correspond to a 51-MeV proton run.

Roberto Iuppa

Silicon microstrip ADC – E_{dep} calibration curve

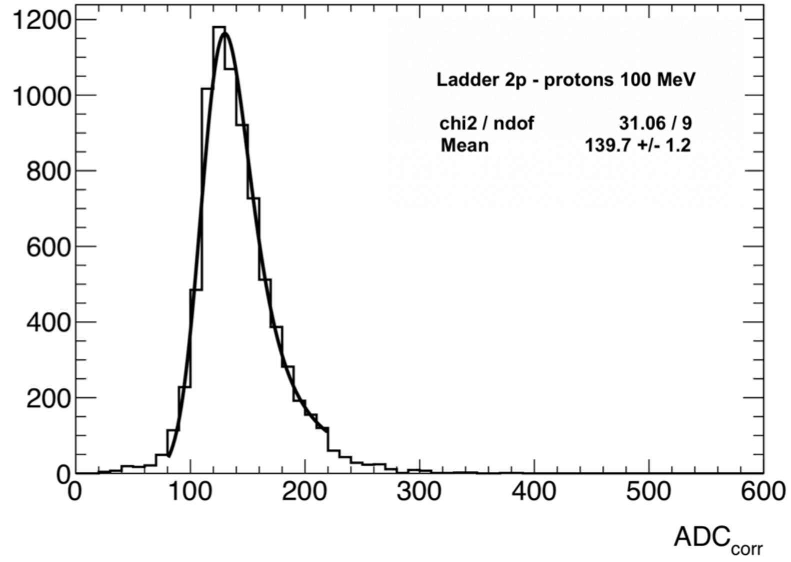

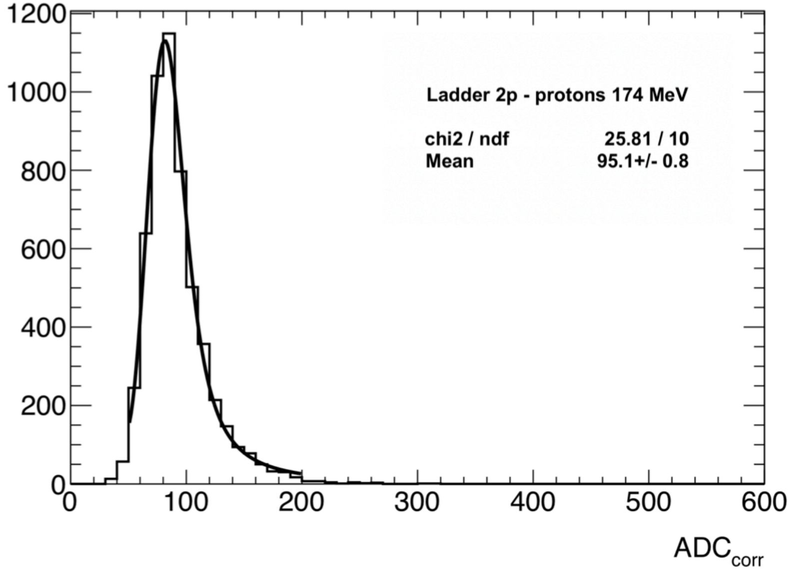

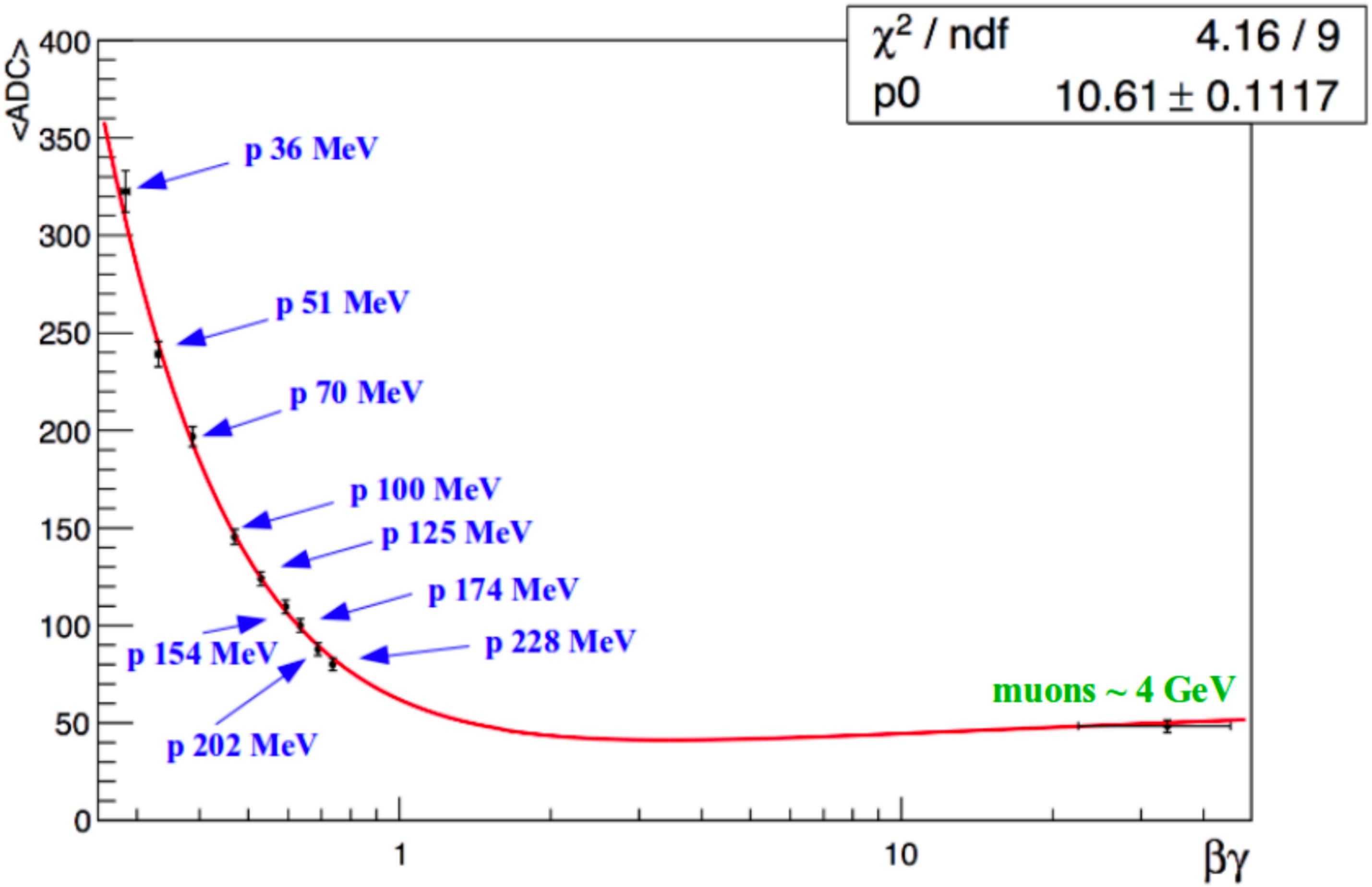

Upper calorimeter calibration

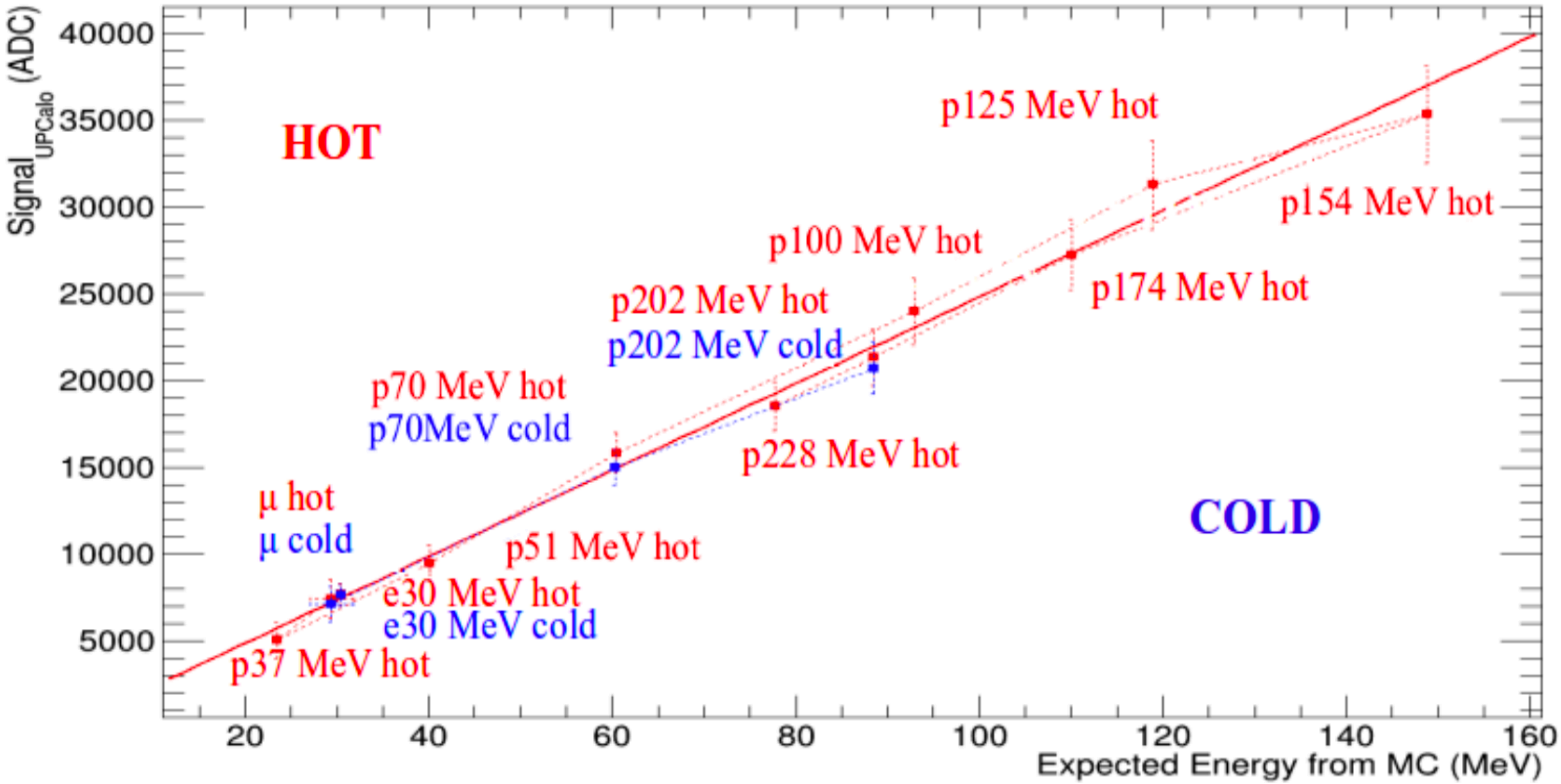

Roberto Iuppa

LYSO calibration

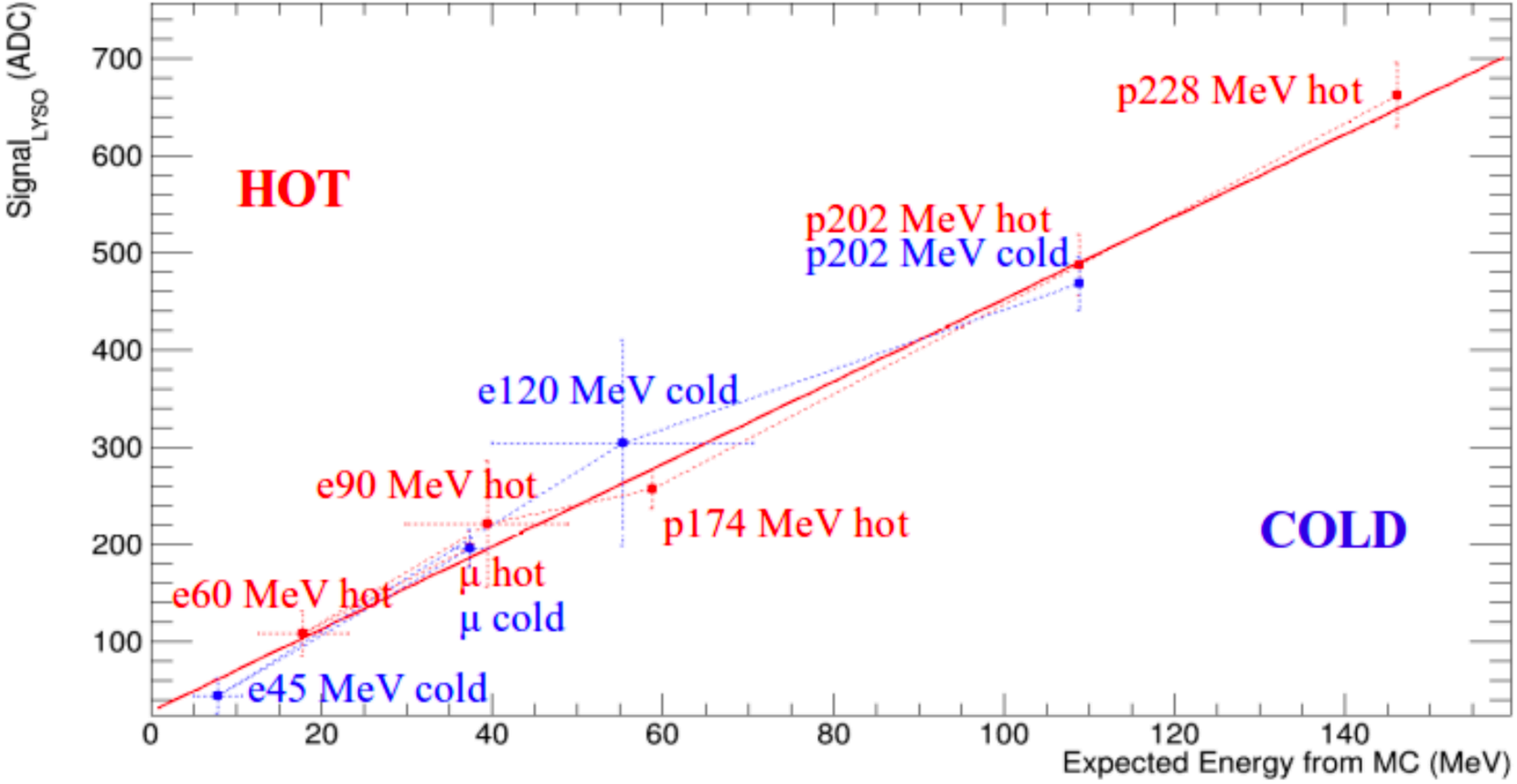

Roberto Iuppa

Particle identification

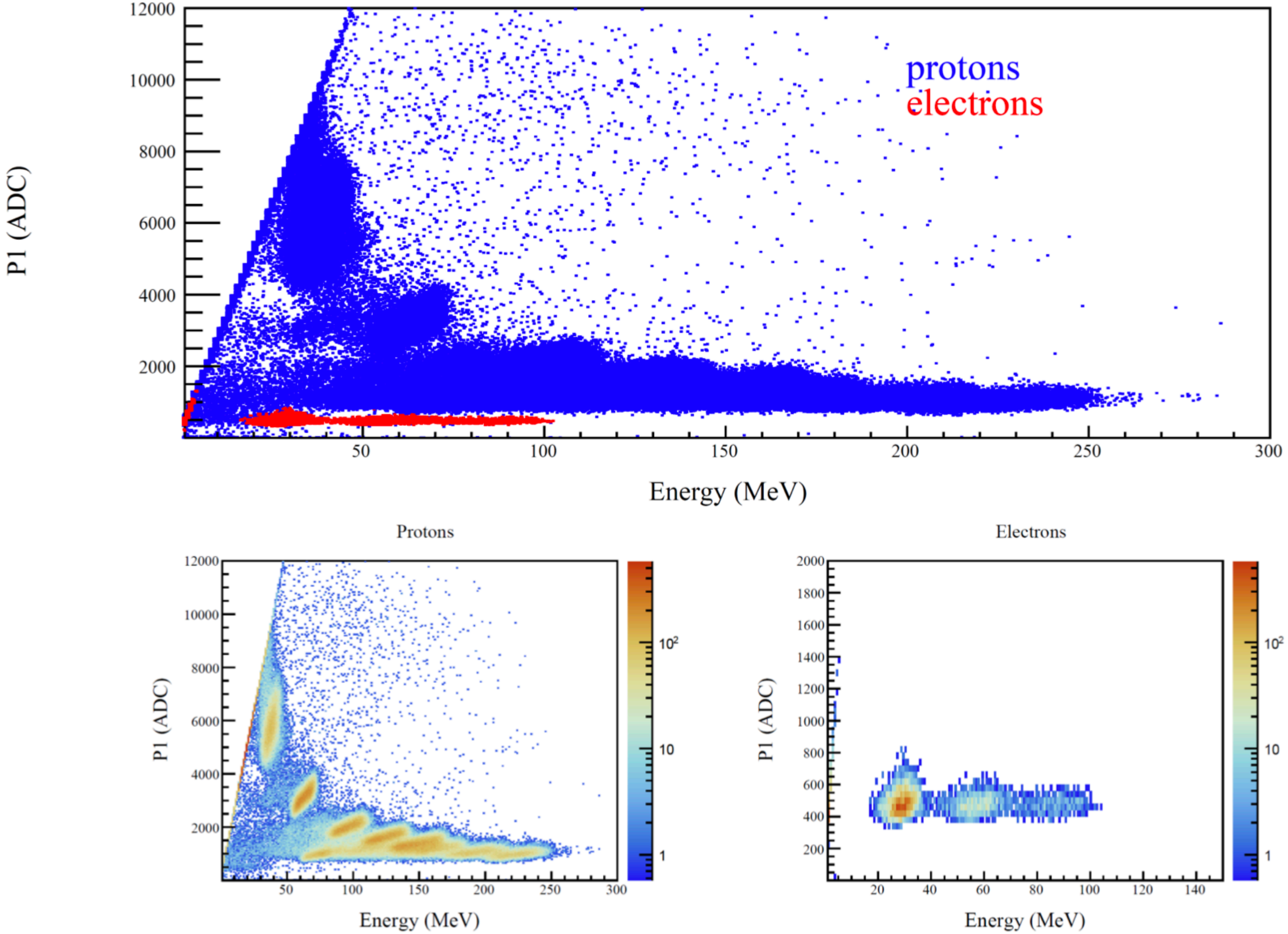

Particle identification

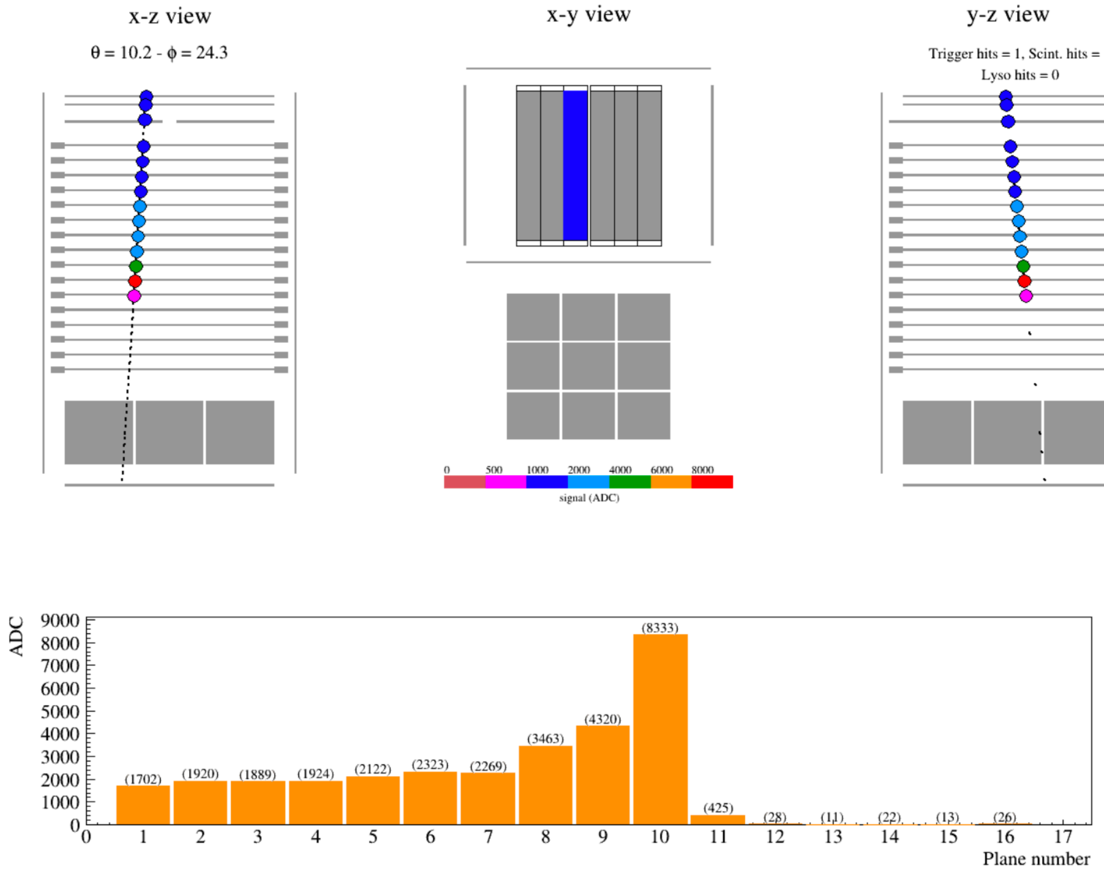

Figure 23: **Longitudinal profile of a ~ 125 MeV proton inside the scintillator tow** a Bragg peak can be clearly spotted on plane 10.

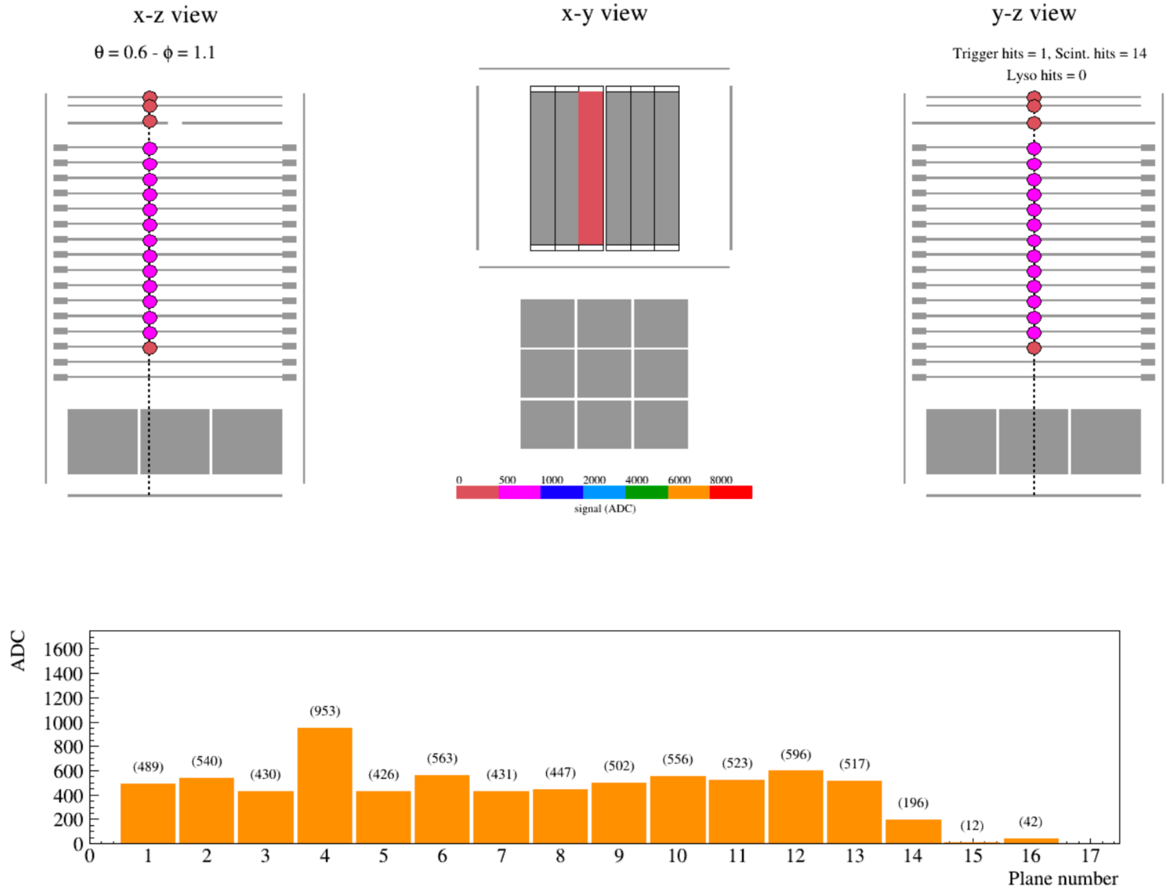

Figure 24: **Longitudinal profile of a ~ 30 MeV electron inside the scintillator tower**: the signal released is almost constant along the distance travelled by the particle up to plane 14.

Arrival direction - DL

Together with the energy reconstruction, the $FCNN_{Kin}$ predicts the arrival direction.

Challenge: EJ200 attenuation length is 380 cm (~x100 the distance between the hit and the closest PMT). Position reconstruction extremely coarse.

The general idea is the following:

- Each plane is poorly sensitive **to the impact position,** but poorly sensitive **does not read as completely blind**;
- **Crossing** the information of **all the 16 planes**;
- **not vertical particle traverses more material** and releases more charge;
- **cos(θ), ϕ are correlated E_{Kin}**;

Arrival direction prediction **improves energy reconstruction.**
No calo **arrival direction** reconstruction **with std methods!**

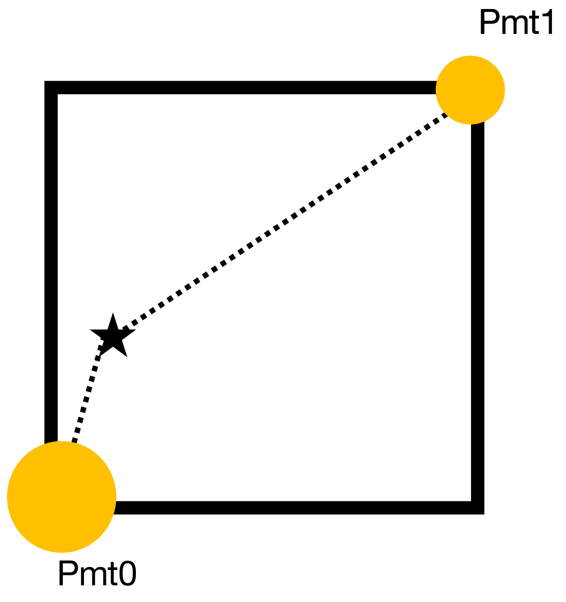

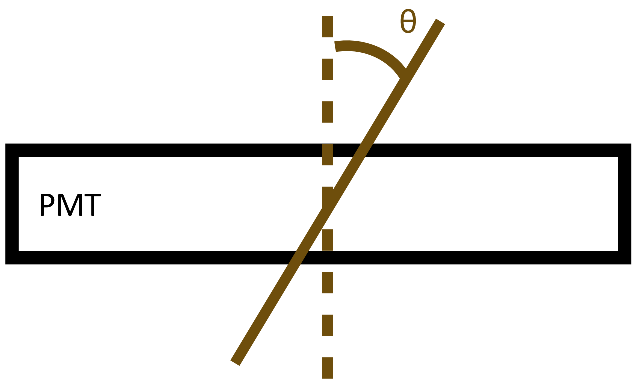

Roberto Iuppa

Arrival direction: deep learning

We used Geant4 to simulate particles (electrons and protons) interacting with a **detector composed by a pile of 16 scintillator planes readout by 32 photo-multiplier tubes**, evenly distributed on the edges of each plane.

Detector

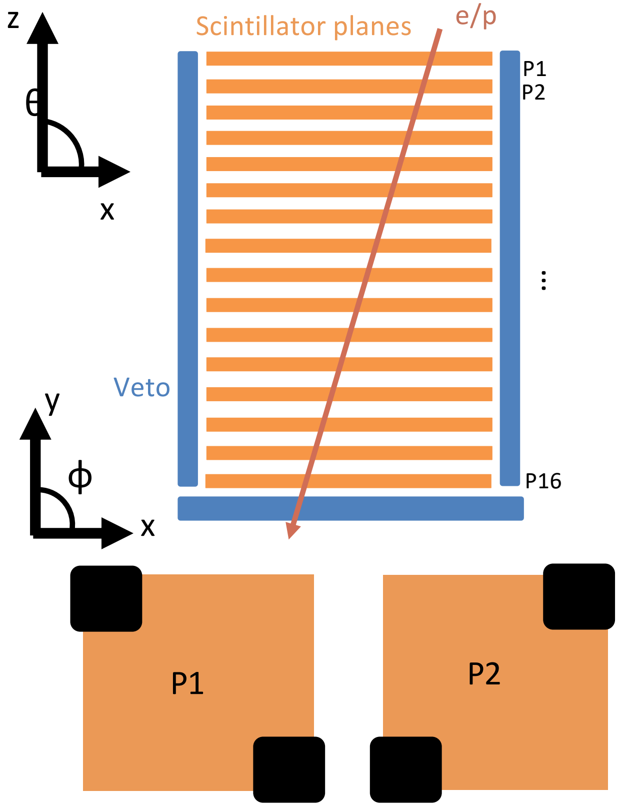

Protons and **electrons** simulated:
(1.5 million events each)

- $0.5 < \cos(\theta) < 1$;
- $0° < \phi < 360°$;
- 30 MeV< E_K < 300 MeV (protons)
  1 MeV< E_K < 100 MeV (electrons)

Selection:

- Traversing P1 and P2, but not hitting the lateral Veto (passing);

Geant4
Event display

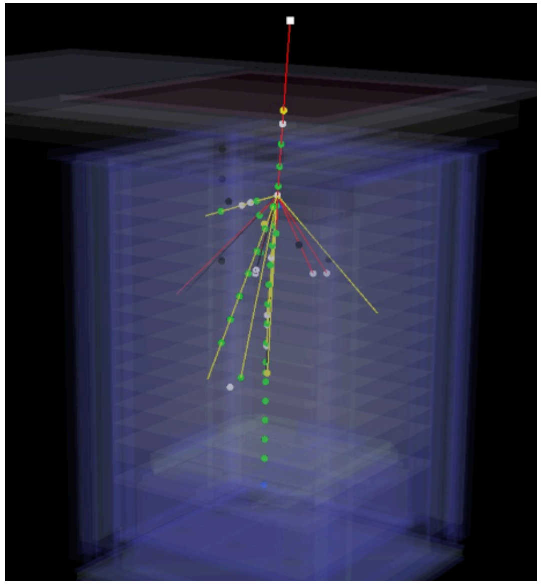

Deep Learning reconstruction strategy

The main elements of the reconstruction chain are **two Fully Connected Neural Networks (FCNNs)** taking as input the signal of photo-multiplier tubes and **giving as output particle-type flag,** polar and azimuthal **angles** in the local frame and **energy of the particle**.

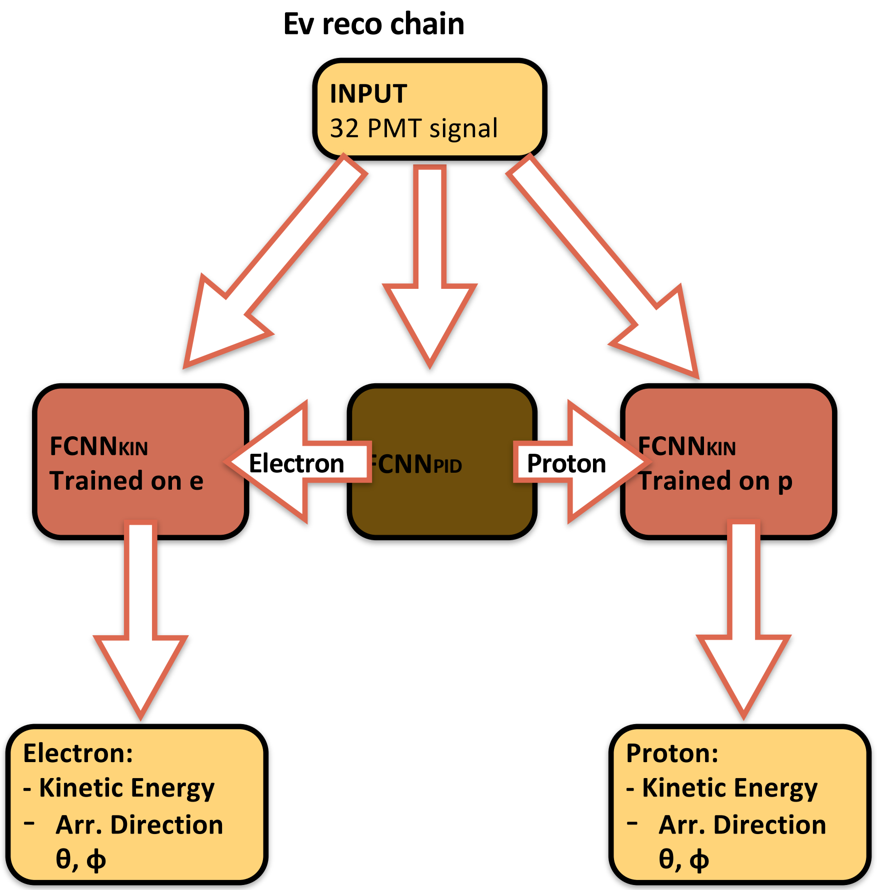

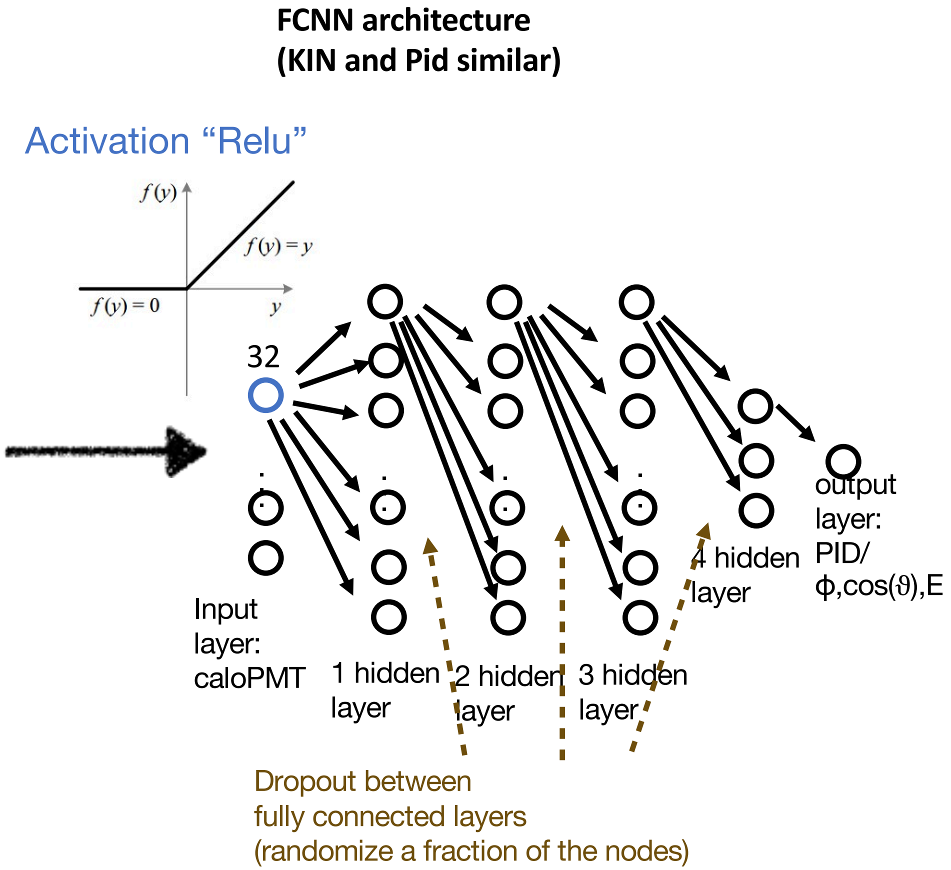

Roberto Iuppa

Fully Connected Neural Network

They consist in a **series of fully connected layers**, where each layer is formed by many units called **"neurons"**:

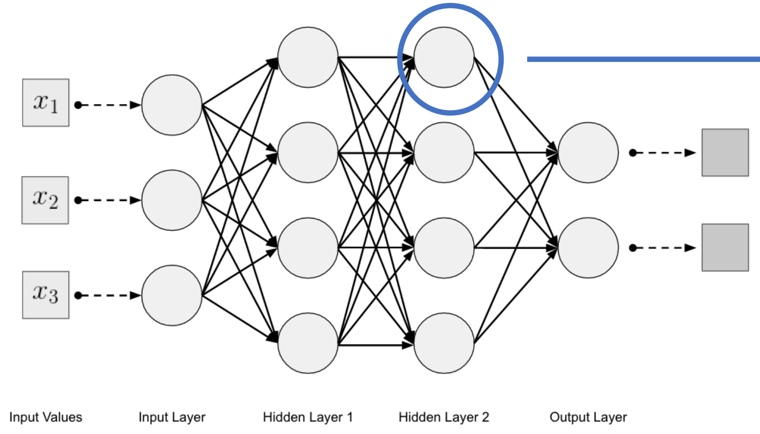

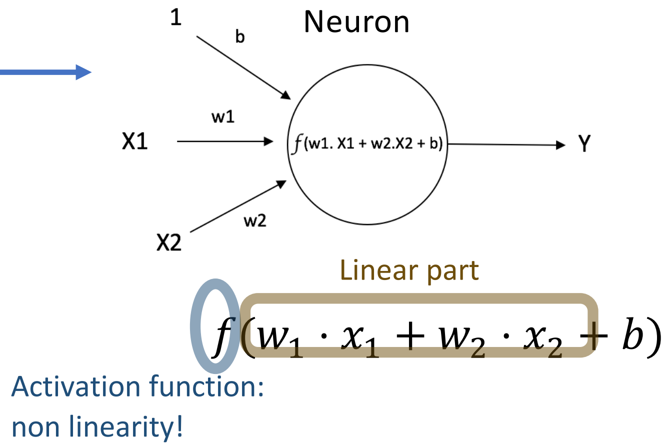

$$f(w_1 \cdot x_1 + w_2 \cdot x_2 + b)$$

Learning procedure → **minimize a scalar called "loss function"** expessed as a function of the weights, w_i:

$$\text{i.e. } L_{MSE} = \sum_{i=0}^{N} \frac{(y_i - y_i^*)^2}{N}$$

- Backpropagation of the error with the chain rule:

$$\frac{\partial L}{\partial W} = \frac{\partial L}{\partial out}\frac{\partial out}{\partial W} = \frac{\partial L}{\partial out}\frac{\partial out}{\partial net}\frac{\partial net}{\partial W} = \cdots$$

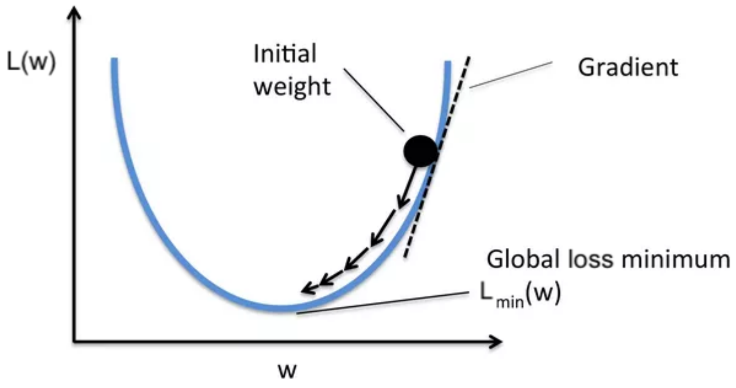

Input distributions

Input variables: 32 PMT signals

Protons

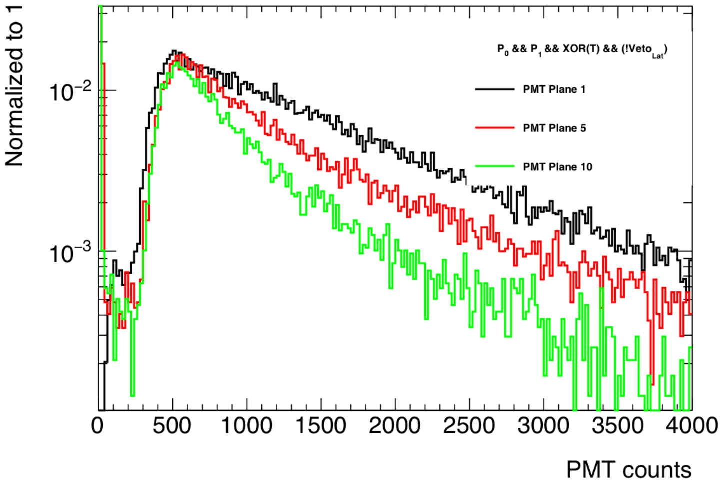

Electrons

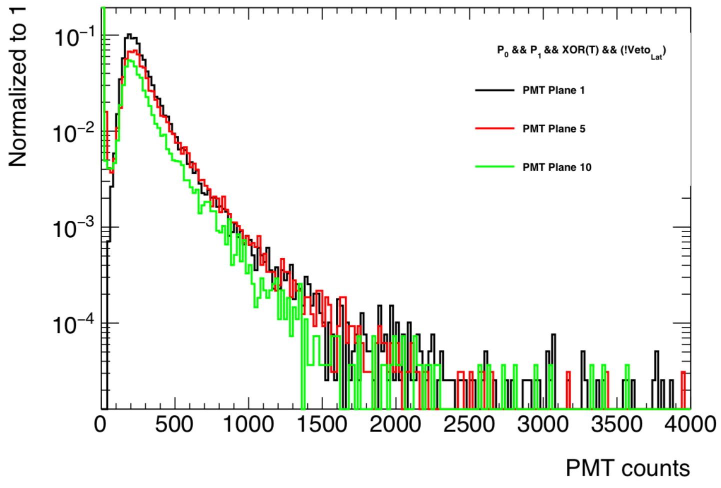

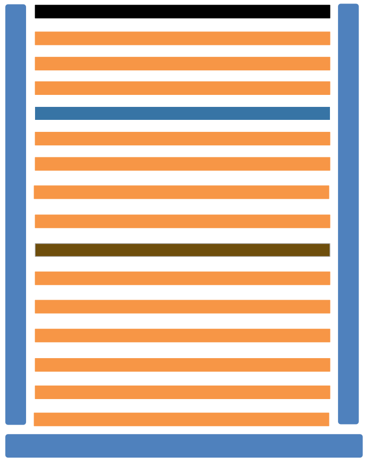

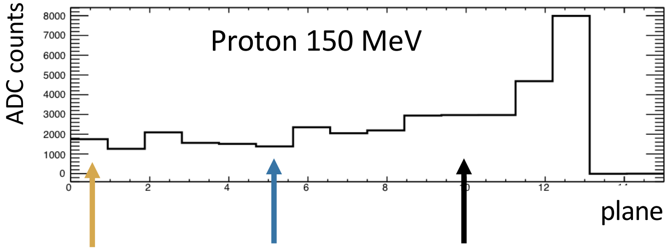

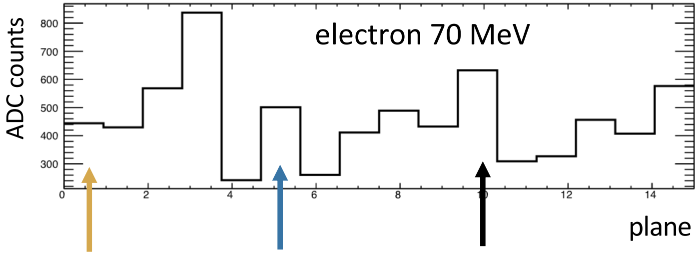

Roberto Iuppa

Target distributions - Generated vs Selected

Target distributions: ϕ, cos(θ), Ekin

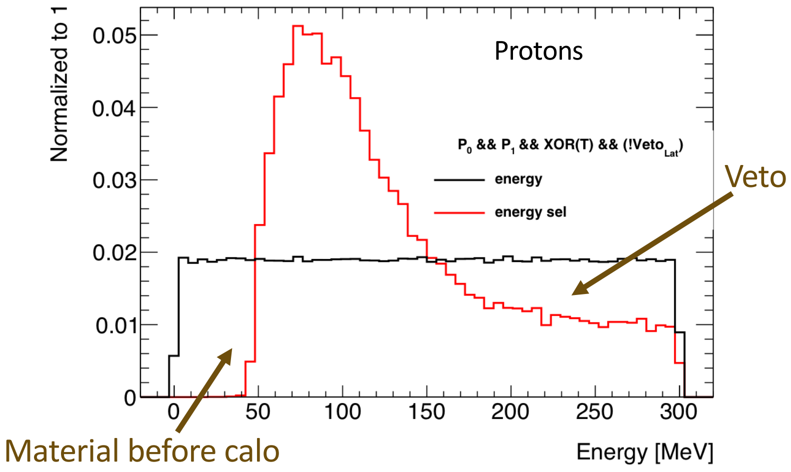

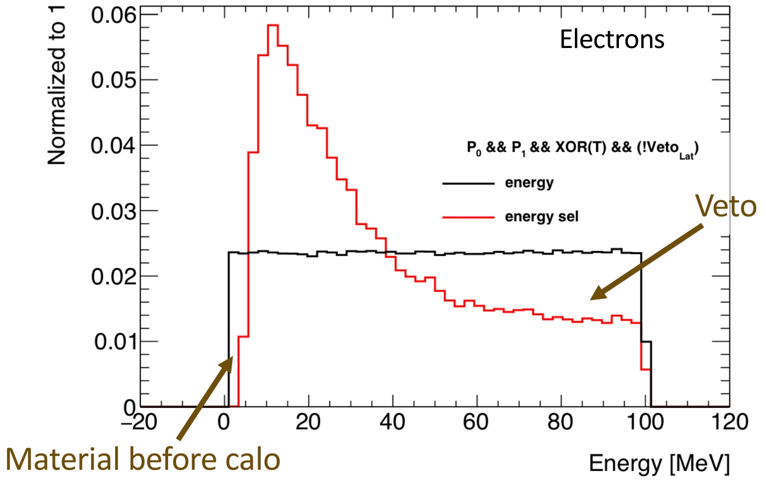

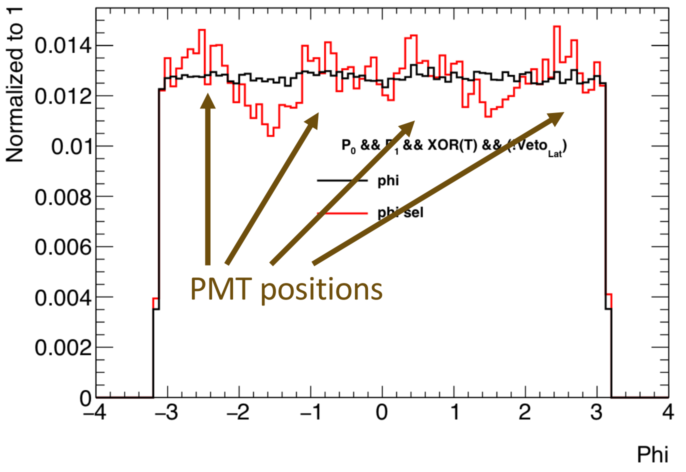

Angular distributions similar for electron & protons

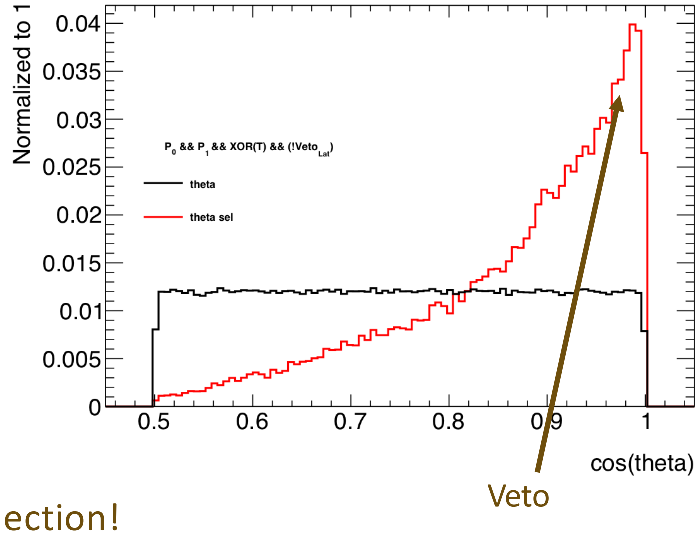

Variables are sculpted after selection!

Roberto Iuppa

The LIMADOU Experiment on the CSES Satellite

Training procedure

The two **FCNNs are trained independently** to keep their prediction (PID and Kin) uncorrelated as much as possible. Therefore, we get **independent predictions at each step** of the reconstruction chain.

- Training dataset split in two parts: **80% for training and 20% for evaluation** (cross validation was used).
- An additional and statistically independent test sample was used to check the FCNNs performance.
- **Number of epochs** ranged between **100-300** and **hyperparameters (**batch size, learning rate, etc…**) optimized**;
- Loss functions: MSE for $FCNN_{Kin}$ (regression) and BCE for $FCNN_{PID}$ (classification);

PID Loss (BCE)

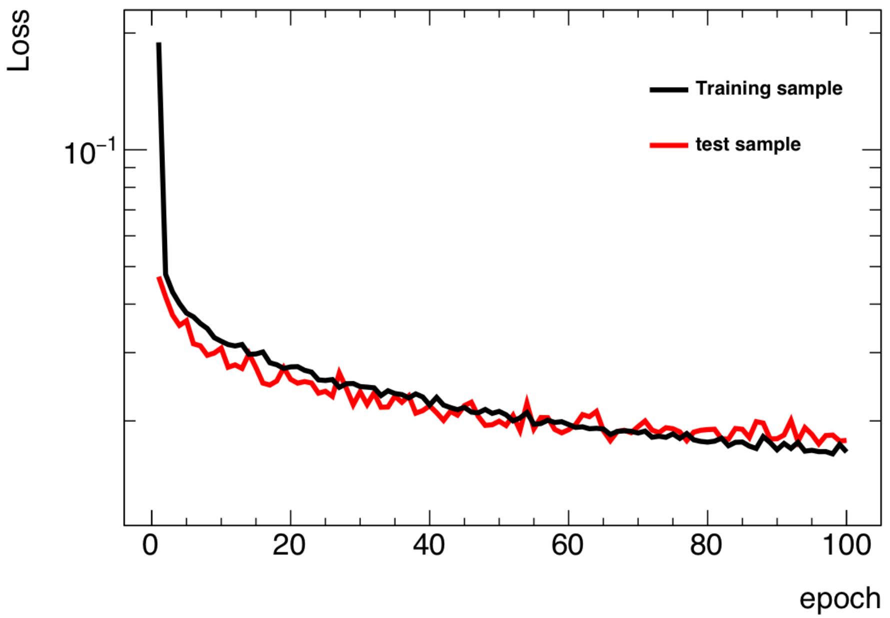

Roberto Iuppa

PID performance - DL

After the training procedure **the accuracy of the PID** based on DL **is 99.3 %** (population are already separated in ADC, small overlap). **Efficiency** and **mistag rate** have been estimated for electrons and protons.

$$Eff_{part} = \frac{N_{ev}(PID = part)}{N_{ev}(TRUTH = part)}$$

$$Mis_{part} = \frac{N_{ev}(PID! = part)}{N_{ev}(TRUTH = part)}$$

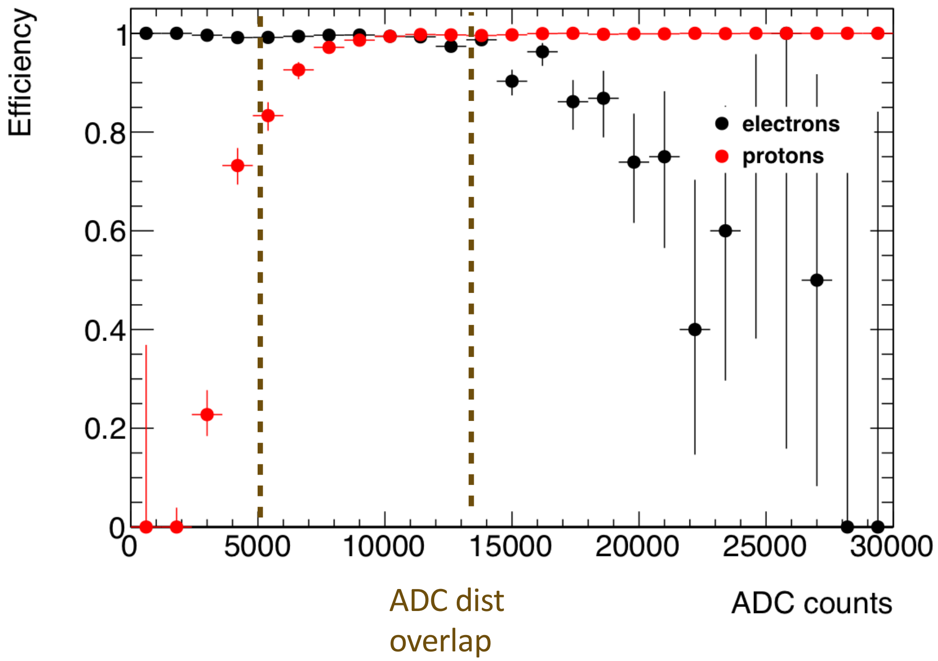

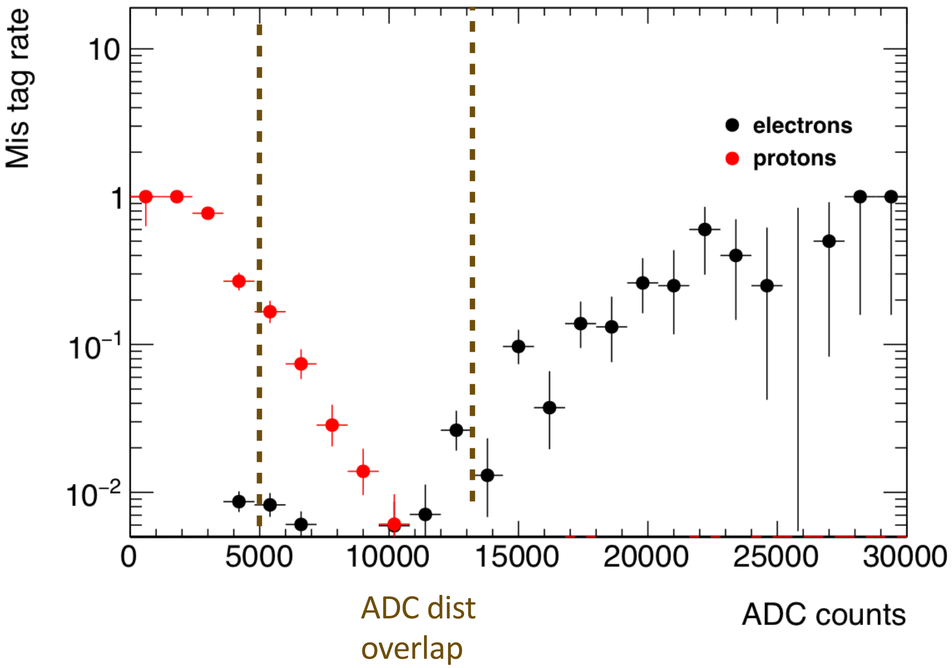

Roberto Iuppa

PID$_{reco}$ performance - DL vs Std

Both the **standard reconstruction (STD)** and the **DL reconstruction (DL)** are cut based: the first cut is optimized on the dE/dx (ADC_{TOT} vs ADC_{P1}) curve, the second cut is optimized on the NN output, to gain the best separation.

STD

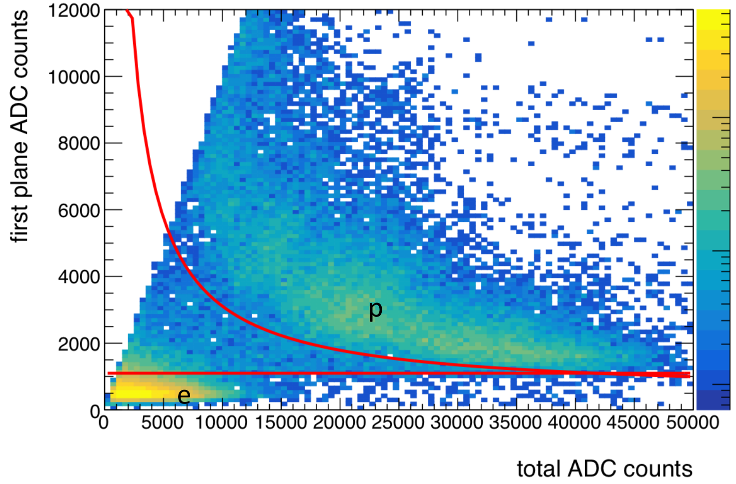

DL

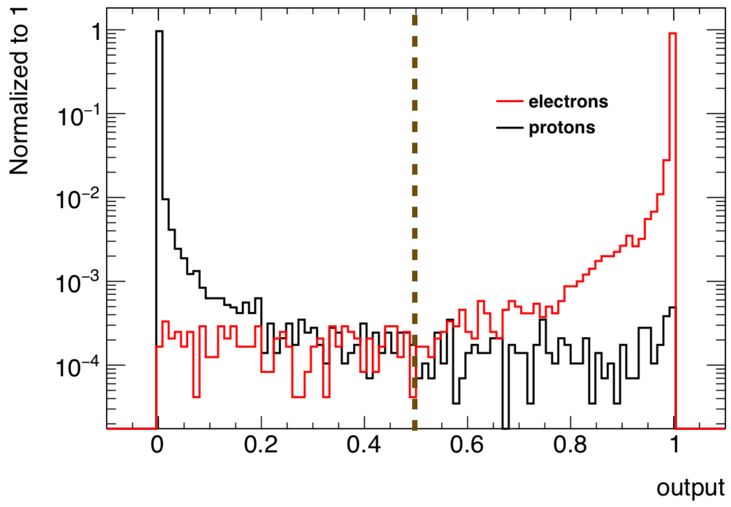

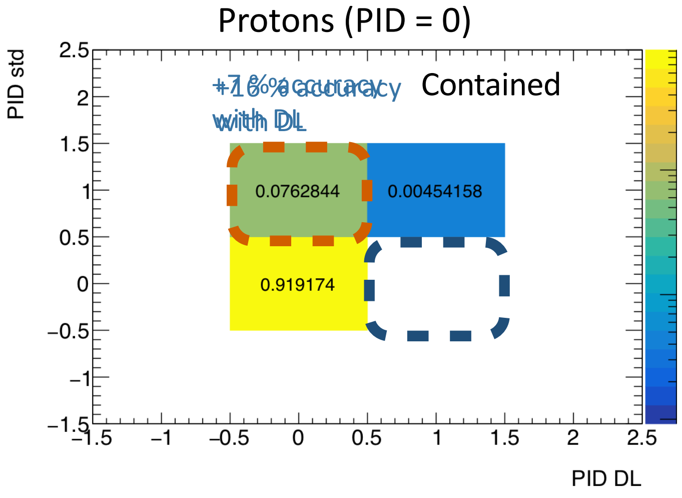

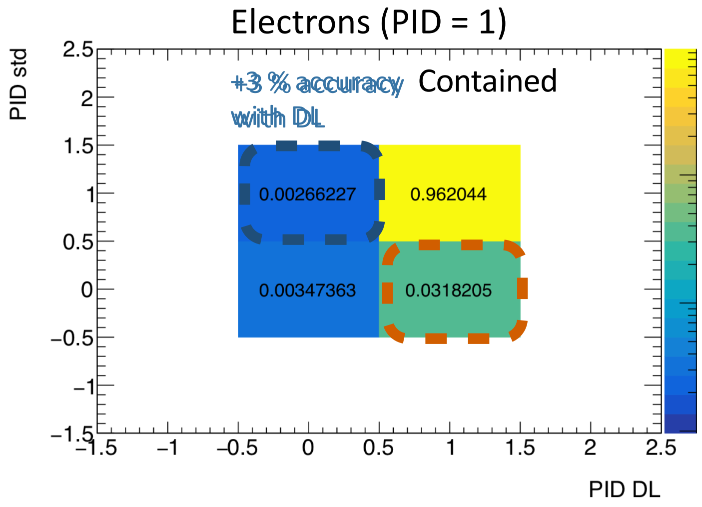

6.5% of such events in 154 MeV *p* test beam

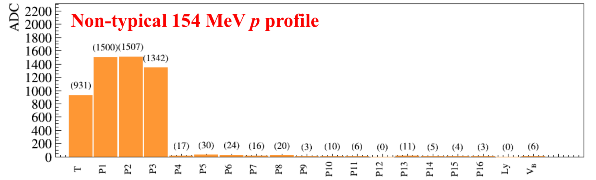

These events are most likely INTERACTING protons inside the Tower

Roberto Iuppa

E_{reco} performance - DL

After the particle identification, the ADC signal collected in each of the 32 PMT is passed to the **second reconstruction network: FCNN$_{kin}$**. It predicts the **kinetic energy of the particle**:

Reco Protons

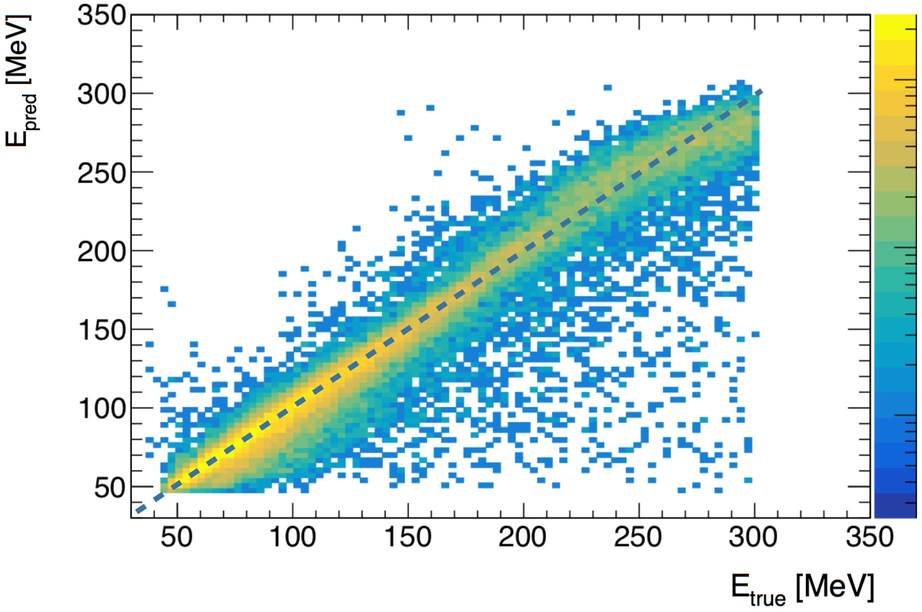

Reco Electrons

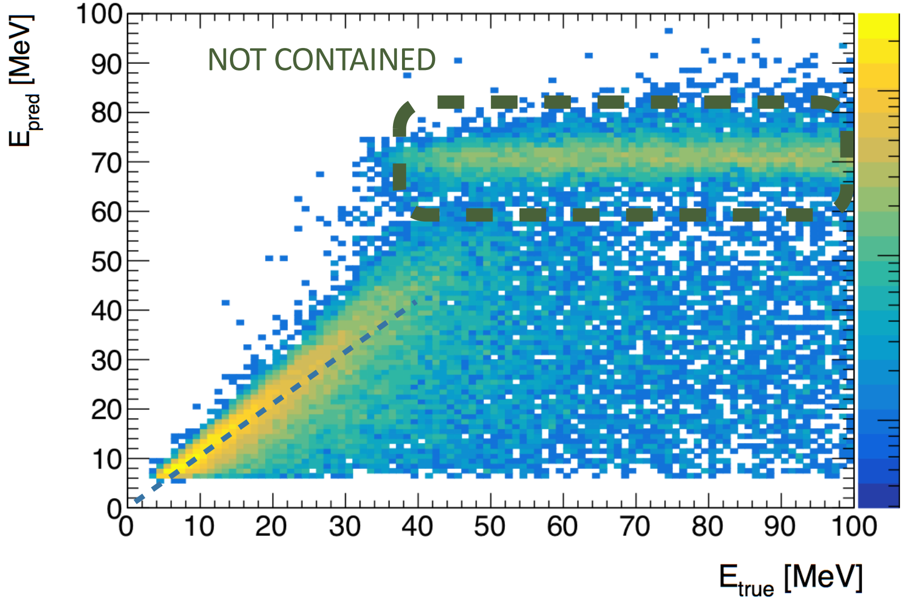

E^{prot}_{Kin} **really good**
even for **not contained** (>175 MeV)

E^{el}_{Kin} good below ~ 45 MeV (contained)
electrons are MIP
(plane ADC counts is constant)

E_{reco} performance - DL vs Std

The standard reconstruction for the energy of a particle works just for contained events. It is realized with a calibration looking at the dependency of “EnergyReco” on “EnergyTruth”.

Reco Protons

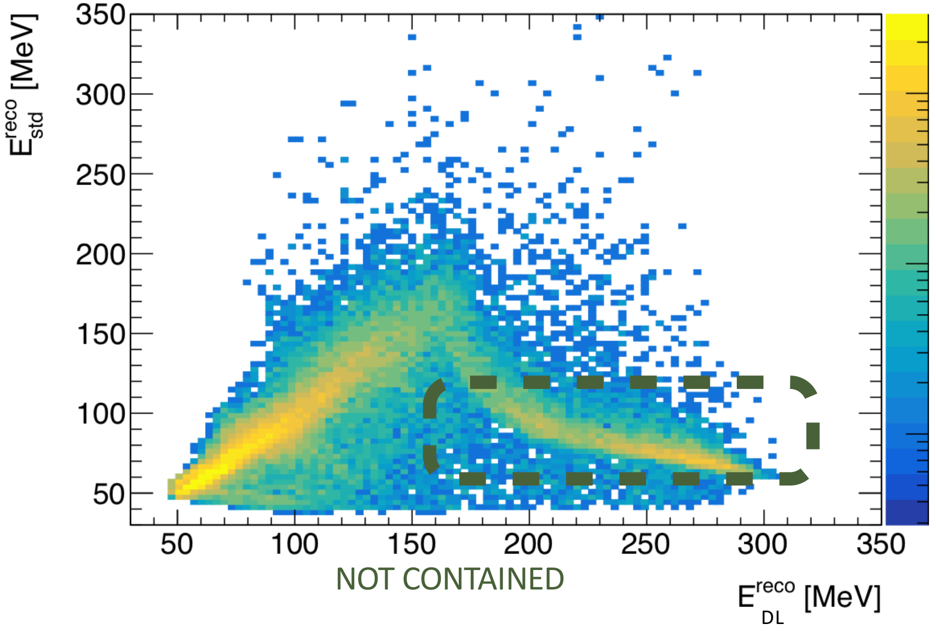

Reco Electrons

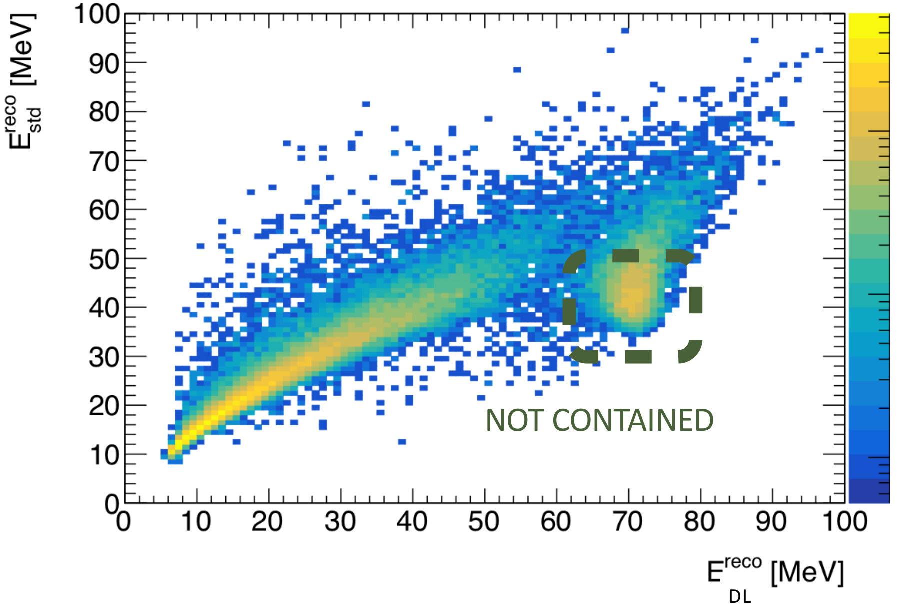

Deep learning is able to **reproduce standard energy reconstruction performance for contained** events and possibly **extend reconstruction to nuclei events not contained**

Roberto Iuppa

Arrival direction - D

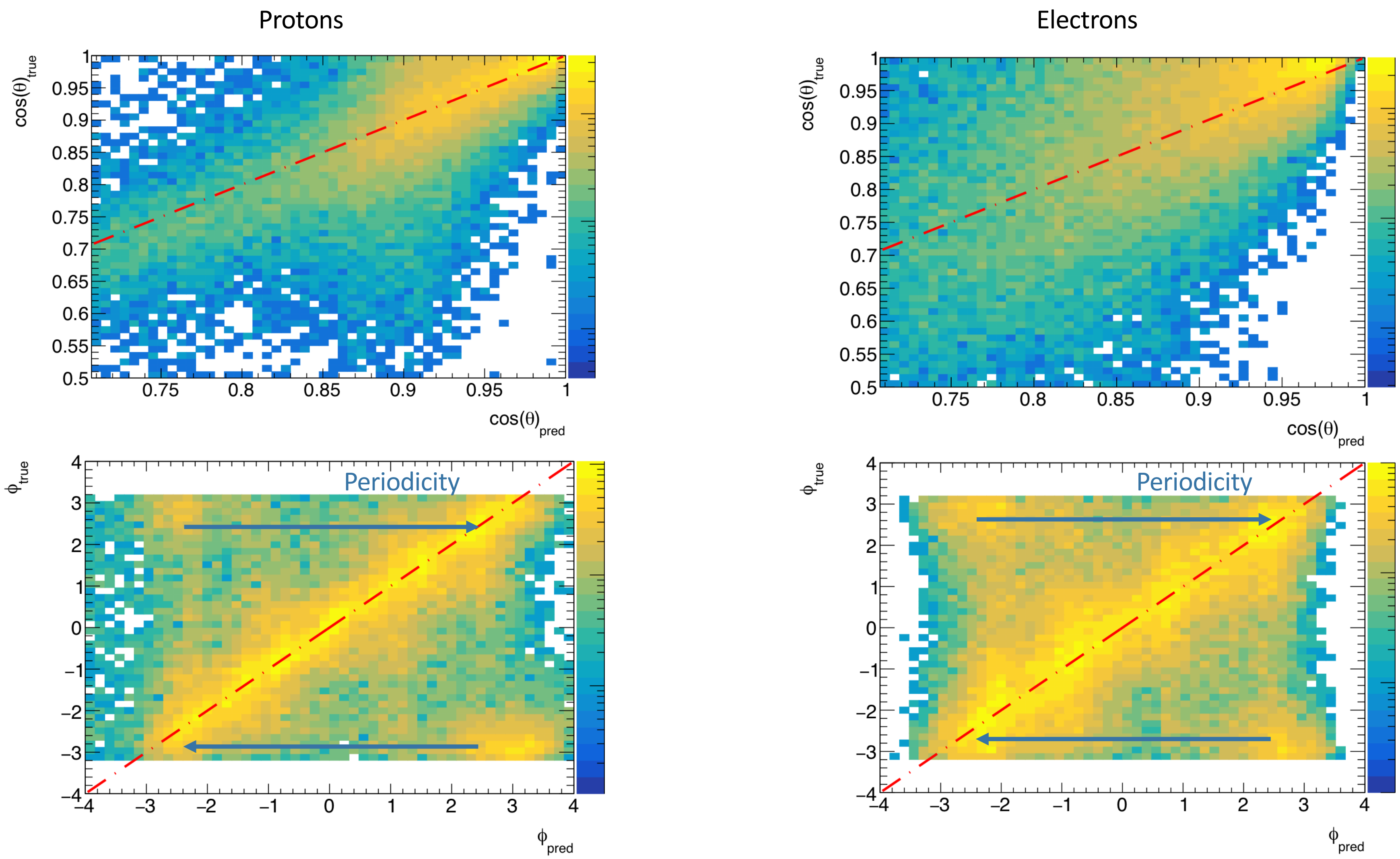

Protons release more signal

More signal → More accuracy

Arrival direction - DL

Ψ is defined as the **angle between the DL-reconstructed incoming direction and the measured one.**

Protons

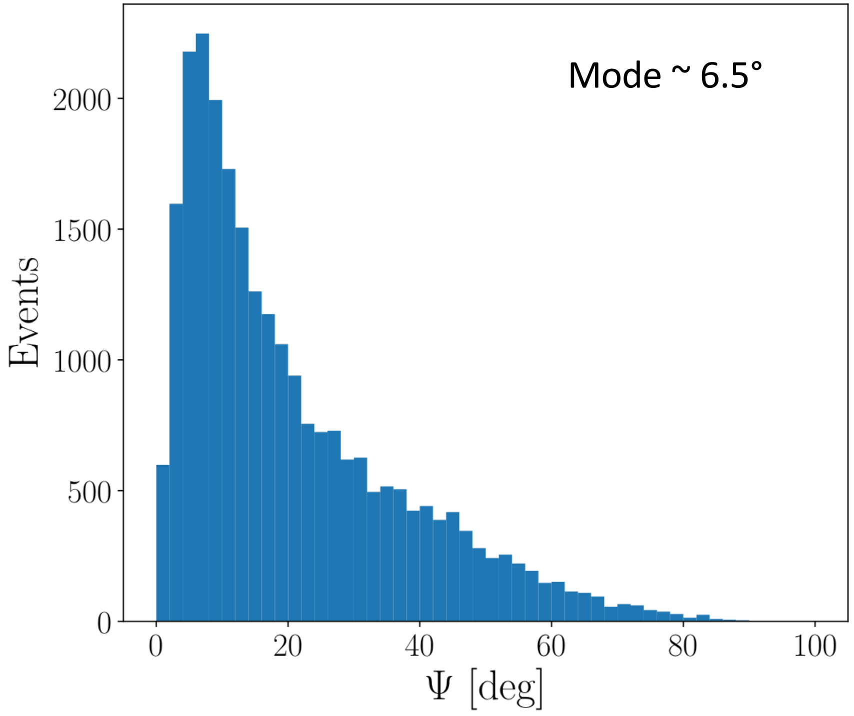

Electrons

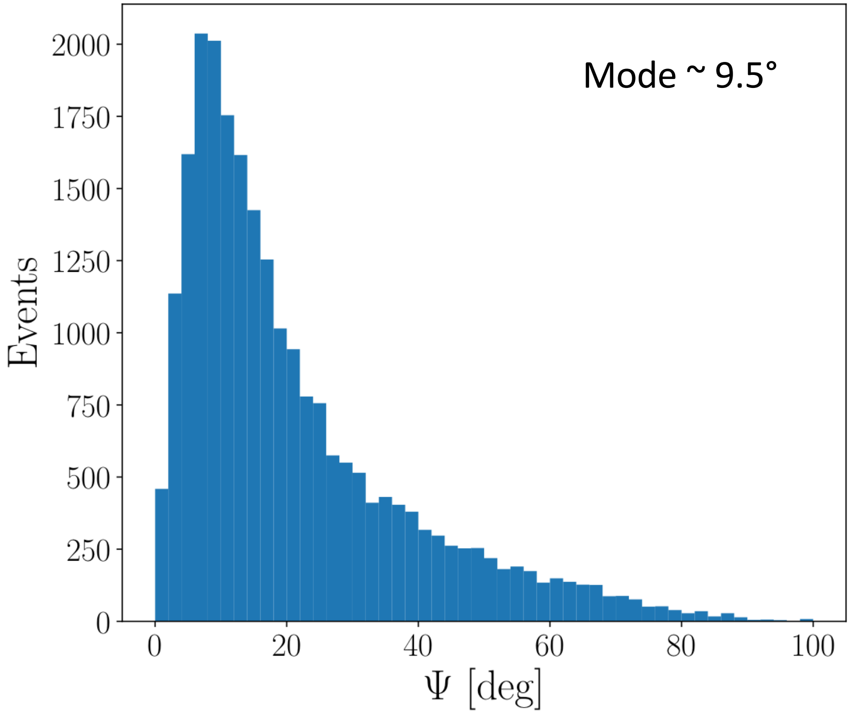

Roberto Iuppa

Results from commissioning phase

The Astrophysical Journal Supplement Series, 243:16 (17pp), 2019 July

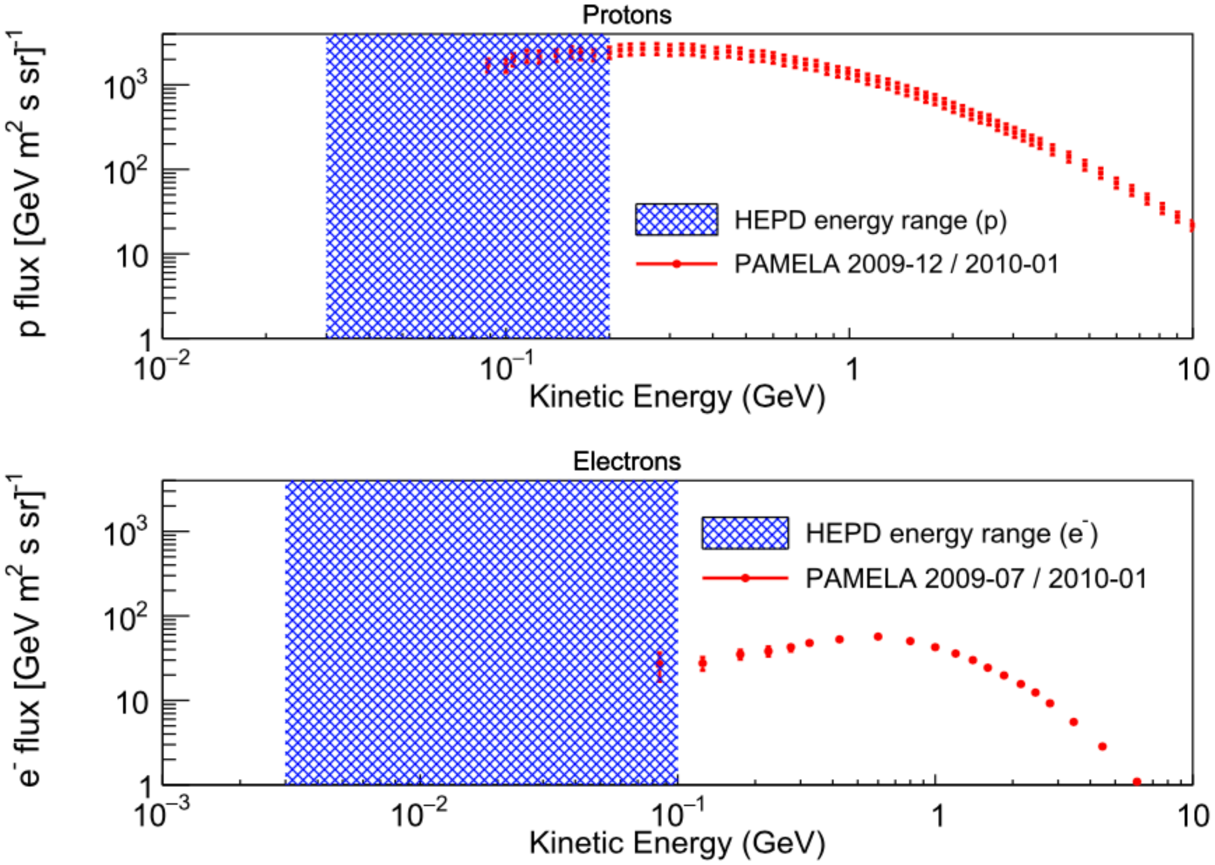

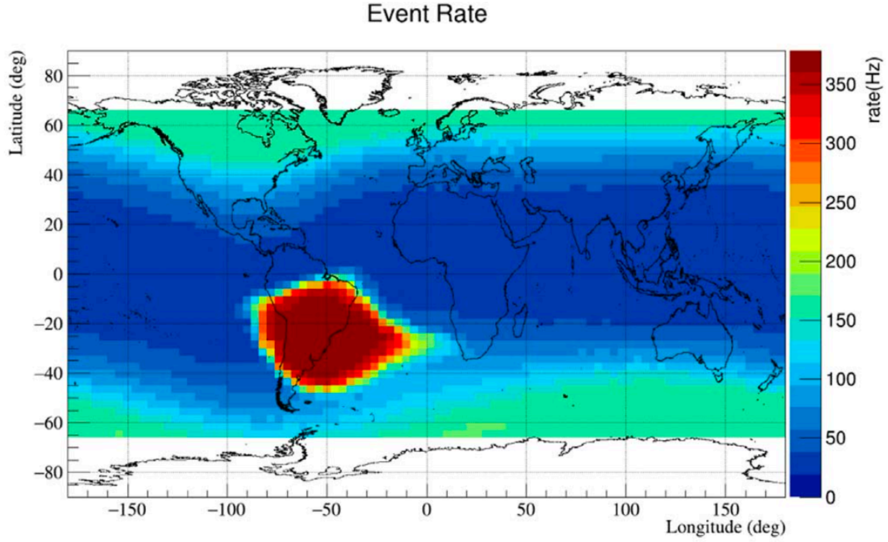

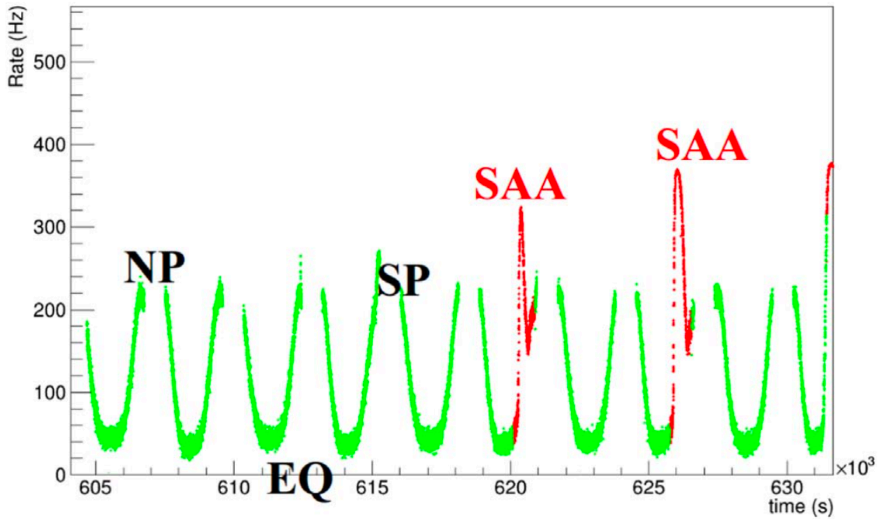

Figure 11. Top panel: HEPD average event-rate map during the period from 2018 May 14 to June 11. The red spot around Brazil represents the SAA, in which the rate counter saturates at about 350 Hz. Bottom panel: HEPD trigger rate as a function of onboard time for a few orbits. Different regions are marked.

Roberto Iuppa

Results from commissioning phase

Roberto Iuppa

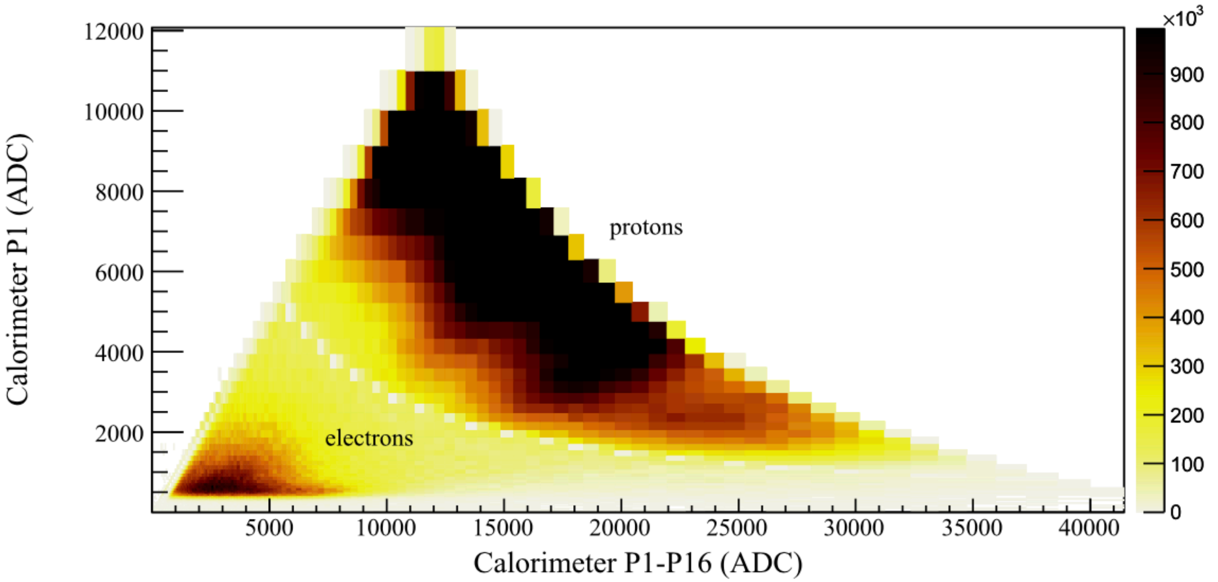

Figure 13. In-flight proton–electron identification by HEPD: energy released in the first plane of the calorimeter (P1) as a function of that released in the full calorimeter (P1 + ... + P16).

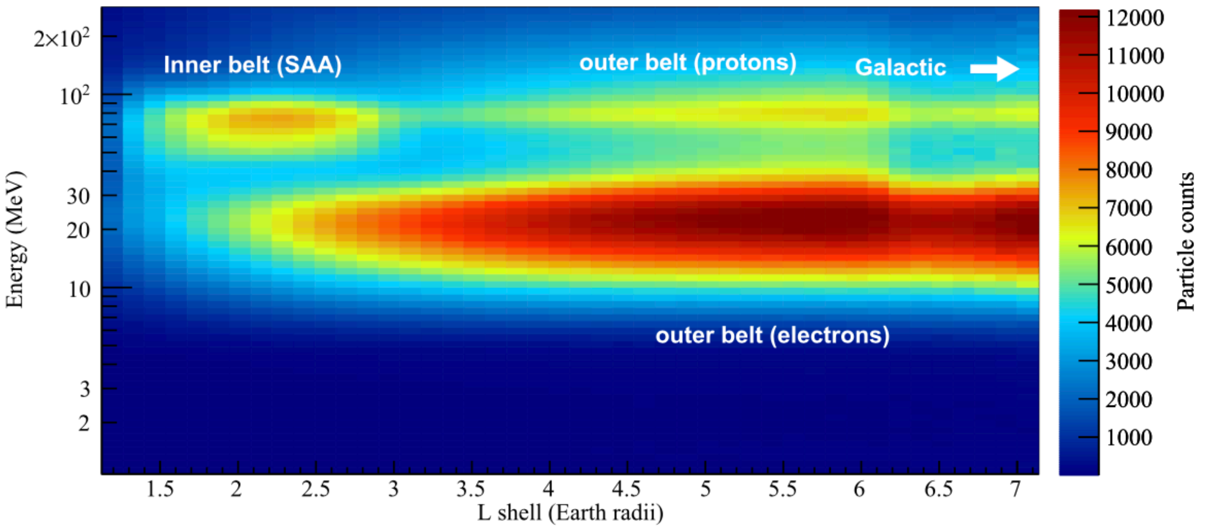

Figure 14. Different particle populations detected by HEPD as a function of L-shell and energy.

Results from commissioning phase

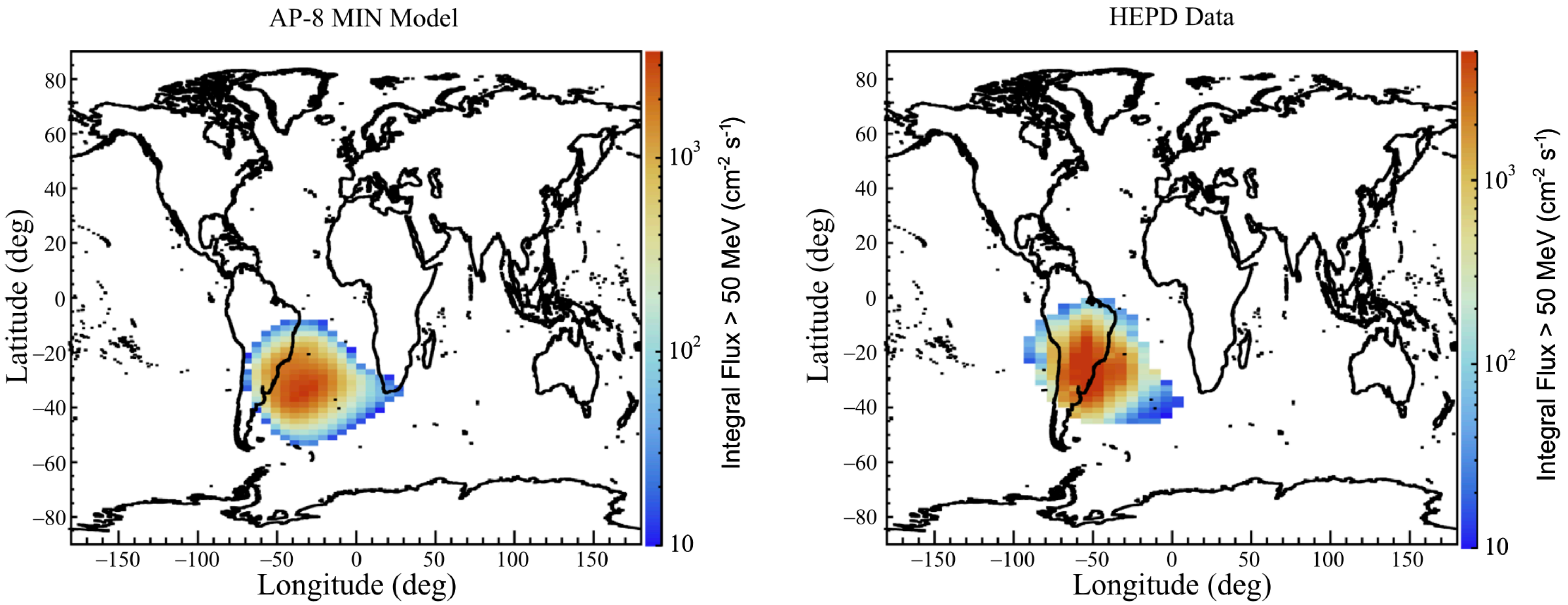

Figure 15. Comparison between trapped-proton geographical distributions inside the SAA obtained through the AP-8 MIN model (by the SPENVIS interface) and HEPD data (2018 August), respectively.

Results from commissioning phase

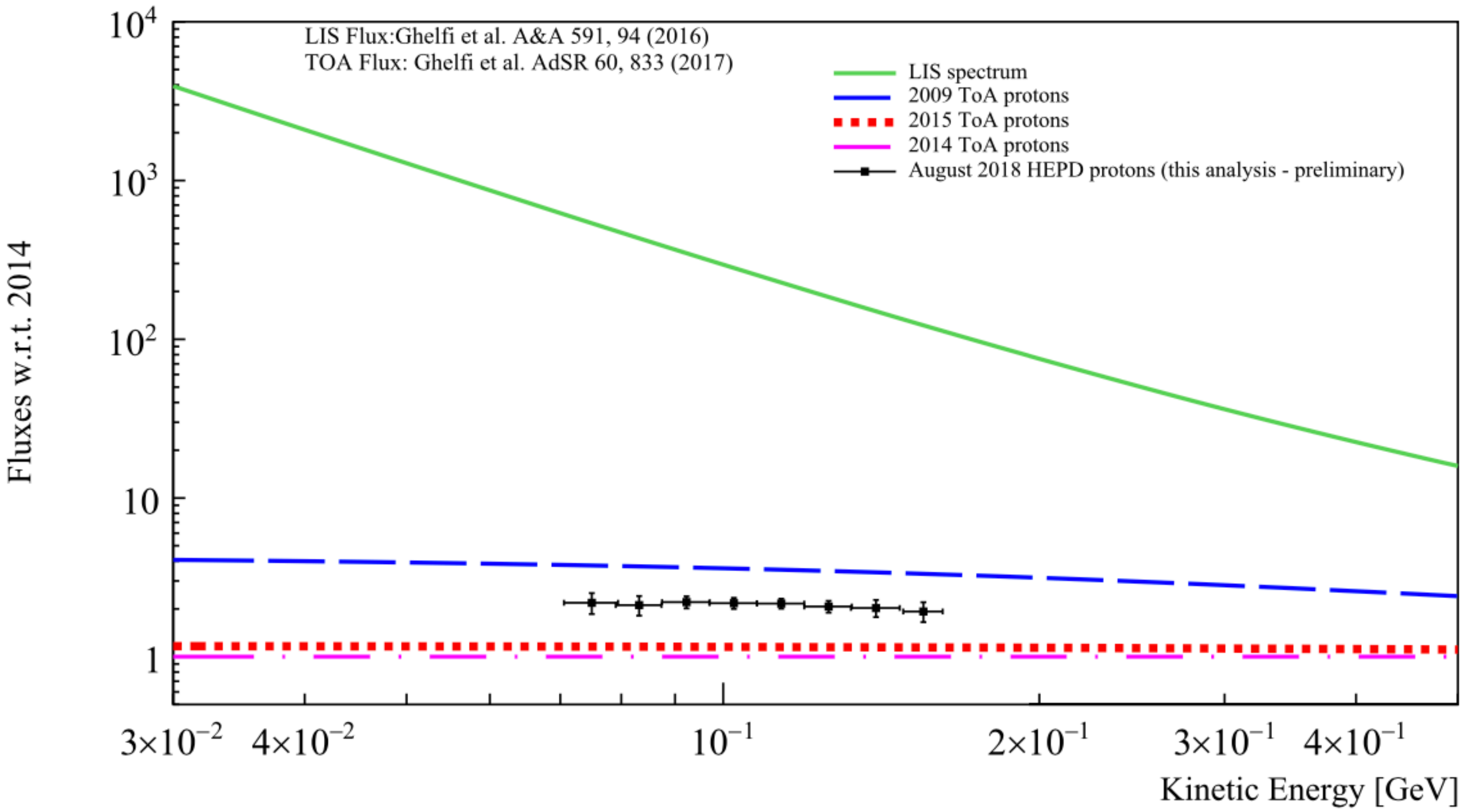

Figure 16. HEPD galactic proton flux (black squares) compared to TOA theoretical fluxes for 2009 (blue dashed line), 2014 (magenta dashed–dotted line), 2015 (red dotted line), and LIS spectrum (green solid line).

Roberto Iuppa

Topics

Roberto Iuppa

lecture 2

the HEPD-02 tracker

- needs
- concept
- spatialize a new technology: how to

CNSA-ASI MOU on CSES-02, Roma March 23,2019

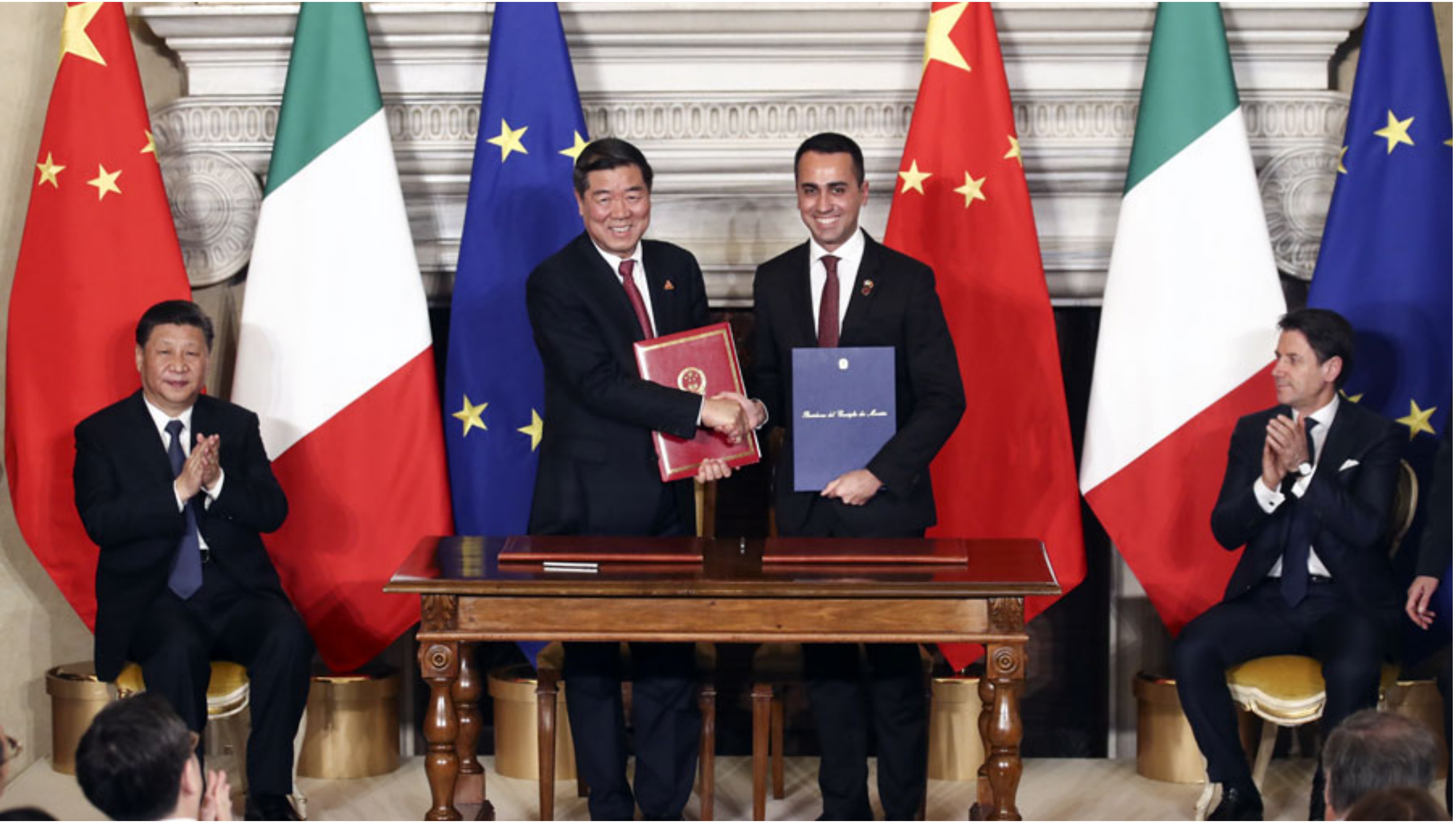

Roberto Iuppa

CSES-02 Milestones

- March,2017, National Development and Reform Commission of China (NDRC)proved CSES-02 project；
- April, 2018, NDRC proved CSES-02 feasibility demonstration；
- Sept. 3, 2018, CEA start the CSES-02 project developing；
- March 23, 2019, CNSA-ASI MOU on CSES-02 cooperation signed in Roma；
- June,2019, NDRC proved the Launching site and TT&C ；
- Dec.4, 2019, authorized by CEA and MEM, ICD proved the CSES-02 preliminary design;
- **Currently，NDRC release the annual budget of CSES-02 and MEM is ready to manage CSES-02 instead of CEA** .

The CSES-02 launch time is fixed no later than March, 2022

Whahat do you see from these plots?

The Astrophysical Journal Supplement Series, 243:16 (17pp), 2019 July

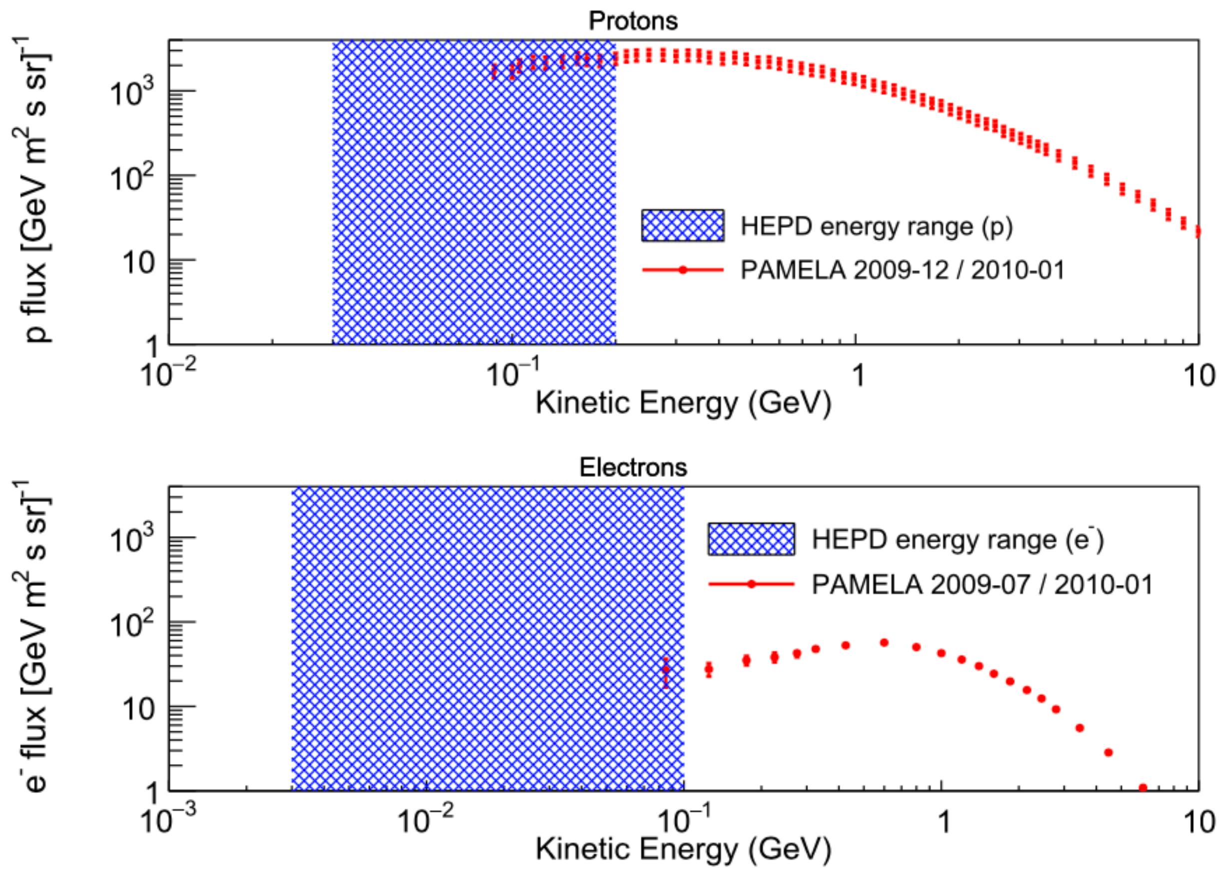

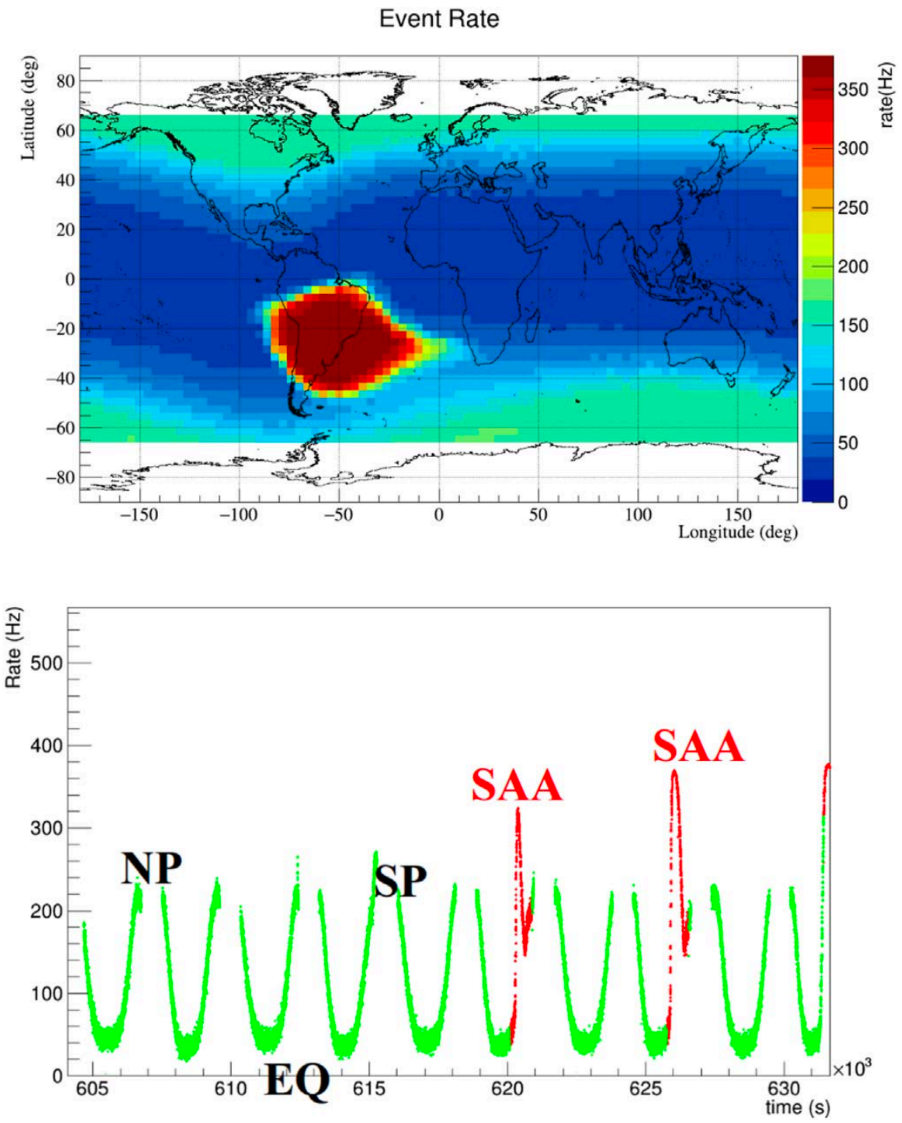

Figure 11. Top panel: HEPD average event-rate map during the period from 2018 May 14 to June 11. The red spot around Brazil represents the SAA, in which the rate counter saturates at about 350 Hz. Bottom panel: HEPD trigger rate as a function of onboard time for a few orbits. Different regions are marked.

Microstrip: custom technology. Very expensive. Noisy.
Difficult to readout and calibrate (it also takes online time → increases dead time). Expensive to readout (VA).
Tracking resolution limited (yet sufficient for HEPD-02)

Roberto Iuppa

The LIMADOU Experiment on the CSES Satellite

Trackers in space: summary

Roberto Iuppa

HEPD is the ideal science case for a change of paradigm

Experiment	Year	Technology	Pitch [µm]	Resolution [µm]	Surface [m²]	Power [W]	Power density [mW/cm²]	Life span [year]
Fermi LAT	2008	Single side	228		74	160	0.2	Ongoing
DAMPE	2015	Single side	121	70	7	90	1.3	Ongoing
PAMELA	2006	Double side	50 (p) 67 (n)	3	0.13	63	48	11
AMS-02	2011	Double side	110 (p) 208 (n)	10 (p) 30 (n)	6.4	734	12	Ongoing
HEPD-01	2018	Double side	182	50	0.088	10	11	Ongoing

Trackers in space: summary

Roberto Iuppa

If you want to find something better than HEPD-01 microstrip, you need something
- Ready (launch 2022!)
- Easy to readout (no time to become a “guru” of some technology)
- Performing better: faster and lower noise

Experiment	Year	Technology	Pitch [µm]	Resolution [µm]	Surface [m^2]	Power [W]	Power density [mW/cm^2]	Life span [year]
Fermi LAT	2008	Single side	228		74	160	0.2	Ongoing
DAMPE	2015	Single side	121	70	7	90	1.3	Ongoing
PAMELA	2006	Double side	50 (p) 67 (n)	3	0.13	63	48	11
AMS-02	2011	Double side	110 (p) 208 (n)	10 (p) 30 (n)	6.4	734	12	Ongoing
HEPD-01	2018	Double side	182	50	0.088	10	11	Ongoing

ALPIDE

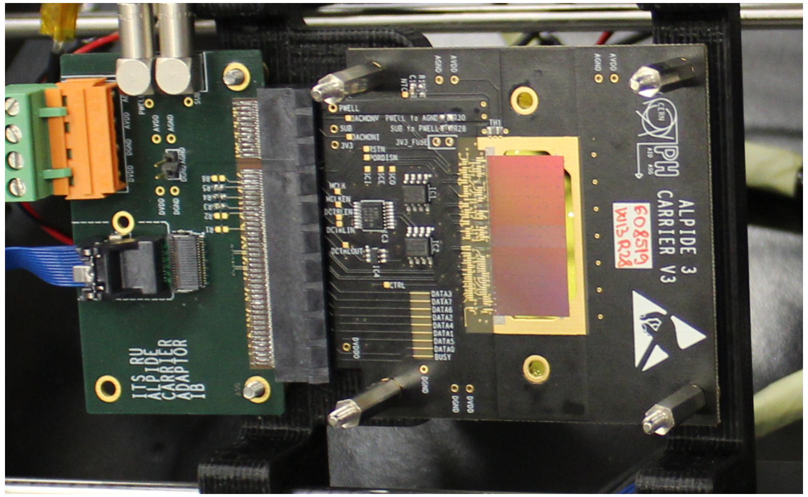

ALPIDE is a MAPS detector designed for ALICE ITS Upgrade.
The requirements for the upgrade are reported in the table.

Parameter	IB	OB	Achieved
Detector size [mm^2]	15 x 30	15 x 30	15 x 30
Detector thickness [µm]	50	100	50 - 100
Spatial resolution [µm]	5	10	4
Detection efficiency	>99%	>99%	>99%
Fake hit rate [evt^{-1} pixel^{-1}]	<10^{-5}	<10^{-5}	<10^{-7}
Integration time [µs]	<30	<30	~2
Power density [mW/cm^2]	<300	<100	<50 *

* The power consumption depends on the detector configuration

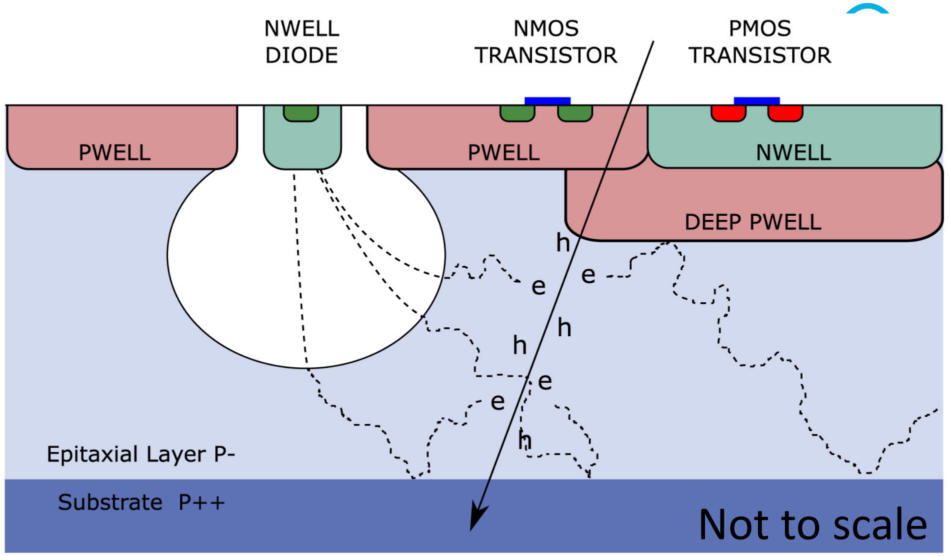

https://doi.org/10.1088/0954-3899/41/8/087002.

- Sparsified readout
- Pixel pitch: 26.88 x 29.24 µm^2
- Columns x rows: 1024 x 512
- Electrode diameter: 2 µm
- Back bias: 0 V to -6 V
- Producer: TowerJazz

ALPIDE: block diagram

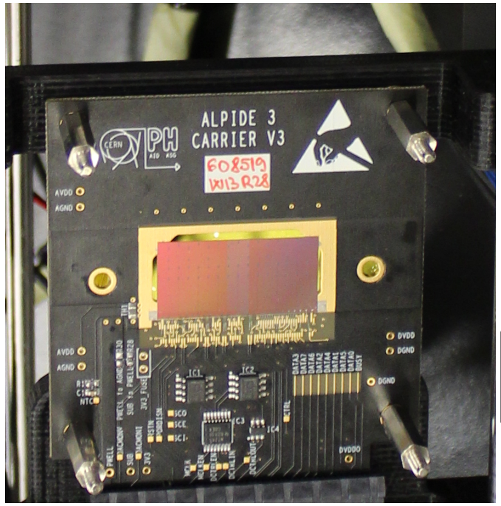

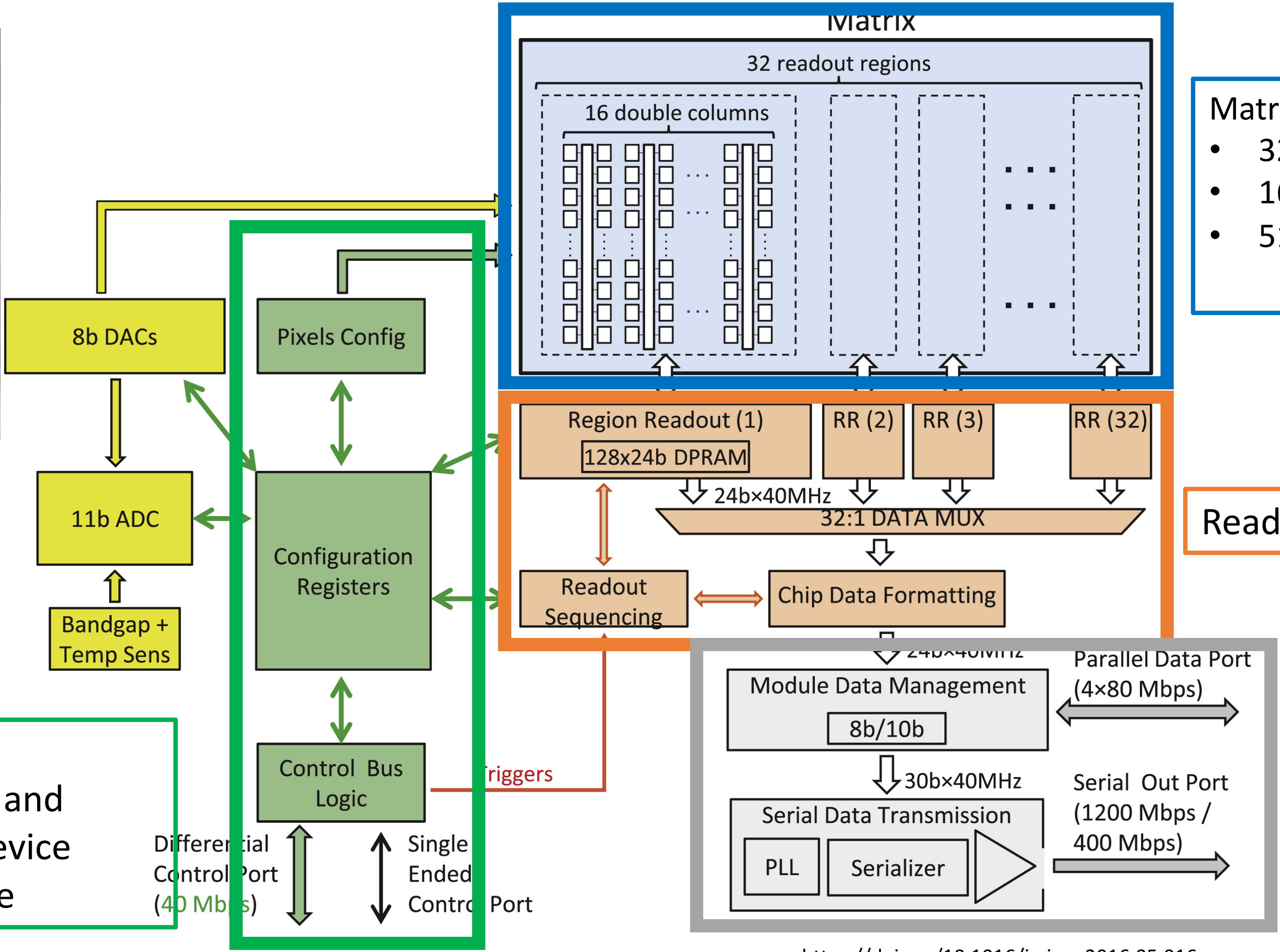

Matrix:
- 32 regions
- 16 double columns/region
- 512 rows/column

Roberto Iuppa

Readout registers (DP RAM)

Data transmission and high speed ports

CRTL line
- Communication and control of the device
- Readout possible

https://doi.org/10.1016/j.nima.2016.05.016

ALPIDE power consumption in ALICE

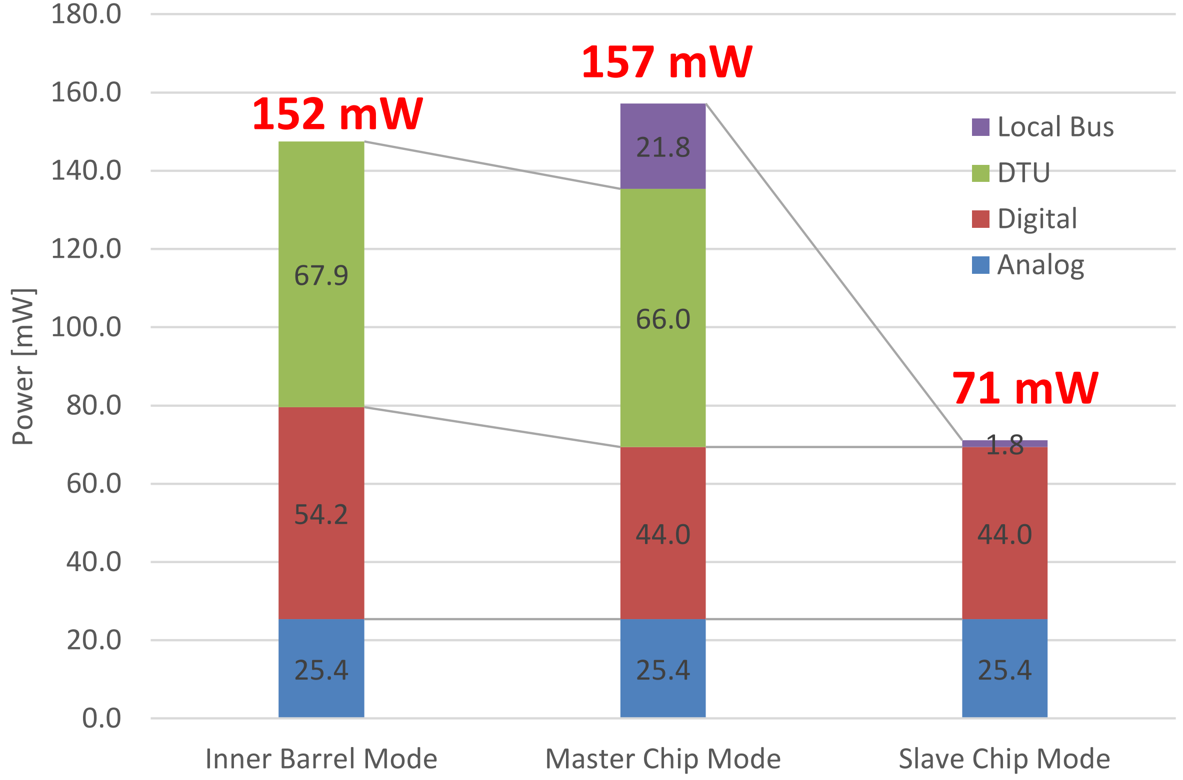

https://indico.cern.ch/event/ 666016/contributions/2722251/attachments/1523408/2380925/ 20170914-ALPIDE-FoCal-Study-Aglieri.pdf

Fermi microstrip power density: 0.2 mW/cm^2
HEPD-01 microstrip power density: 10 mW/cm^2

Inner barrel stave power consumption:

- Nine IB mode detectors: 1.4 W

IB power density: 34 mW/cm^2

OB stave power consumption:

- One Master chip mode: 157 mW
- Six Slave chip mode: 426 mW
- Full stave (two columns of seven detectors): 1.2 W

OB power density: 18.5 mW/cm^2

https://doi.org/10.1088/0954-3899/41/8/087002

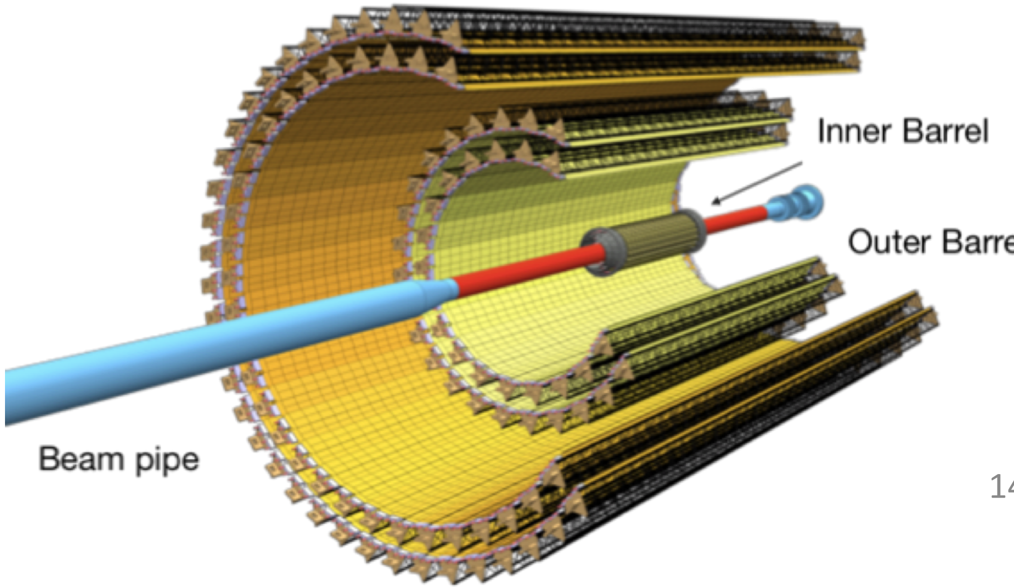

Roberto Iuppa

ALPIDE response to low energy nuclei

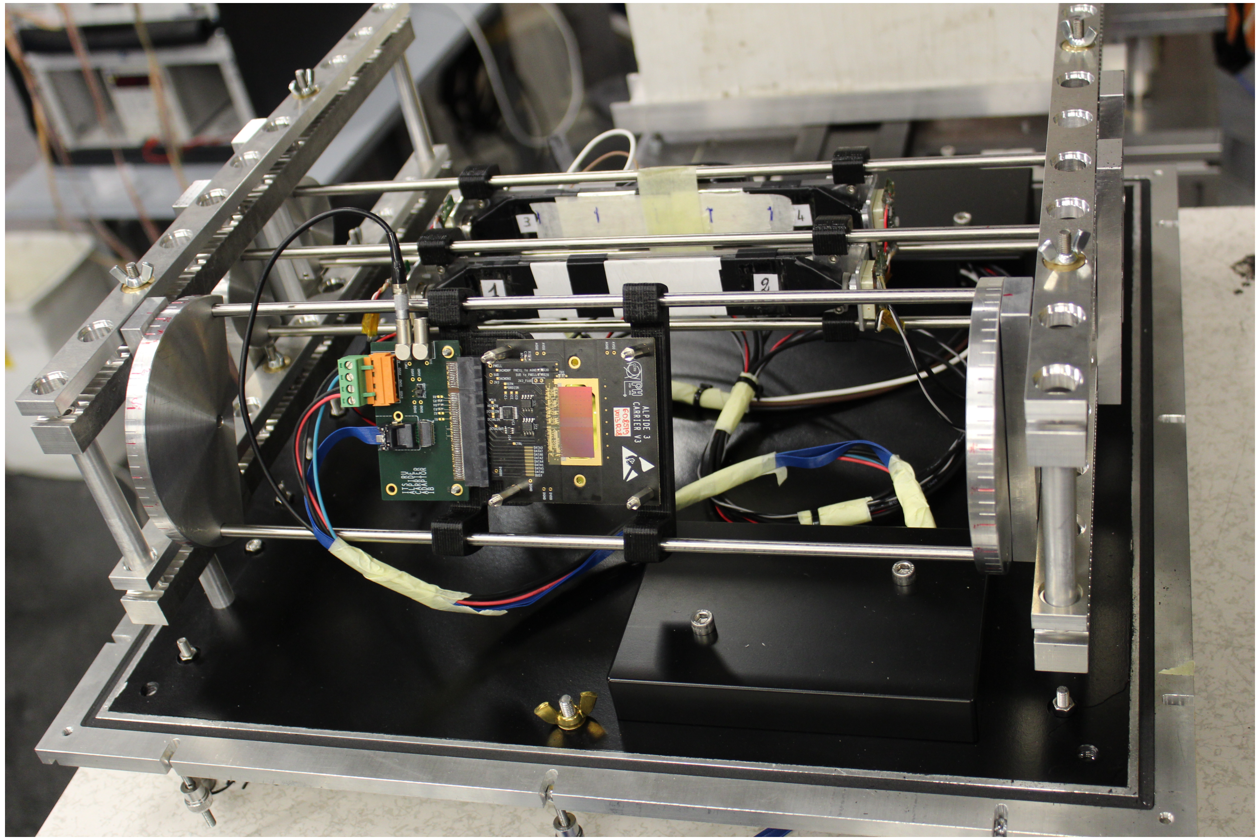

Roberto Iuppa

Experimental setup for beam tests (LNS and TN)

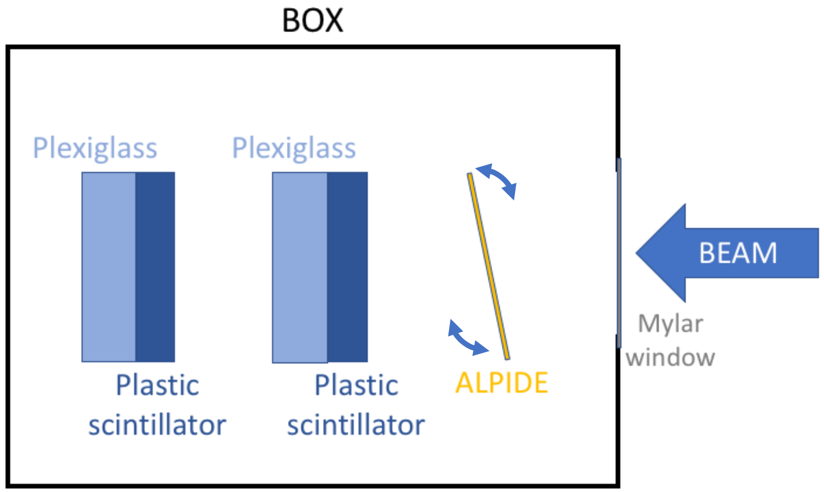

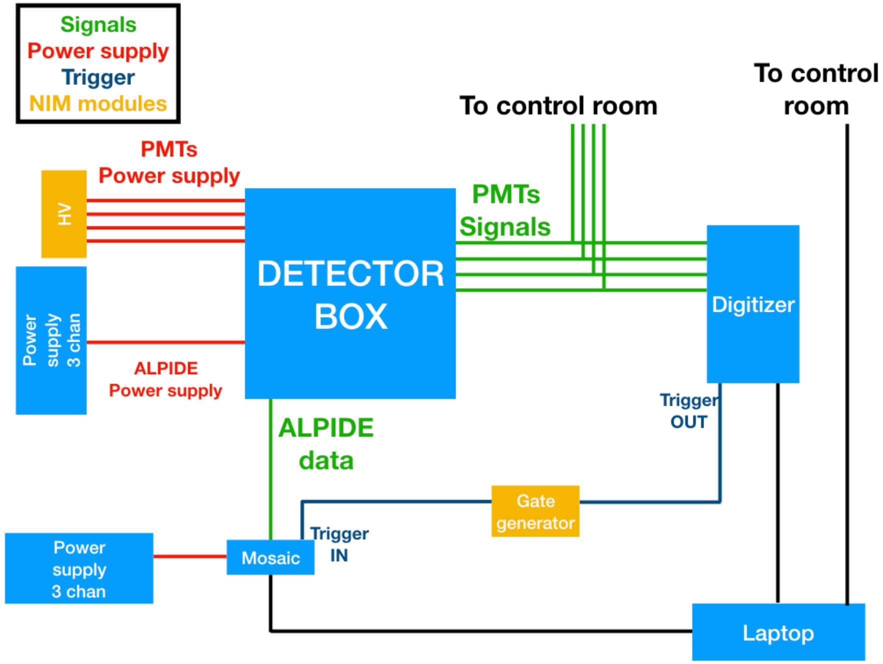

- The experimental setup was composed by an **ALPIDE sensor** and two **EJ200** plastic scintillator bars (2x30x150 mm^3) used to give a trigger signal;
- The scintillators were **readout by two PMTs** for each bar;
- The signal of the PMTs was processed by a CAEN DT5725 digitizer, that saved the waveforms and gave the trigger signal to the MOSAIC board used to control ALPIDE;
- Waveforms from PMTs were also collected by a Lecroy oscilloscope.
- The **energy** of the beam was **62 MeV/amu** and we tested the sensor with **protons**, **He**, **C** and **O** in Catania @ LNS.
- The same setup was used with **20 MeV to 220 MeV protons** in Trento @ APSS Proton Therapy centre

Roberto Iuppa

Cluster size studies: MIPs

- ALPIDE has a binary readout, the only information is the address of pixels over threshold.
- In principle, this readout limits the spatial resolution to pitch/$\sqrt{12}$
- A study of cluster shape as a function of the impact position on the pixel and incidence angle can provide a more precise information (https://doi.org/10.1016/j.nima.2018.04.053)

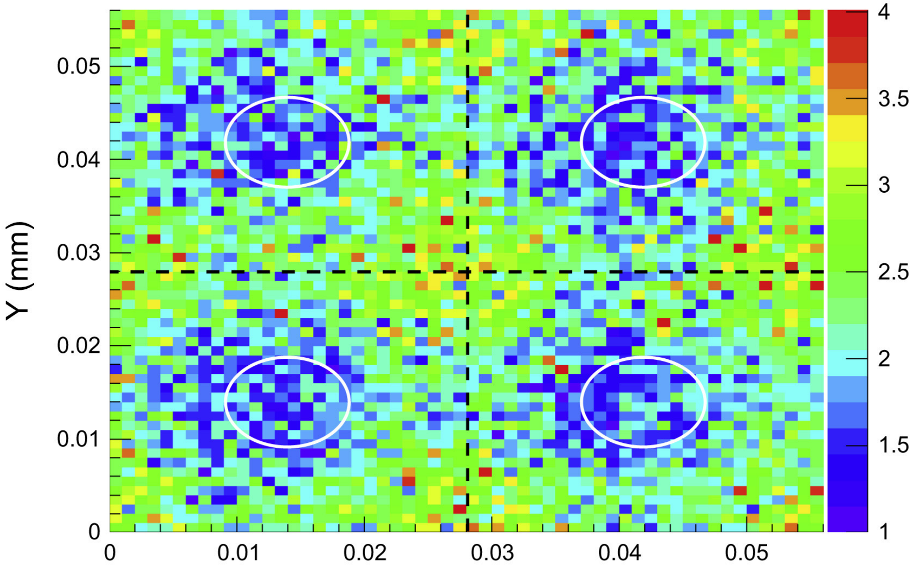

https://doi.org/10. 1016/j.nima.2015.09.057

Cluster size as a function of impact position on pixel for MIPs

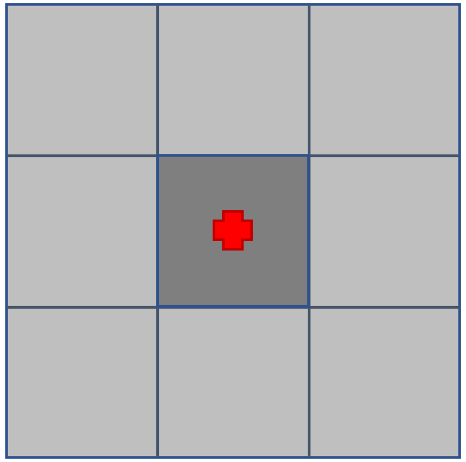

Cluster size: 1

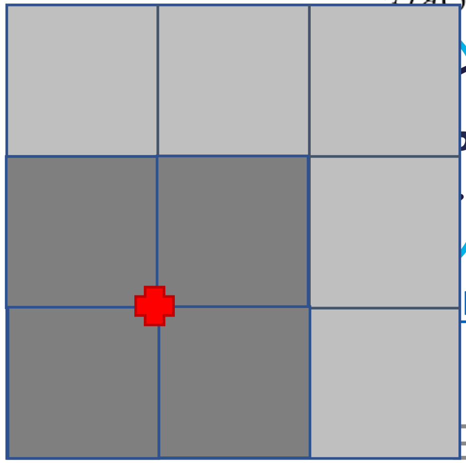

Cluster size: 4

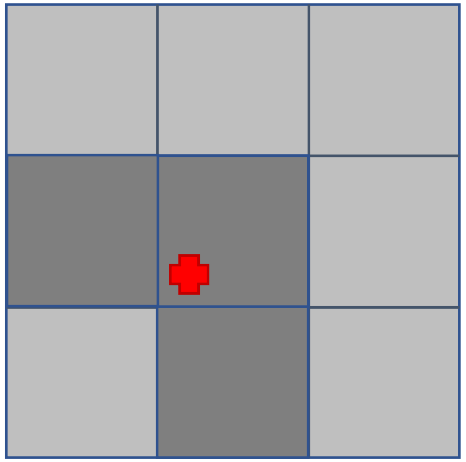

Cluster size: 3

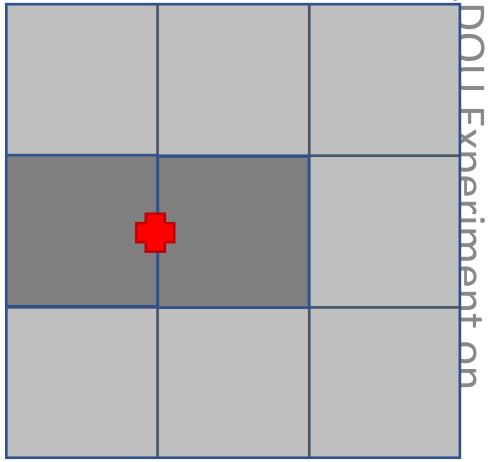

Cluster size: 2

luppa

Cluster size studies: low energy nuclei

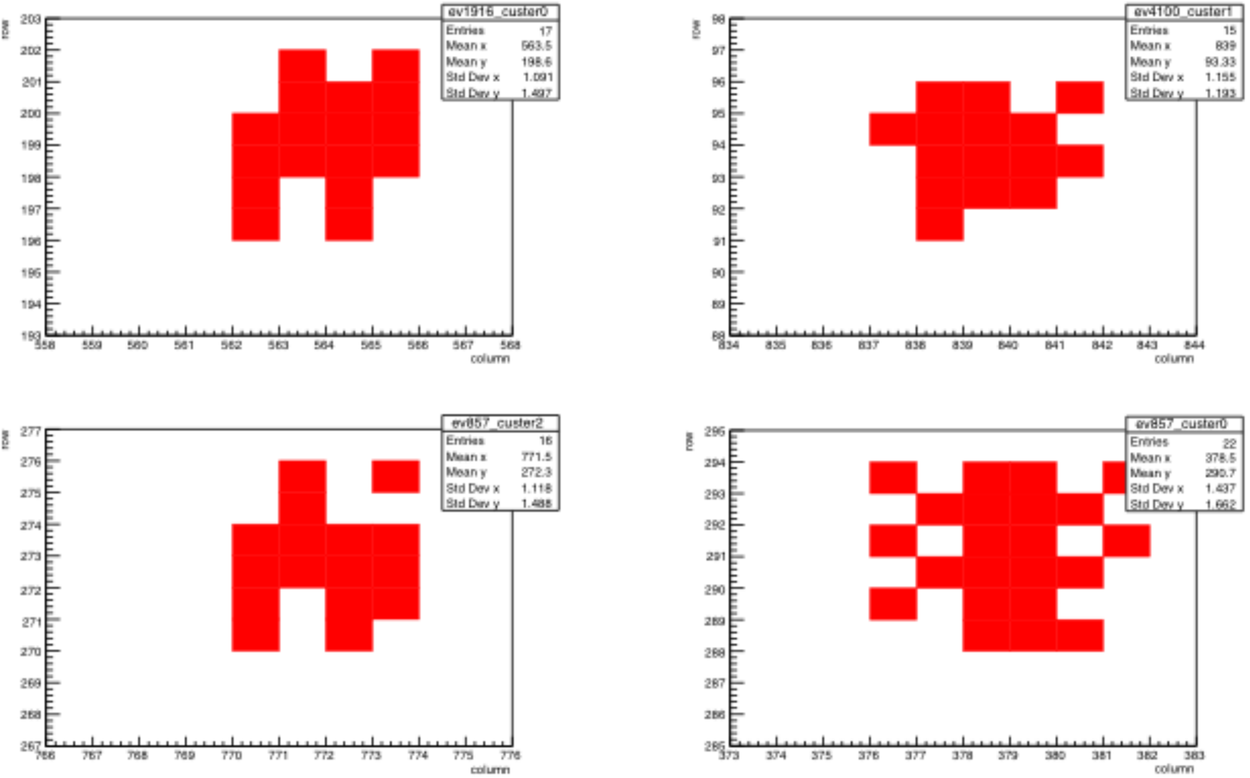

Data collected with 62 MeV/a.m.u. He

- Low energy nuclei produce larger clusters because of the diffusion-driven charge collection
- The number of possible combinations is huge when cluster size enlarges
- The characterisation of the clusters can provide interesting information for event reconstruction algorithms
- Other approaches are required to acquire all the possible information from these structures

Roberto Iuppa

Single cluster event selection

- How do we define a cluster?
- A possible indication comes from the RMS of the pixel position along columns (x axis) and rows (y axis) of ALPIDE
- Data acquired with 220 and 20 MeV protons are used as reference to tune the analysis.
- Events with $RMS_x<2$ and $RMS_y<2$ have been selected for the analysis

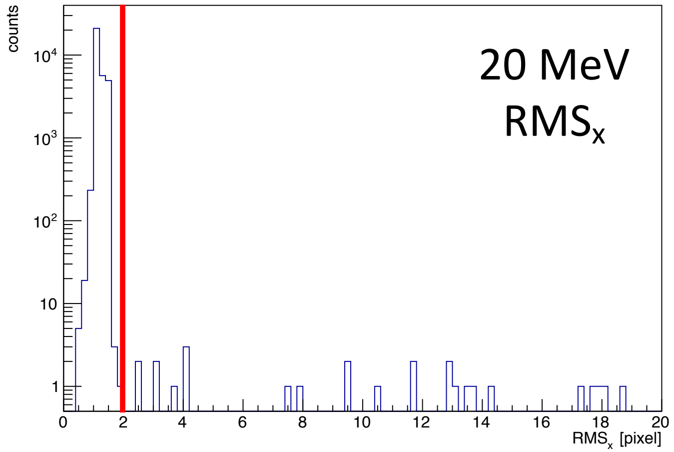

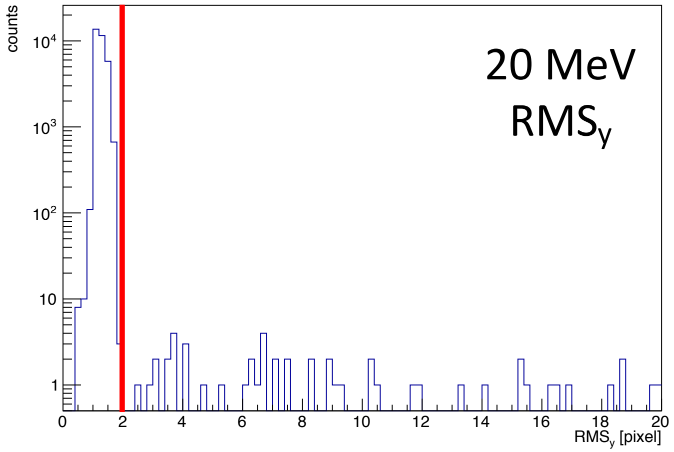

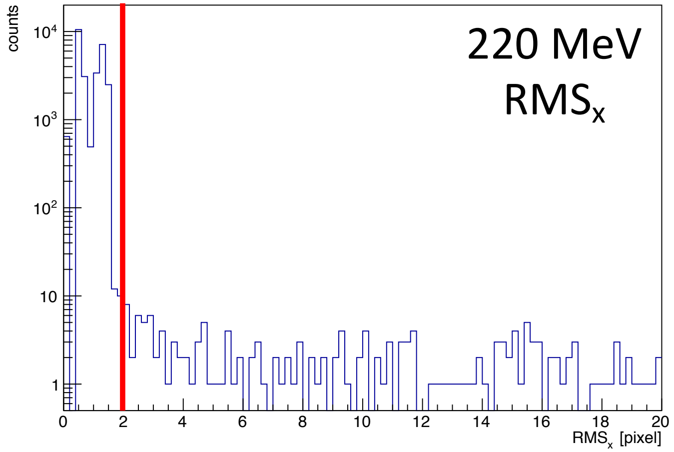

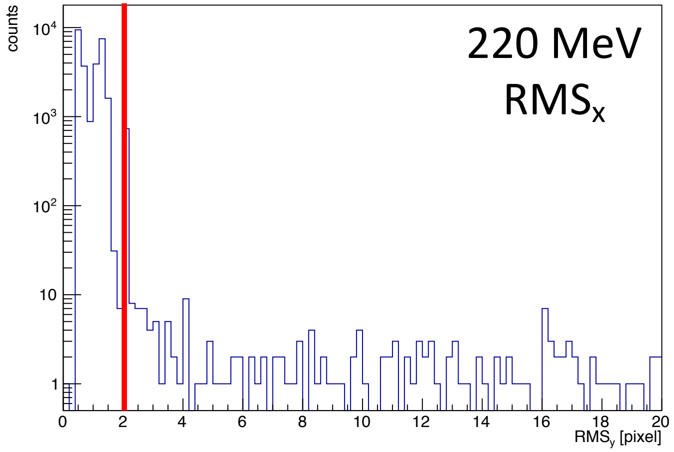

Stacked analysis

Stacking cluster procedure (applied event by event):

- Calculation of mean along x and y
- Subtraction of mean from all the pixel coordinates
- The new coordinates are used to fill a 2D histogram
- The histogram is normalised
- Integral of the histogram gives the average cluster size

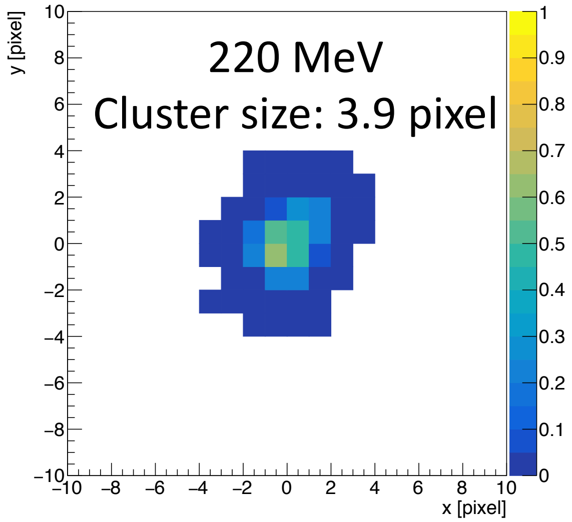

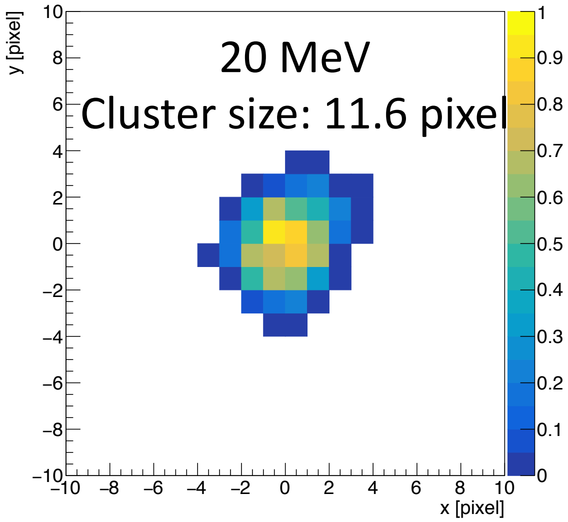

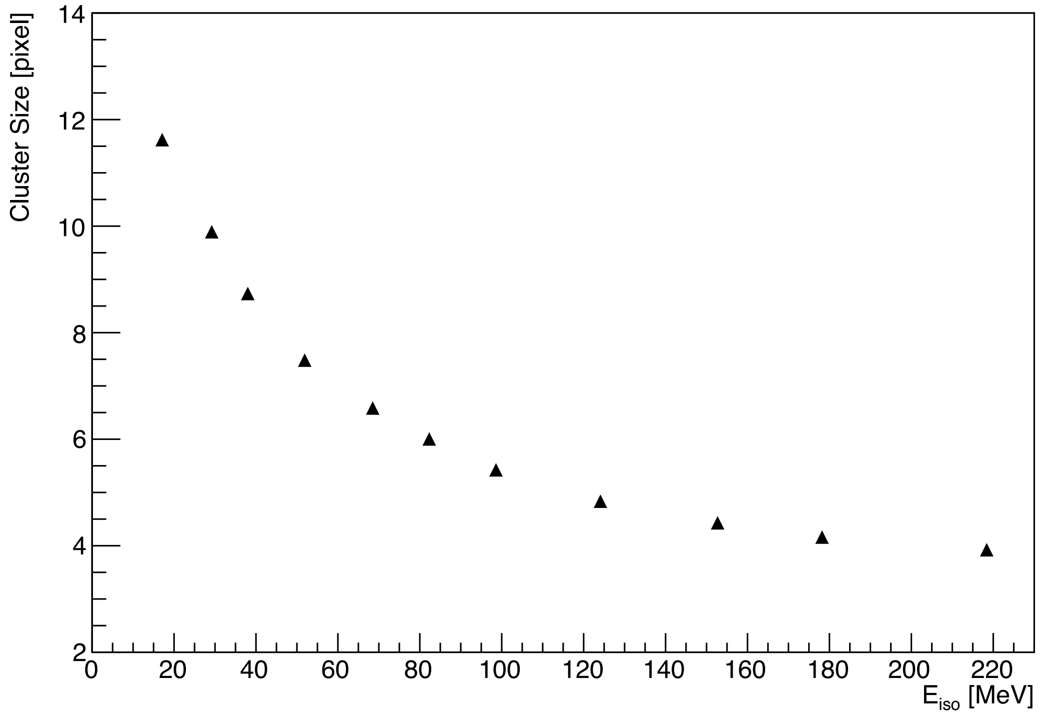

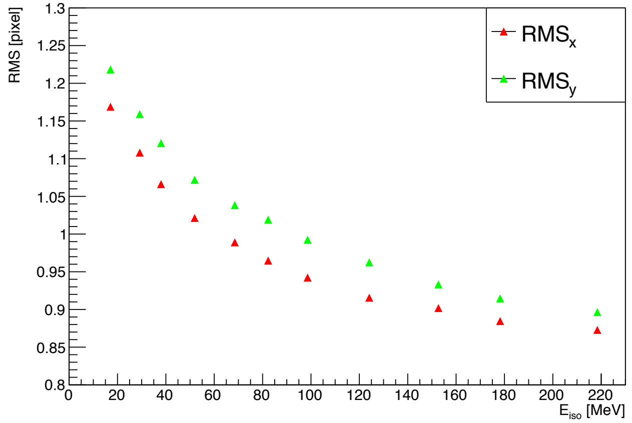

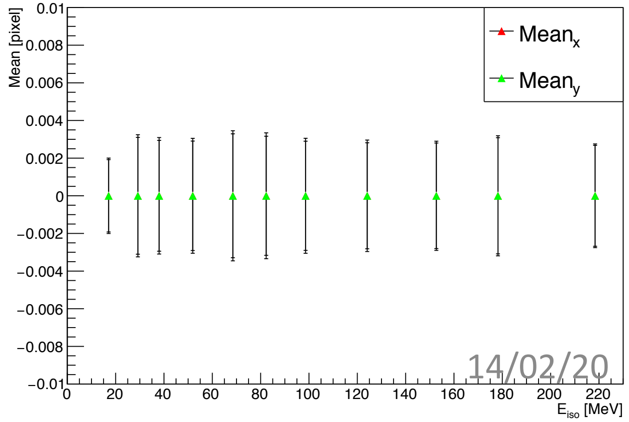

The same procedure has been applied to de data collected with different energies in between.

14/02/20

Study of inclined tracks: stacked analysis

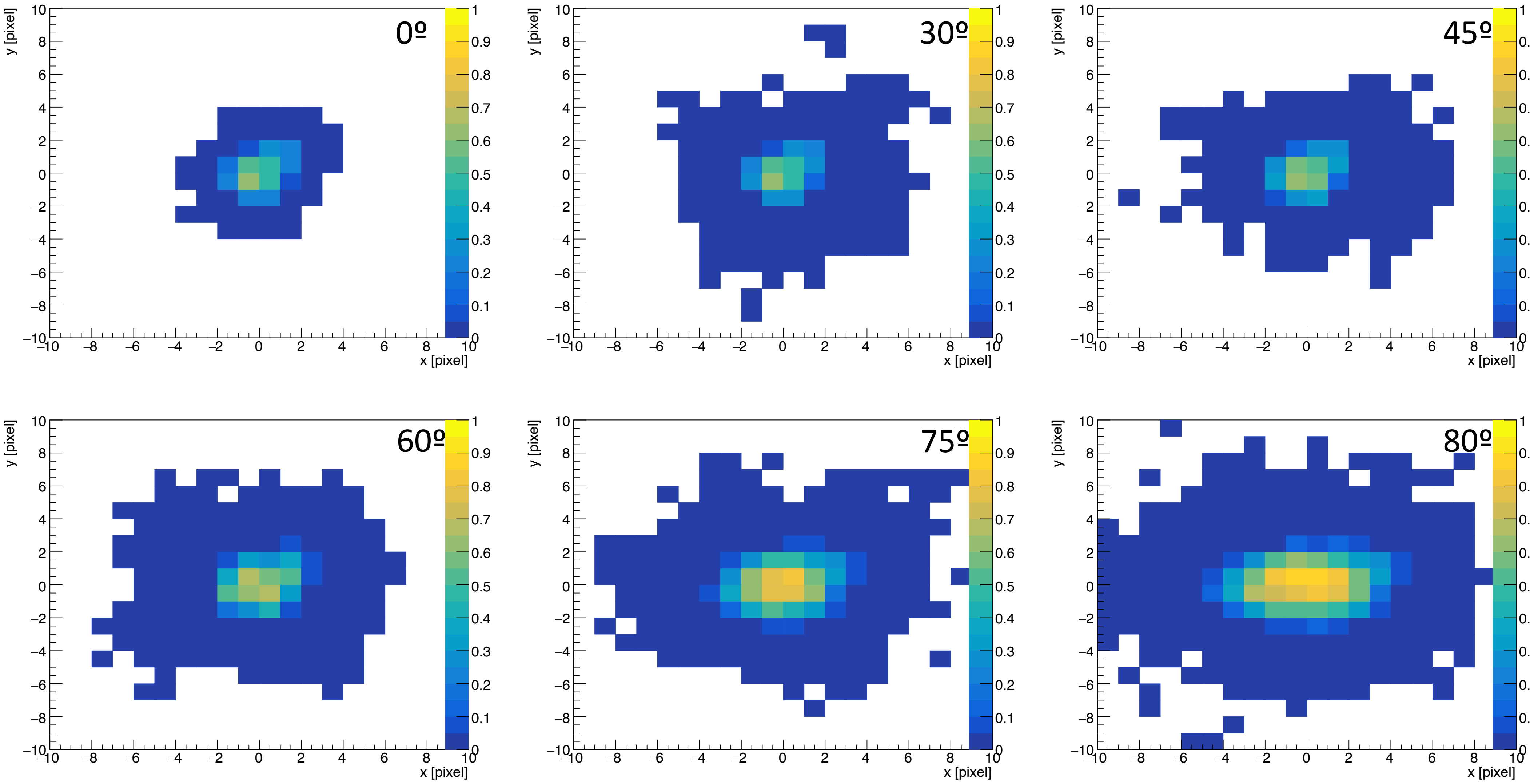

220 MeV protons

Roberto Iuppa

Study of inclined tracks: model

- The model we propose to describe the cluster size evolution is really simple;
- There are **two parameters** to be determined by the fit
- The **IC** parameter quantifies the **intrinsic cluster size** produced by the nucleus on the silicon;
- The **intrinsic cluster size** is **expected to increase with Z,** since the charge produced inside epitaxial layer increases
- The second parameter **T** is the effective **thickness of the epitaxial layer**.
- As shown in the plot, the model perfectly describes the results obtained from GEANT4 simulation of the setup, where diffusion is not included.

$$f(x) = IC \cdot \left(1 + 2 \cdot \sqrt{\frac{\pi}{IC}} \cdot T_{eff} \cdot \tan\theta\right)$$

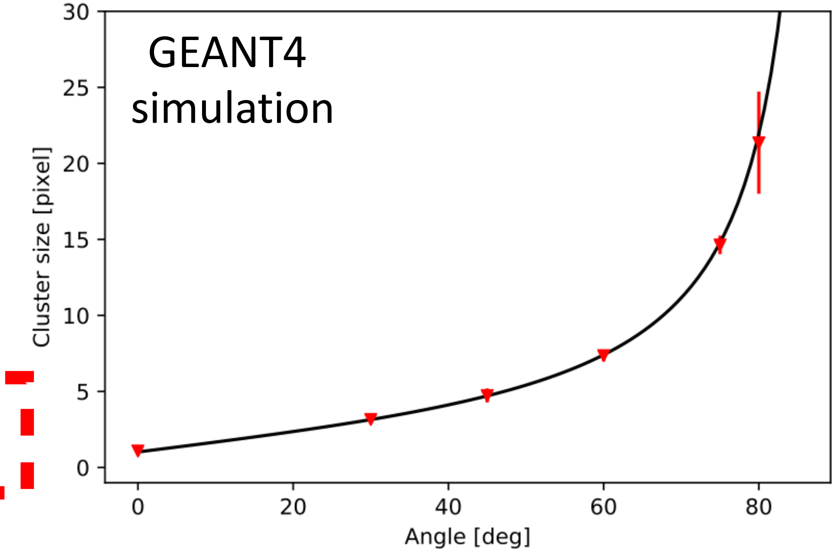

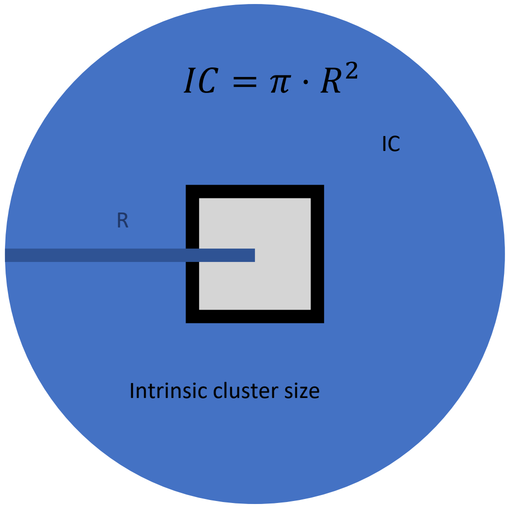

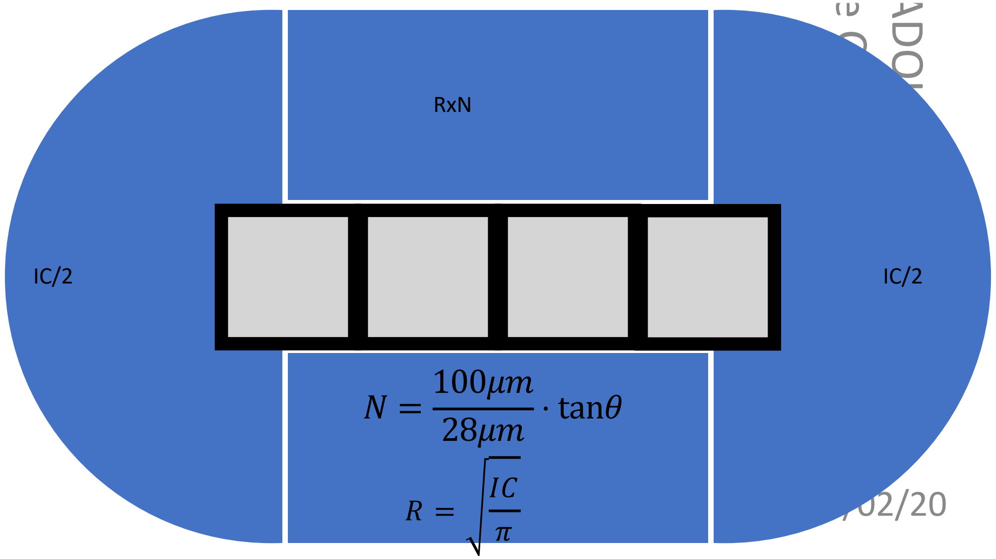

Angle dependence on Z

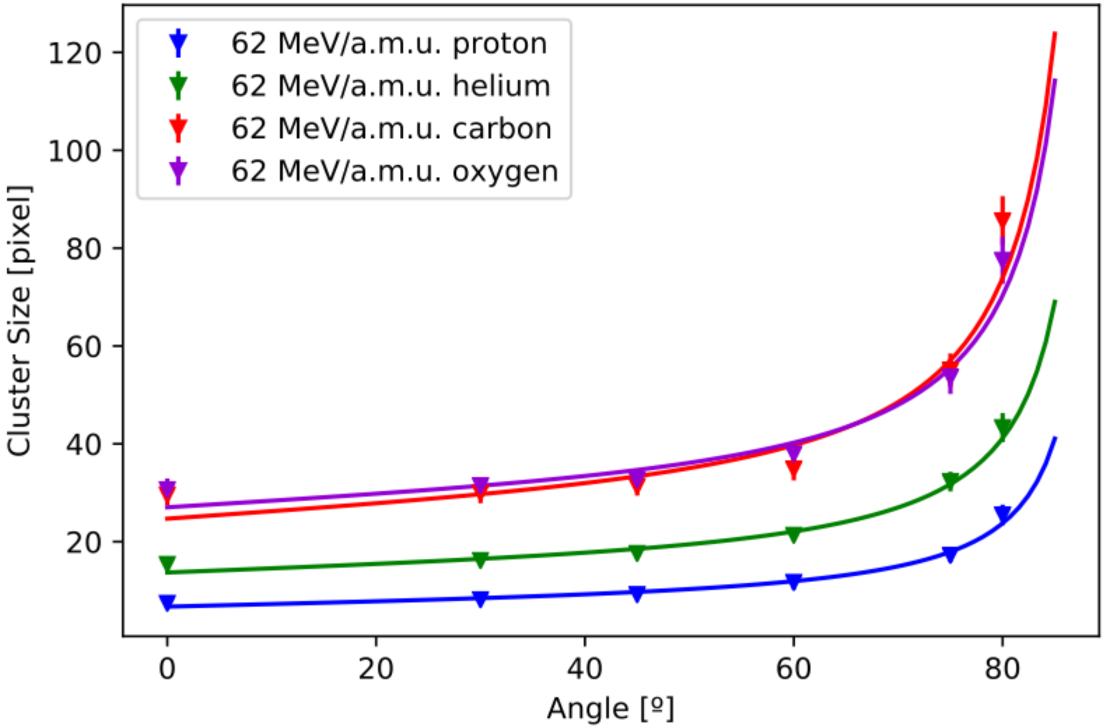

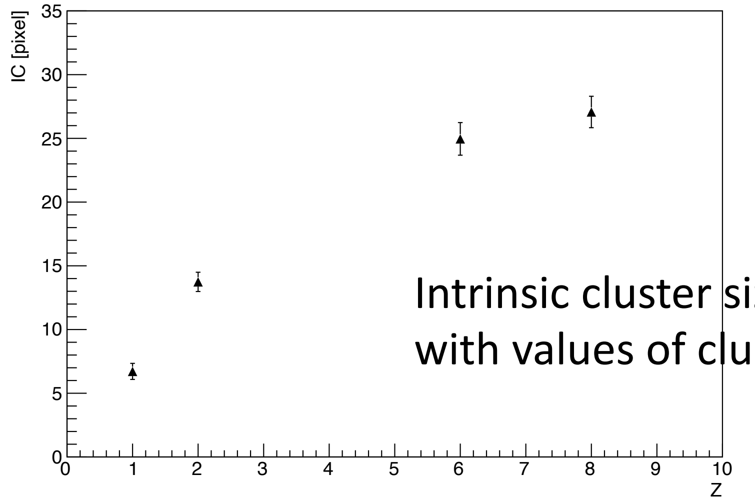

Intrinsic cluster size coherent with values of cluster size at 0º

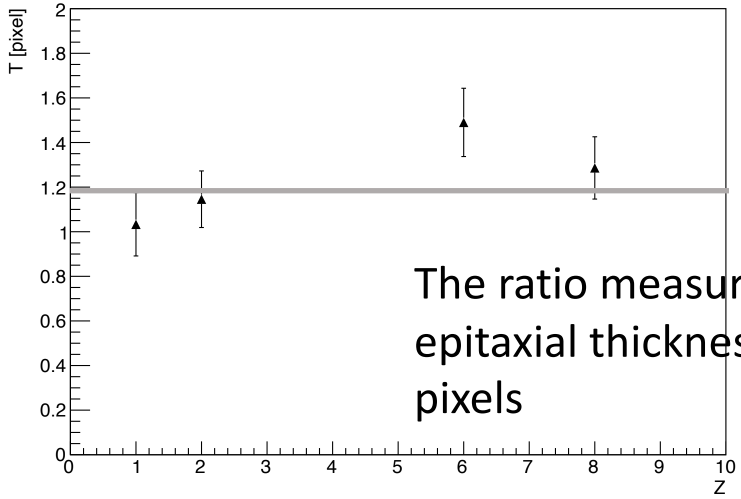

The ratio measured-to–nominal epitaxial thickness is 1.15±0.07 pixels

- 62 MeV/a.m.u. nuclei @ Catania LNS
- Cluster size obtained from **gaussian fit** on the cumulative distributions
- As expected, **cluster size increases with Z.**
- Saturation of intrinsic cluster size for Z ≥6

Angle dependence on other parameters

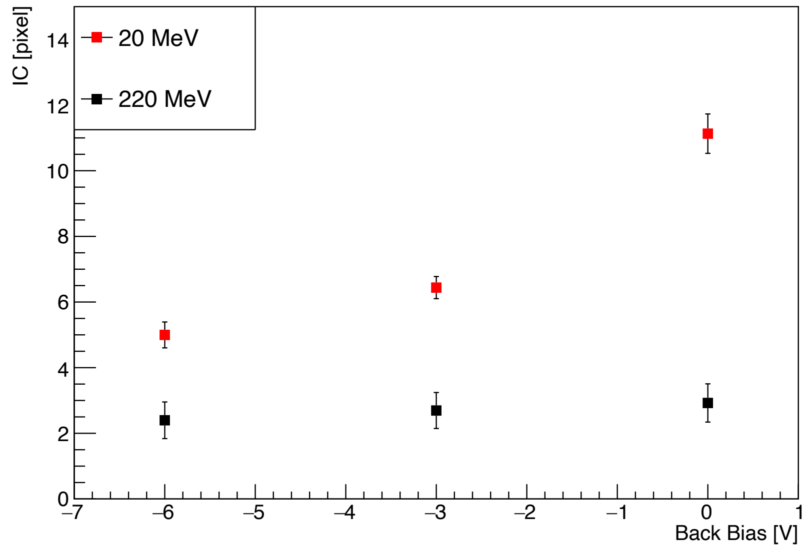

Cluster size effects strongly reduced with the maximum depletion

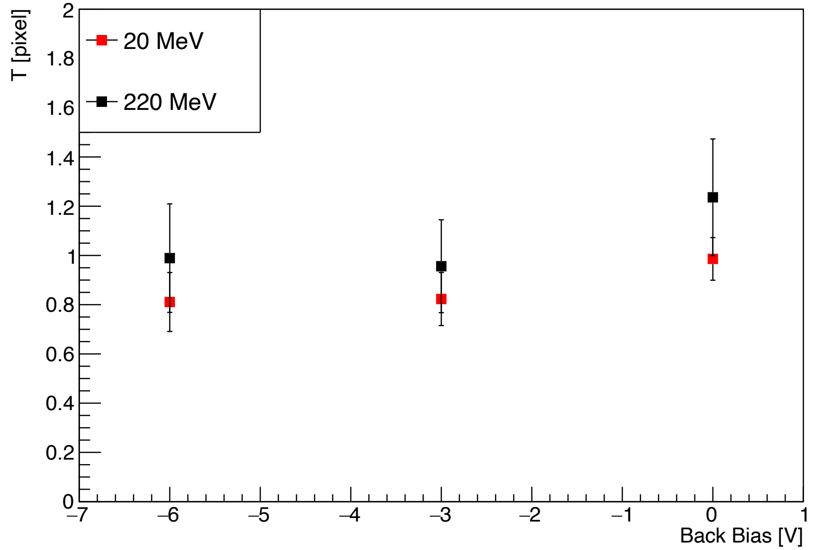

- 20 and 220 MeV protons @ Trento APSS Proton therapy centre, different back bias values
- The results of the best fits give a **epitaxial thickness of about 25 $\pm$ 3 µm**, in agreement with the nominal value, quoted to be between 19 µm and 40 µm (http://inspirehep.net/record/1429449/)
- When the back bias is applied, the charge collection is more efficient and the cluster size decreases.
- The smaller values obtained for the thickness is related to the lower IC

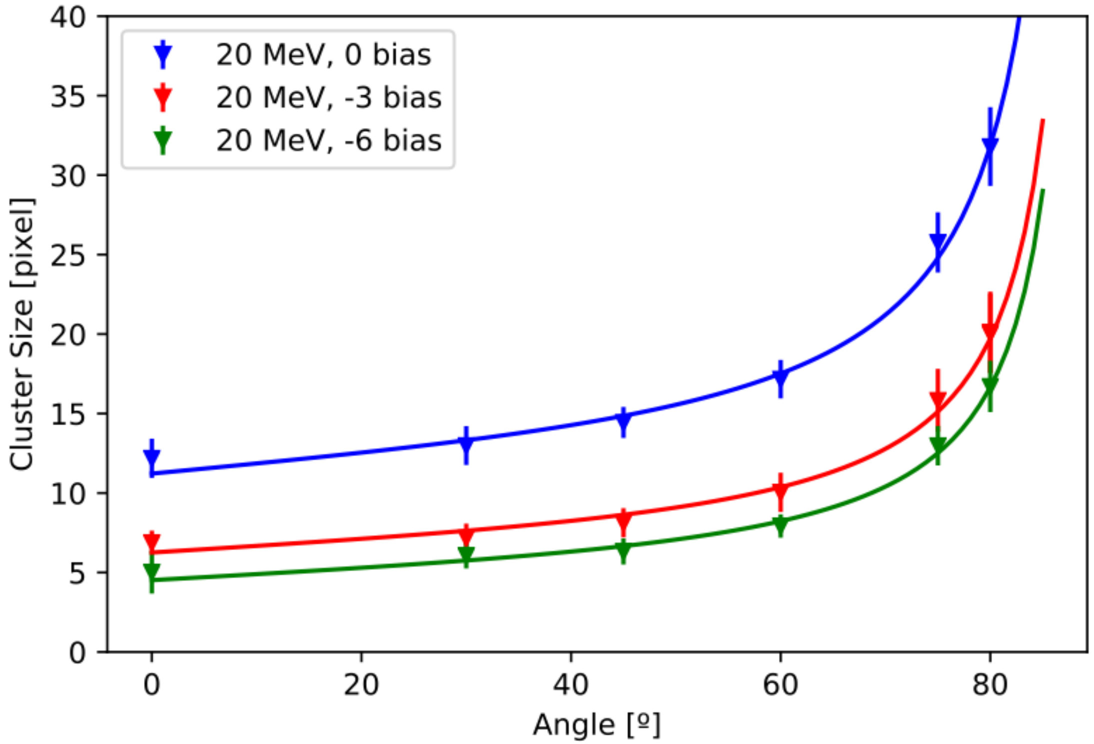

Roberto Iuppa

TCAD simulation

- The TCAD simulation aims to **reproduce** the **cluster size results**.
- Because of the **high computing power required** by the simulation, we use the symmetry of the system to explore larger domains.
- **Heavy Ion model** is used to simulate the energy deposition on silicon
- The charge diffusion is followed for **2 µs** after the charge release
- **Three different domains** are used to explore the effects of particles hitting different pixel positions
- Only **vertical hits** are simulated.
- **Three thicknesses** of epitaxial have been simulated

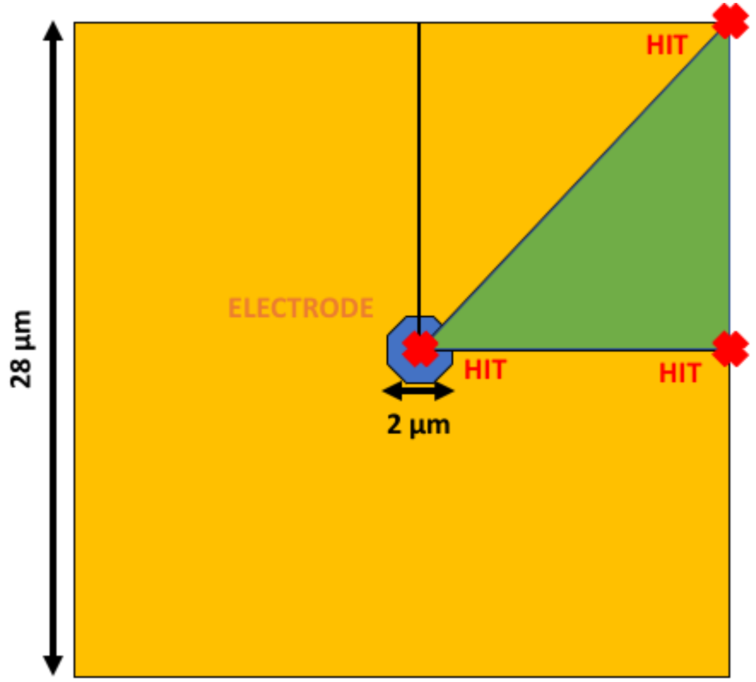

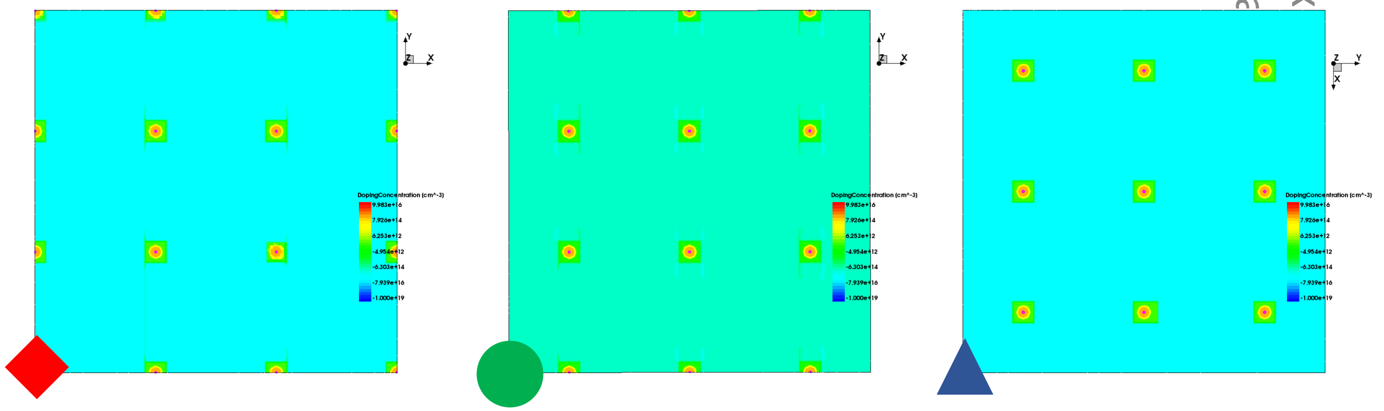

Roberto Iuppa

The LIMADOU Ex the CSES Sa

TCAD simulation: cluster size calculation

- Current on each collection electrode is plot as a function of the time
- Current is integrated to calculate the charge collected
- **Number of electrons is compared with the threshold set on ALPIDE during test beams**
- The number of electrode over threshold after 1 μs from the interaction gives the **cluster size**
- The calculation is extended to the enlarged domain.

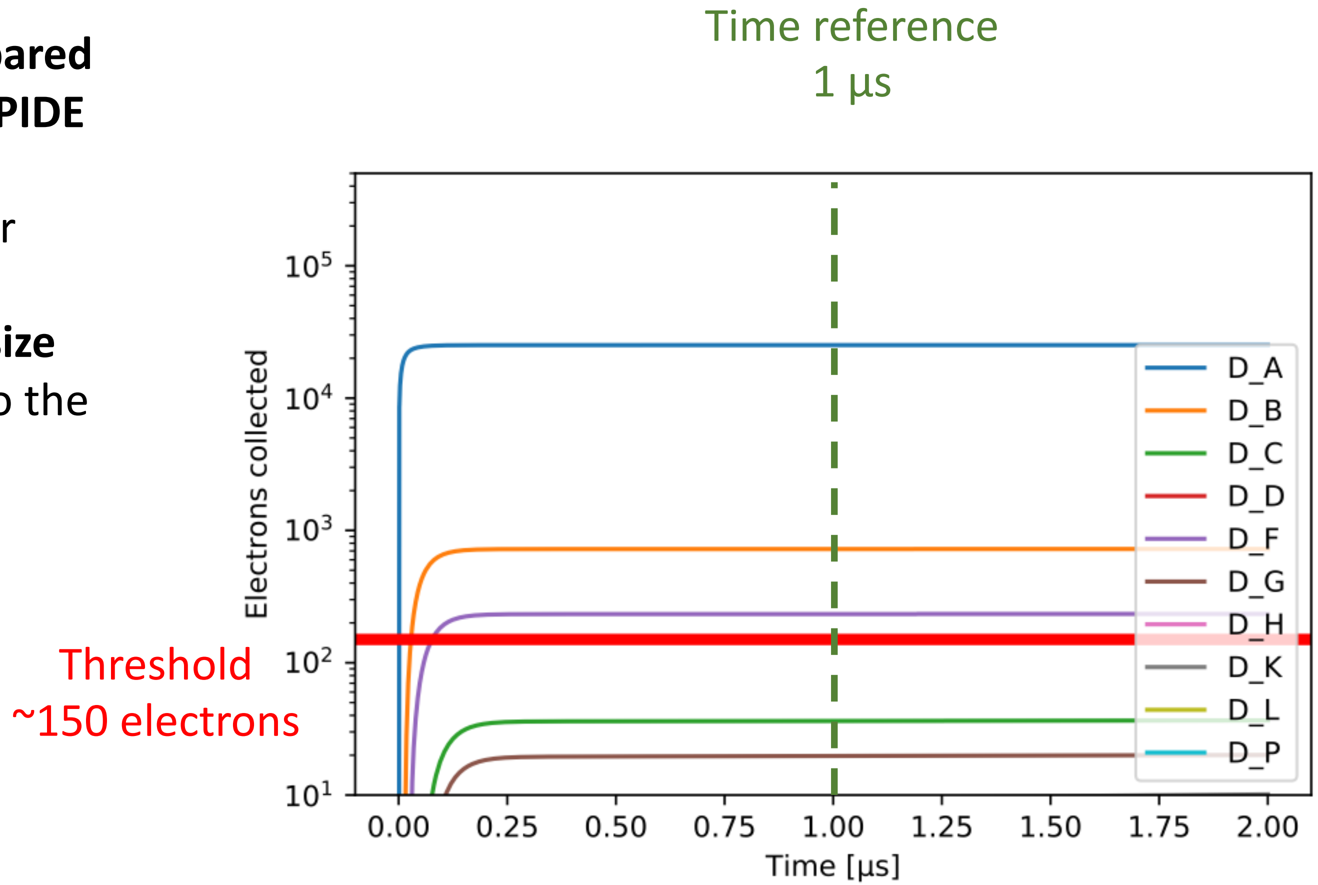

Roberto Iuppa

TCAD simulation: comparison with data

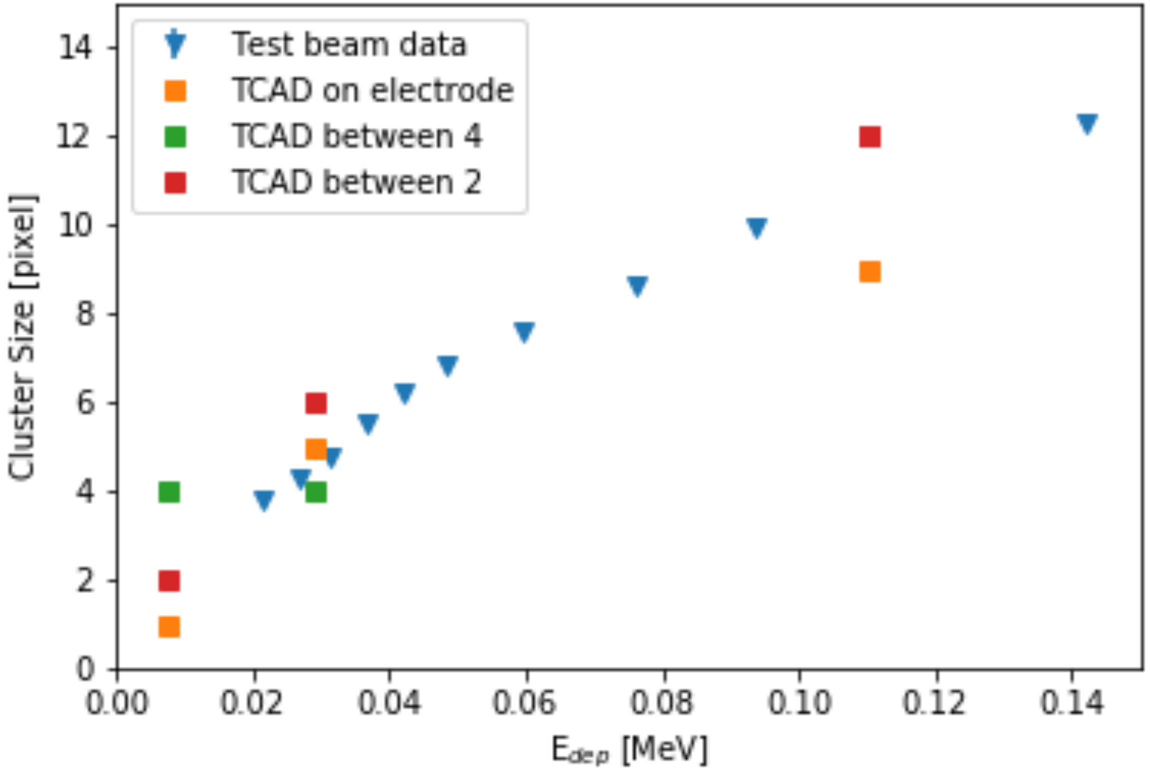

- To compare the **data** from test beam and from TCAD simulation , both are **expressed as a function of the energy deposited in silicon** (from GEANT4 simulation)
- Data are compared with the **25 µm thick simulations**
- The **agreement is good**, since the **simulated points represents the limit cases**, in which the charge collection efficiency is maximum (hit on electrode) and minimum (hit between 4 electrodes).
- Points from simulation embrace those from data along all the explored range.

Roberto Iuppa

Power consumption measurements in Trento

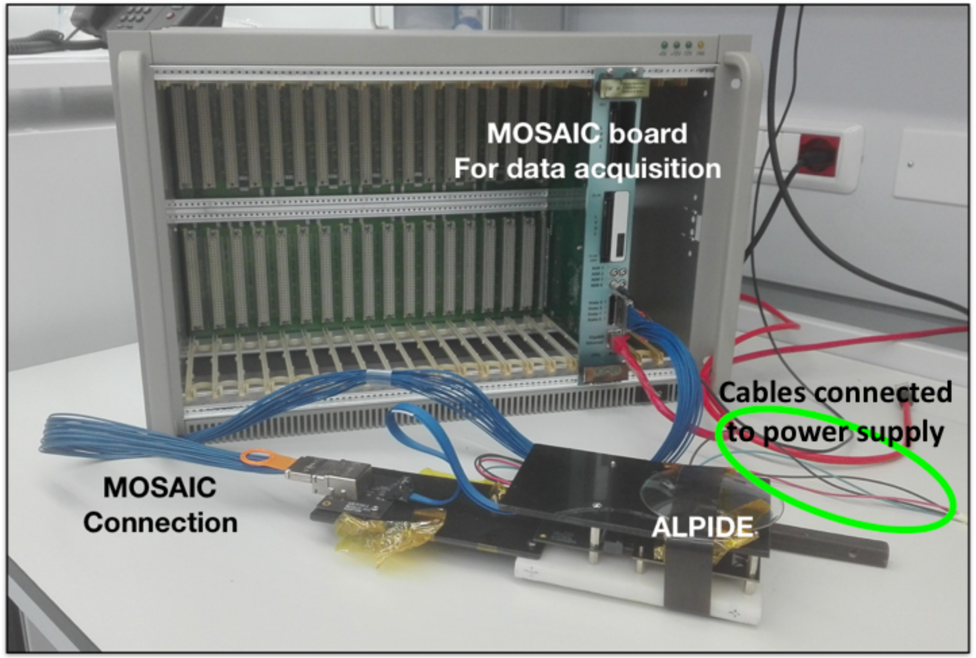

Measurement of transfer function is made sending a sinusoidal wave generated by a waveform generator trough a 1 kΩ resistor. Voltage measured on the resistor is compared to the output of the current probes

Roberto Iuppa

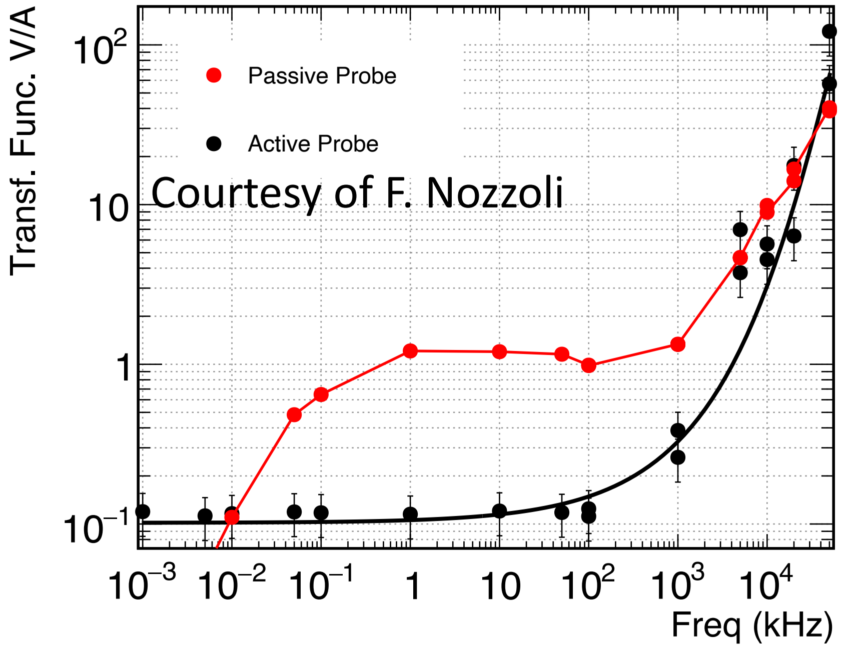

Setup for the measurements:

- **ALPIDE single chip**
- MOSAIC board for the readout
- Power supplier (not shown in picture)
- Passive current probe
- Active current probe
- Laptop (not shown in picture)
- Oscilloscope (not shown in picture)

In collaboration with B. Di Ruzza and F. Nozzoli

Power consumption measurements

Features tested:

- Power consumption during **communications via CTRL line**
- Power consumption during **readout through high speed line**
- Power consumption during **threshold scan**
- Tests are designed by ALICE collaboration to characterise the detectors during ITS assembly

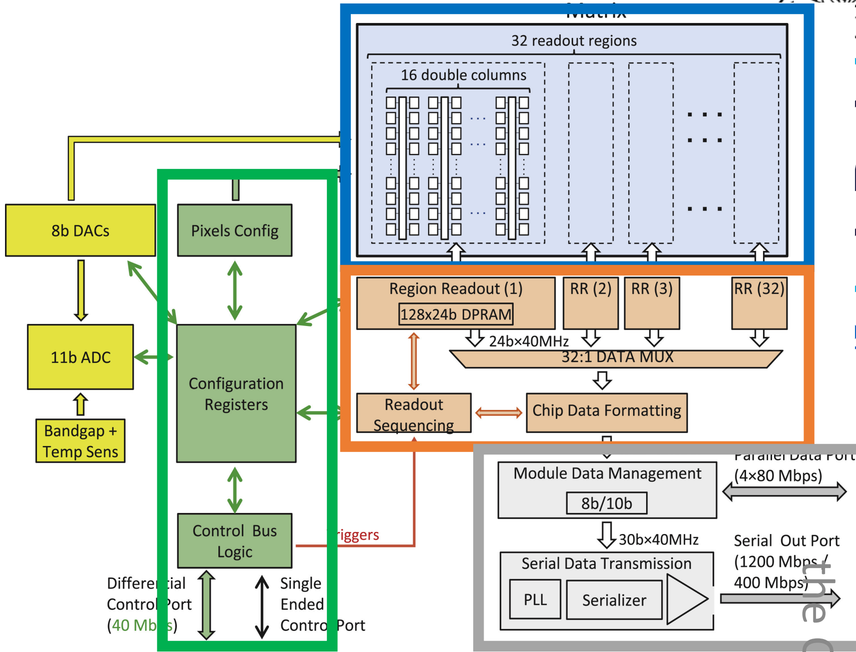

https://doi.org/10.1016/j.nima.2016.05.016

Test	CTRL line status	High speed line status	Analog current [mA]	Digital current [mA]	Power consumption [mW]	Power density [mW/cm²]
FIFO test	**ON**	**OFF**	12	53	125	26
Digital scan	**ON**	**ON**	12	134	240	54
Threshold scan	**ON**	**ON**	12	134	240	54

Power consumption reduction: how to?

Power consumption have to be reduced to fit requirements of the HEPD-02 payload.
From power consumption characterisation, **the high speed line is the most consuming element of the detector**.

The first solution is to **move the readout to the CTRL line**.
It avoids to activate the PLL block and allows to reduce the clock frequency.

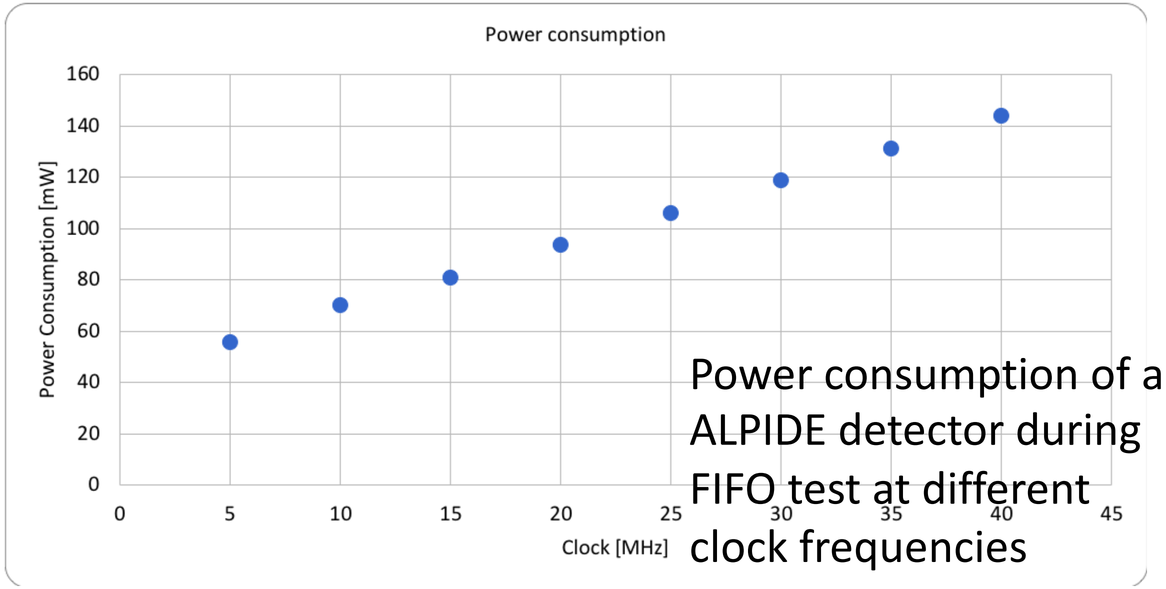

Power consumption of a ALPIDE detector during FIFO test at different clock frequencies

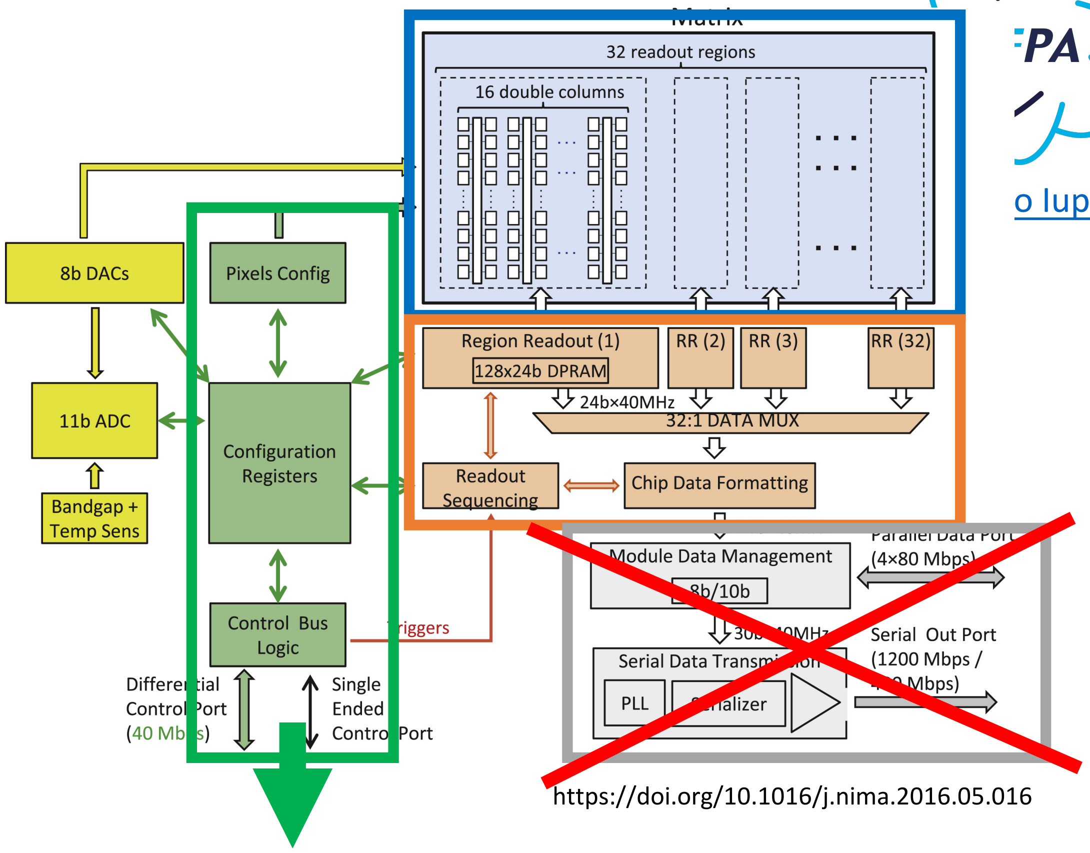

https://doi.org/10.1016/j.nima.2016.05.016

ALPIDE control and data readout

Power consumption reduction: clock-on-demand

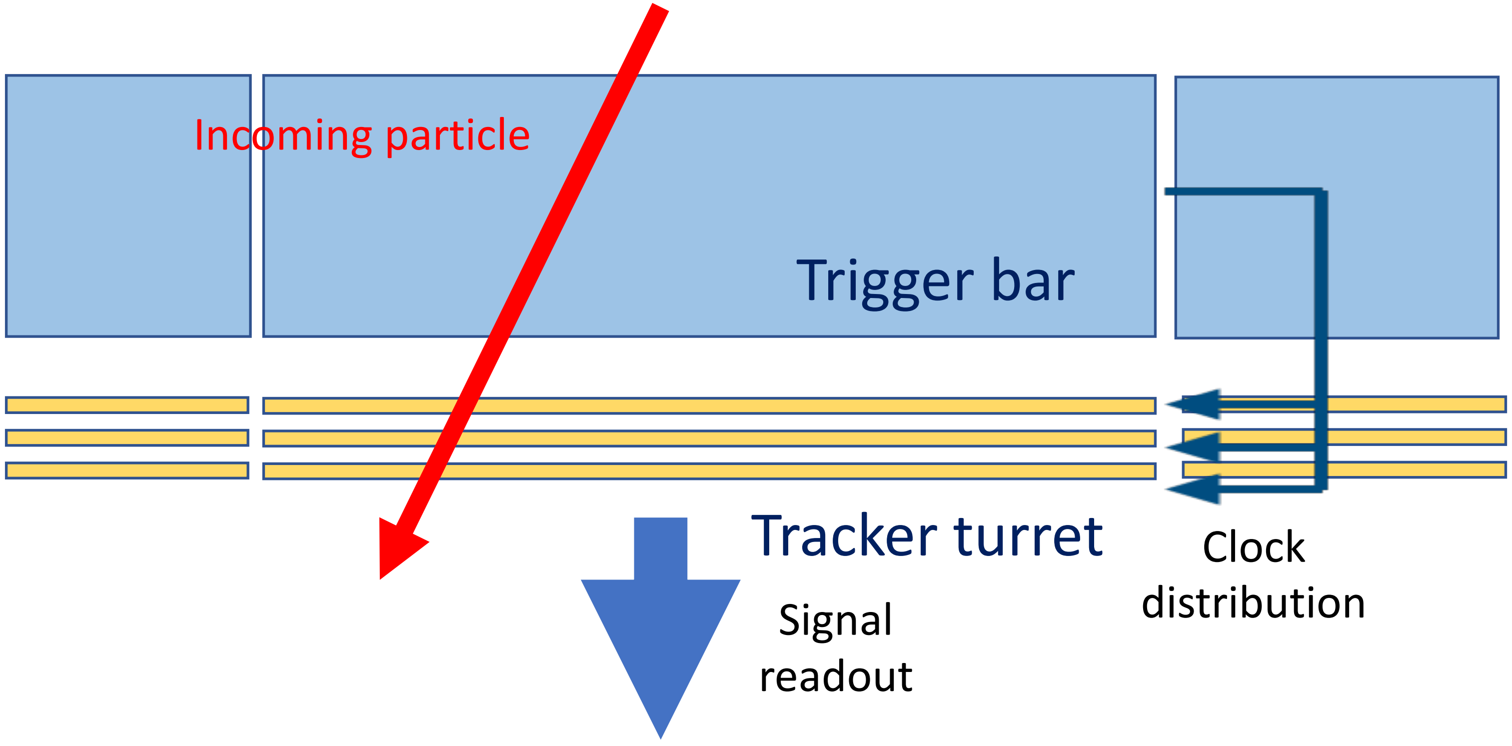

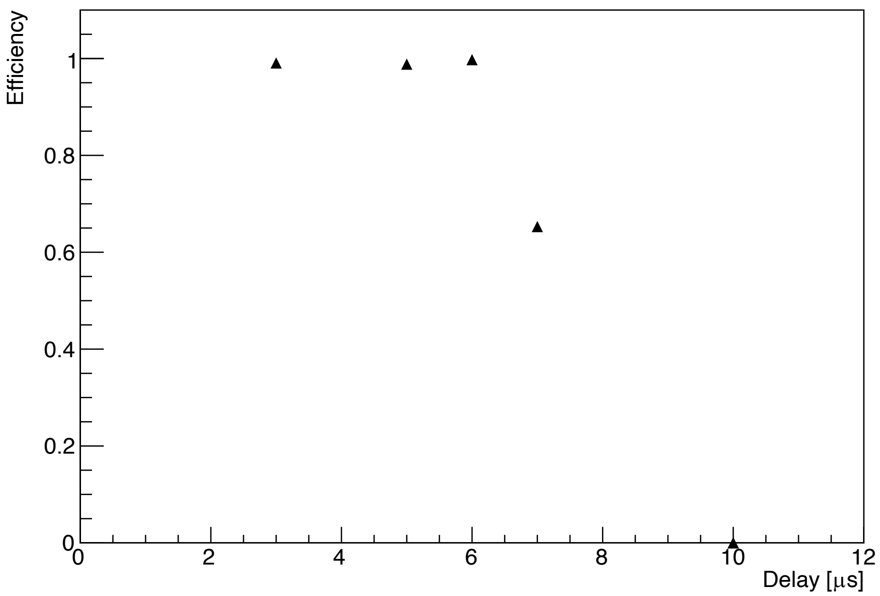

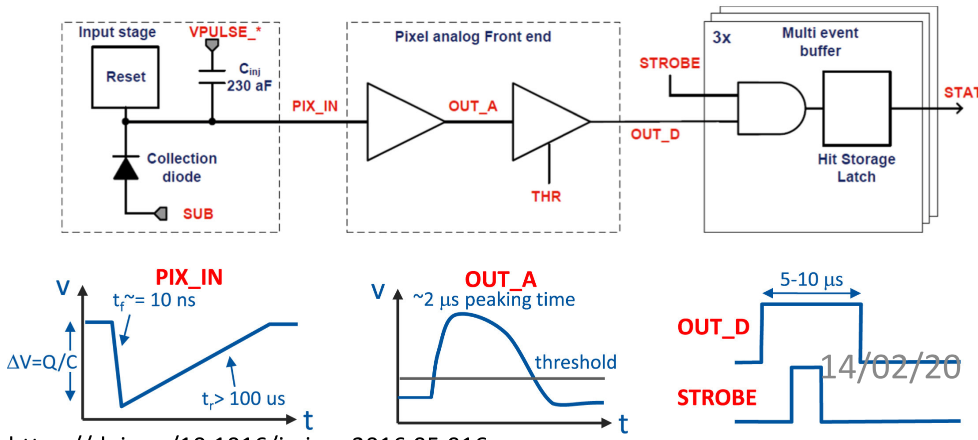

https://doi.org/10.1016/j.nima.2016.05.016

- Analog front-end is kept constantly powered on
- The digital part is needed only for the readout of the data
- The clock is distributed only after the trigger signal is produced
- The smart segmentation of trigger allows to distribute the clock only to the section of tracker involved on the event

Power consumption reduction: clock-on-demand

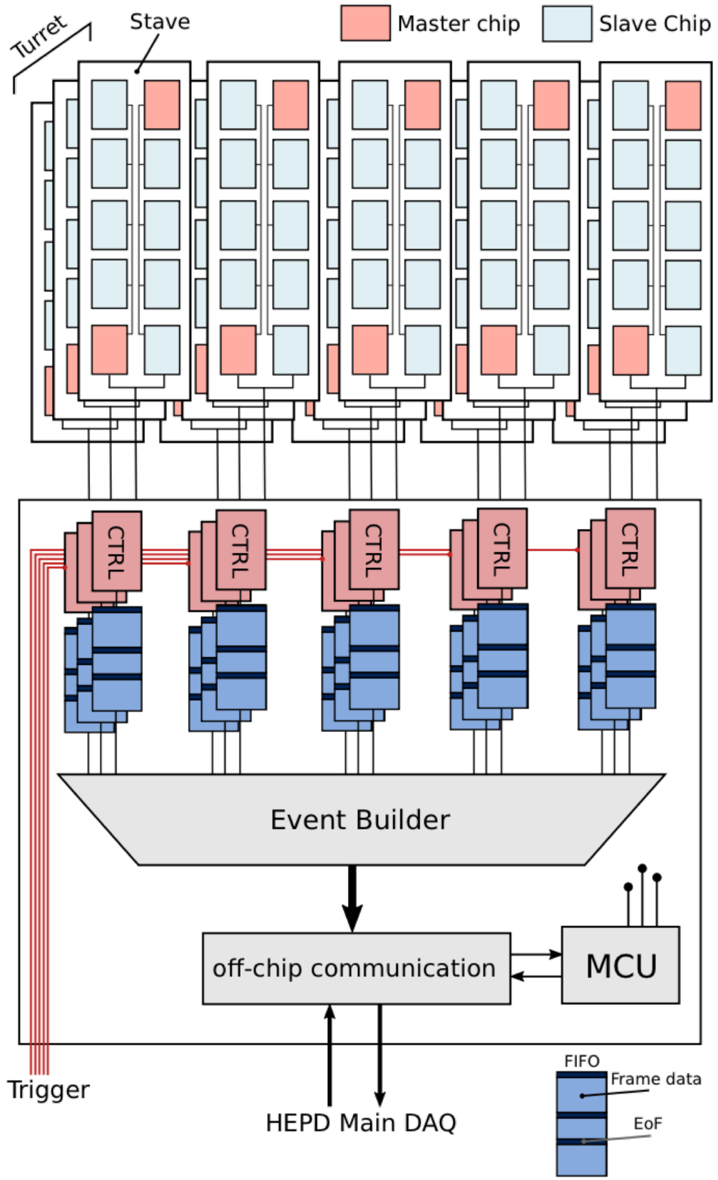

Turrets are kept in a low power state until their operation is needed.

- Clock signal is provided to a turret only when a trigger is received.
- Triggered turret is read in parallel and then unclocked immediately after.

→ ~50% reduction in power consumption.

Roberto Iuppa

Full tracker power consumption

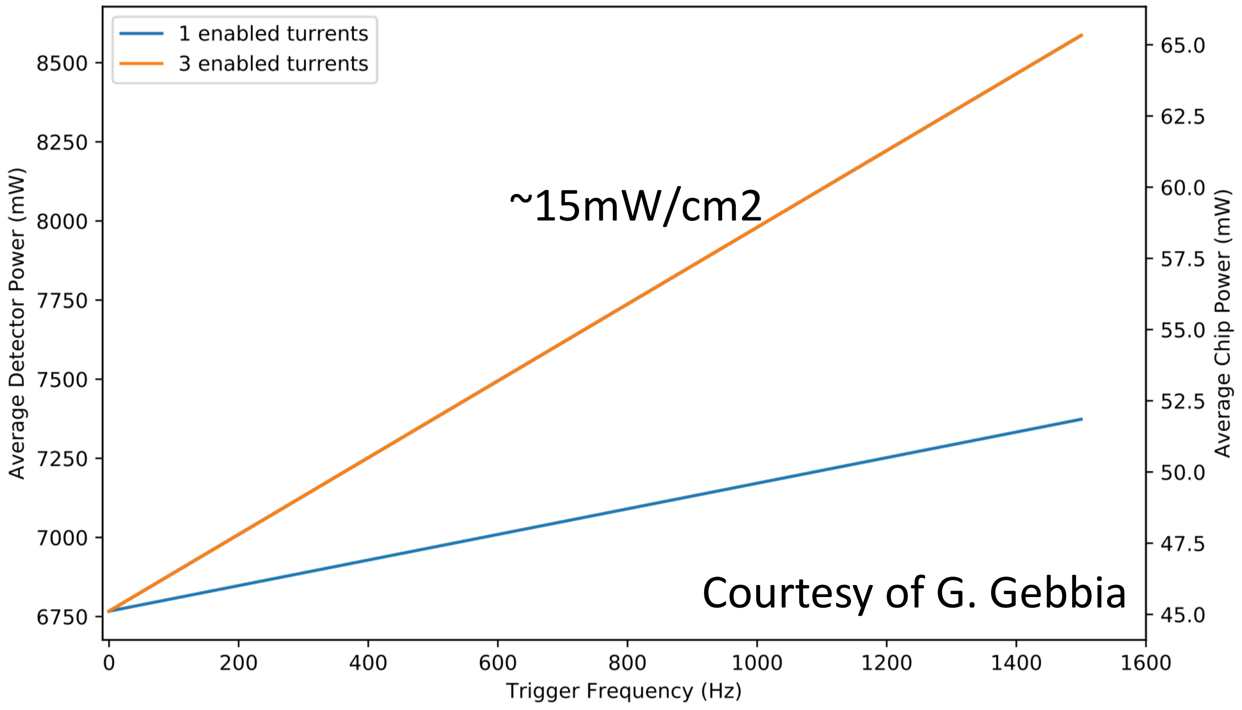

- Power consumption is plot as a function of trigger rate
- To increase the probability to intercept the section of the tracker hit by the particle, three turrets are read out
- Power consumption of the full tracker in this configuration is well below the 10 W of HEPD-01 tracker
- The maximum trigger rate will be defined by the dead time required for the readout.

Roberto Iuppa

Cold plate stratigraphy choice: thermal simulation

Proposed Stratigraphy

HIC support layer:

Material/Sub-Laminate	Thickness (mm)	Orientation (Deg)	Layers
Fleece	0.02		1
K13D2U_EX1515_67-...	0.120	90	1
K13D2U_EX1515_67-...	0.120	0	1
K13D2U_EX1515_67-...	0.120	90	1
Fleece	0.02		1

Lateral ribs:

Material/Sub-Laminate	Thickness (mm)	Orientation (Deg)	Layers
Fleece	0.02		1
K13D2U_EX1515_67-...	0.120	0	~15
Fleece	0.02		1

LOAD CASE: conservative approach. Better results expected if conductivity is higher. Waiting for results of tests on prototypes

- Single Thermal Interface;
- Laminate with Standard Conductivity (HC) CF: K = 200/200/0.5W/(mK)
- End-Block Joints with Silver-Epoxi Adhesive.

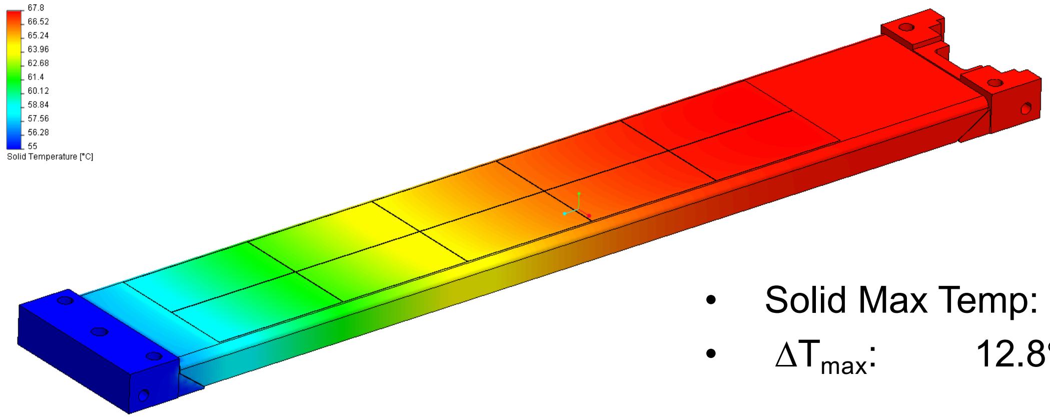

- Solid Max Temp: 67.8°C;
- ΔT_{max}: 12.8°C.

- Double Thermal Interface;

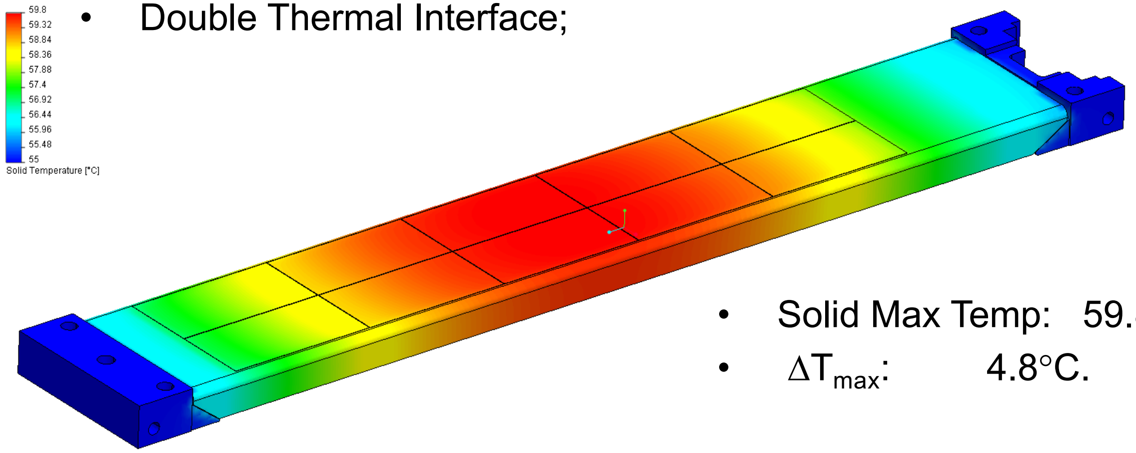

- Solid Max Temp: 59.8°C;
- ΔT_{max}: 4.8°C.

Roberto Iuppa

HEPD-02 tracker

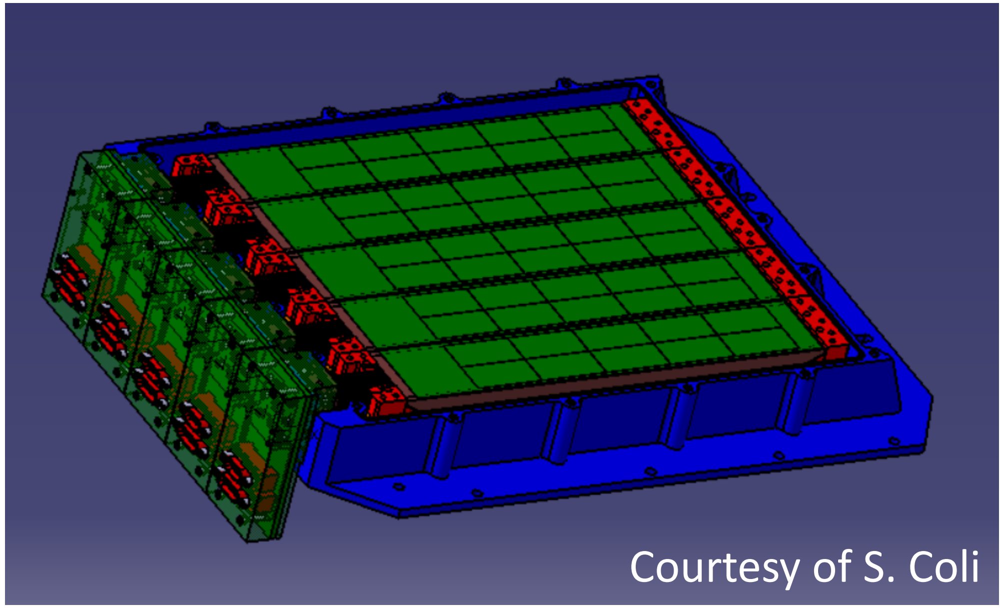

HEPD-02 tracker is **divided in five turrets**.
Each turret is independently connected to the support structure.
The **turret contains three planes of sensitive elements**, called staves.
Stave design has been developed from the ALICE OB stave.

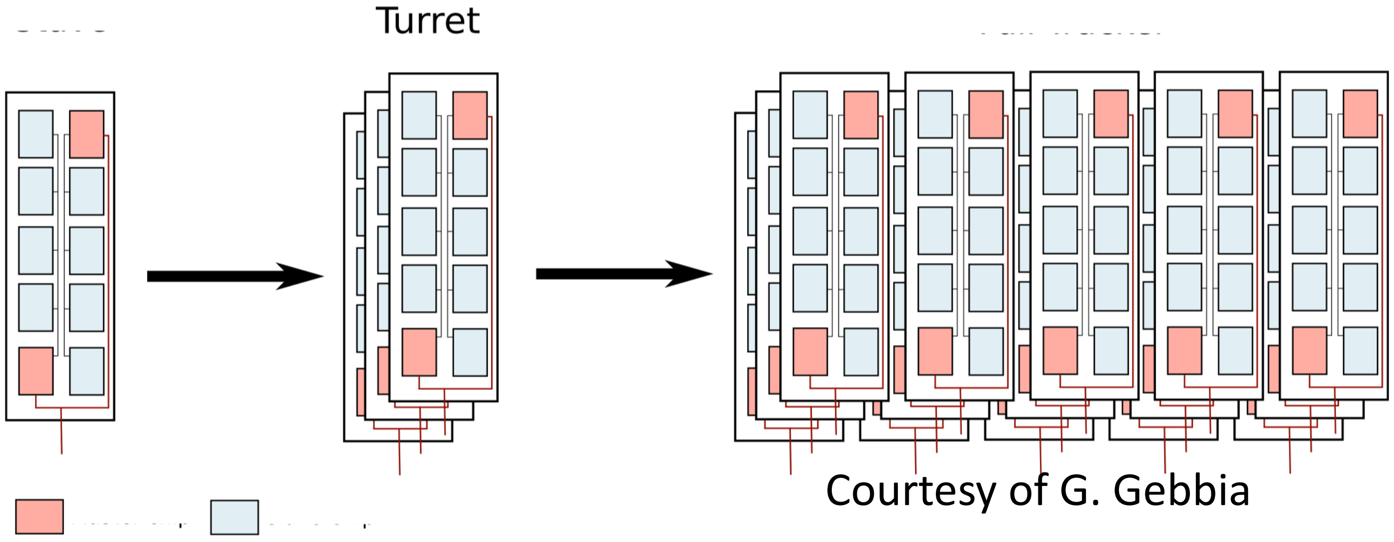

Courtesy of G. Gebbia

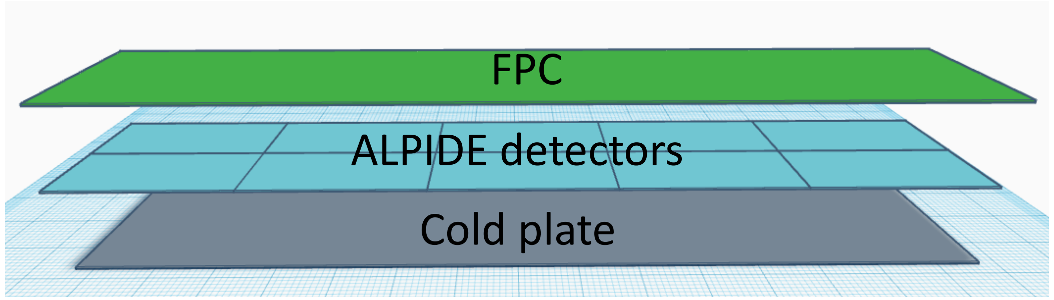

Main features of the stave:

- Two columns of ALPIDE detectors
- One master and four slave chips for each stave
- FPC (different designs proposed)
- Cold plate for thermalisation in carbon fibre

Roberto Iuppa

HEPD-02 tracker

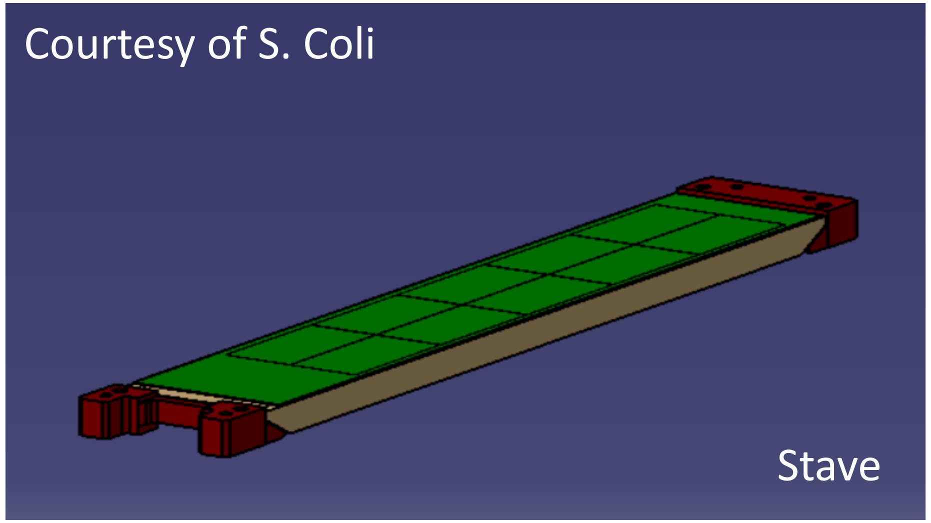

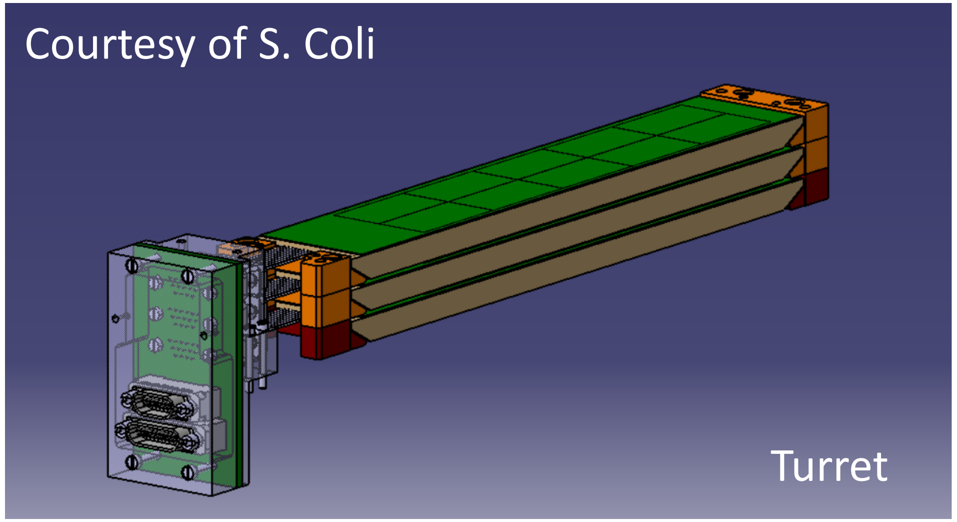

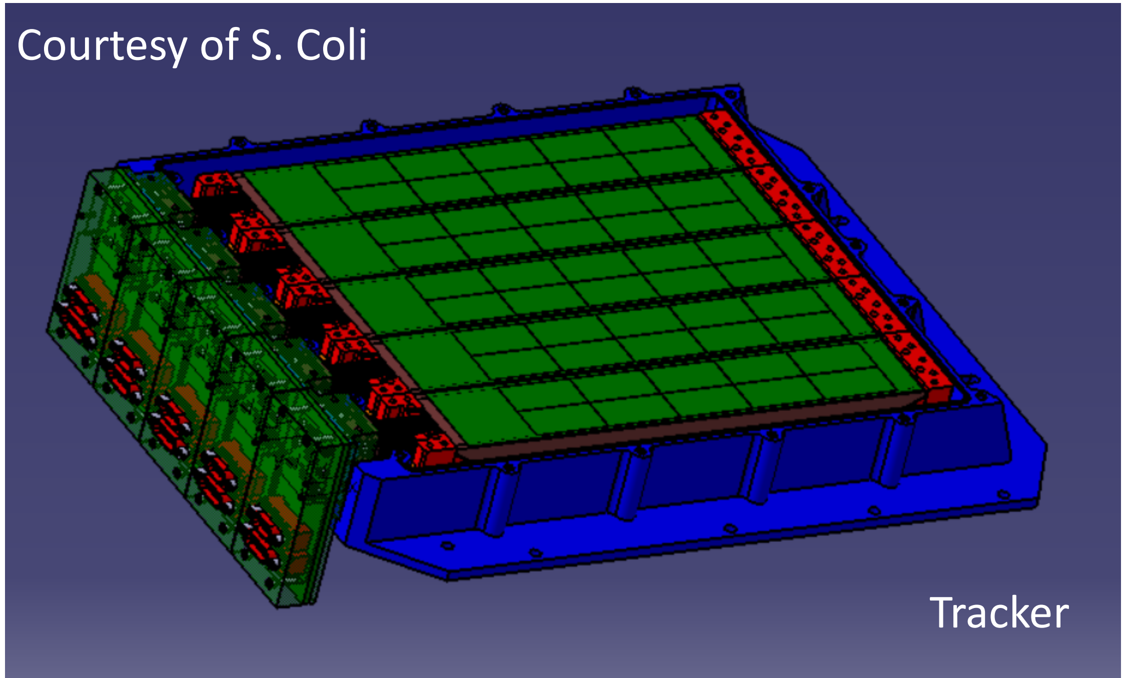

Roberto Iuppa

Stave stratigraphy

Stave element	Material	Thickness [µm]	X_0 [%]
Glue	Araldite	130	0.029
ALPIDE	Si	50	0.053
FPC lines	**Cu**	**36**	**0.251**
FPC	Kapton	135	0.048
Cold plate	Carbon fibre	350	0.134
TOTAL			0.515

Stave element	Material	Thickness [µm]	X_0 [%]
Glue	Araldite	130	0.029
ALPIDE	Si	50	0.053
FPC lines	**Al**	**50**	**0.056**
FPC	Kapton	115	0.040
Cold plate	Carbon fibre	350	0.134
TOTAL			0.312

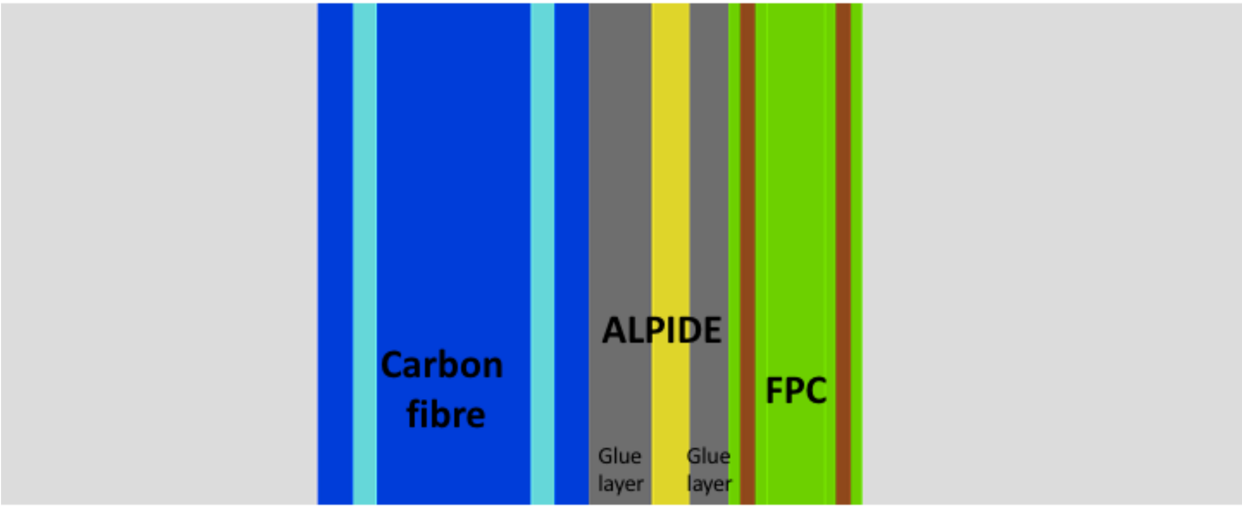

The simulation includes the satellite **window** and **thermal blanket** and **three staves.**

Stave structure:

- FPC (Composed of Kapton and metal lines)
- ALPIDE
- Cold plate

Tables compare the effects of ALICE OB FPC and ALICE IB FPC on X_0

Both the configurations have been simulated to evaluate **thresholds for protons and electrons and multiple scattering for electrons**.

Performance: thresholds

2 planes of tracker

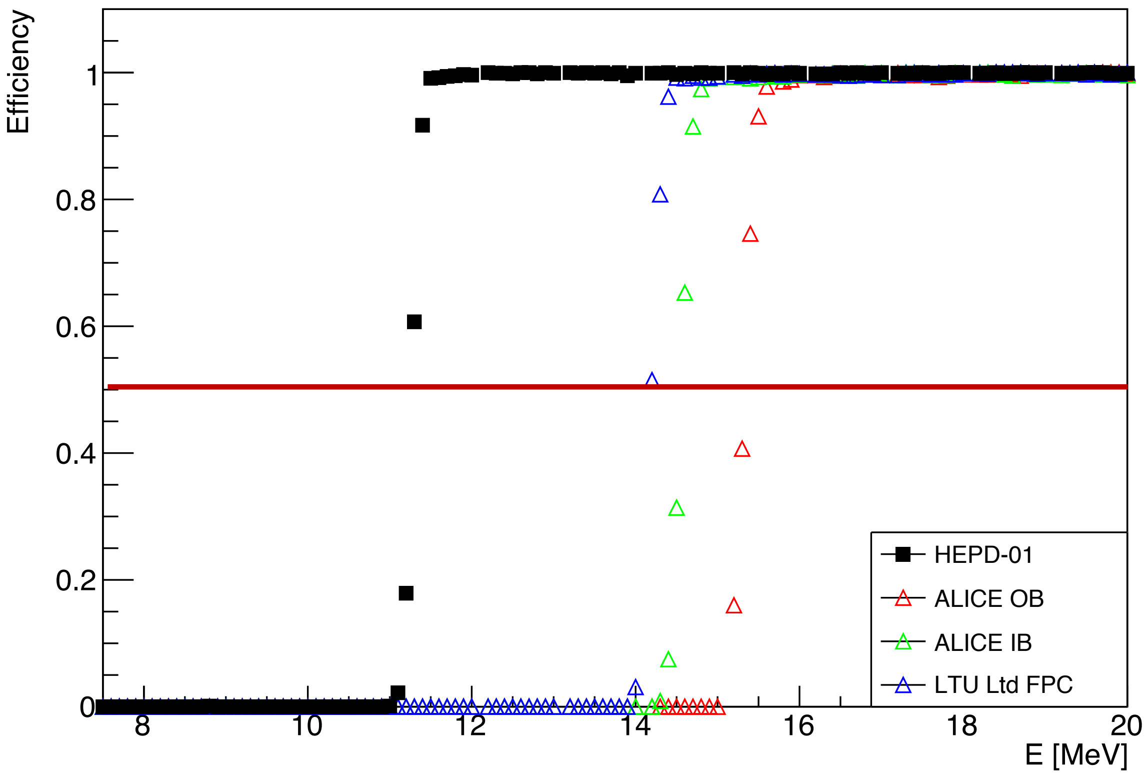

Protons

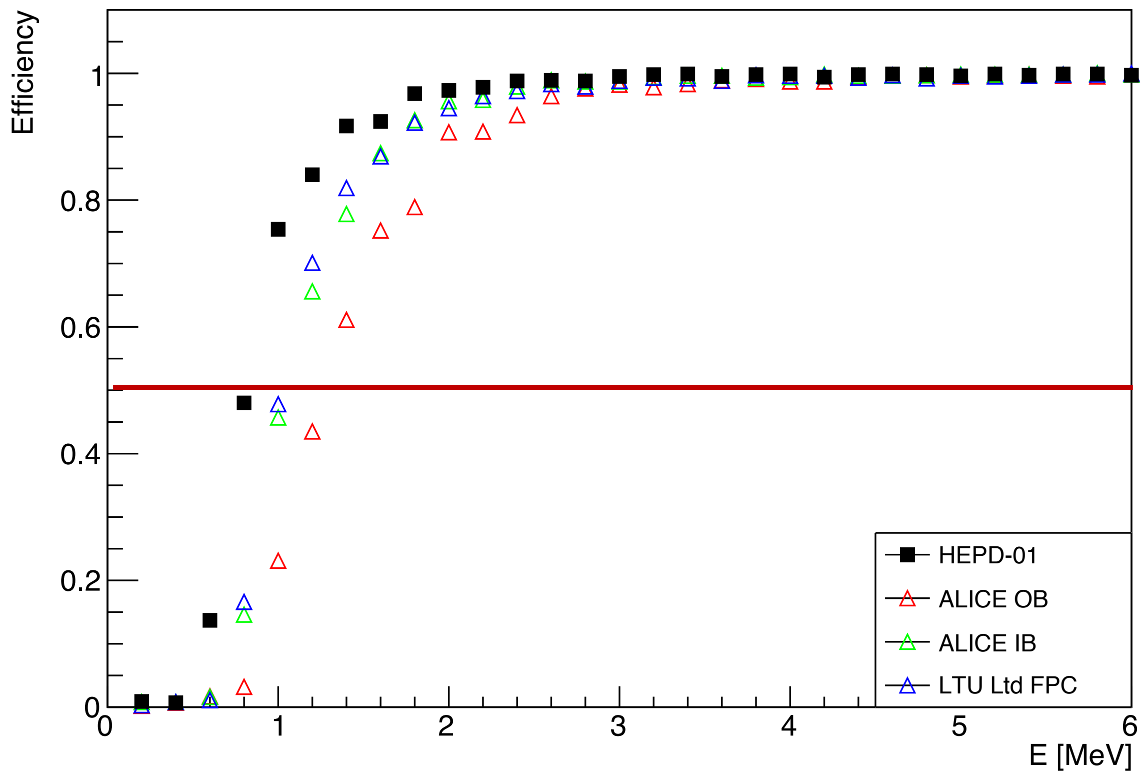

Electrons

Stave stratigraphy:

- 50 µm ALPIDE
- 350 µm Carbon Fibre
- FPC according previous tables

Space compliance tests: Vibration tests

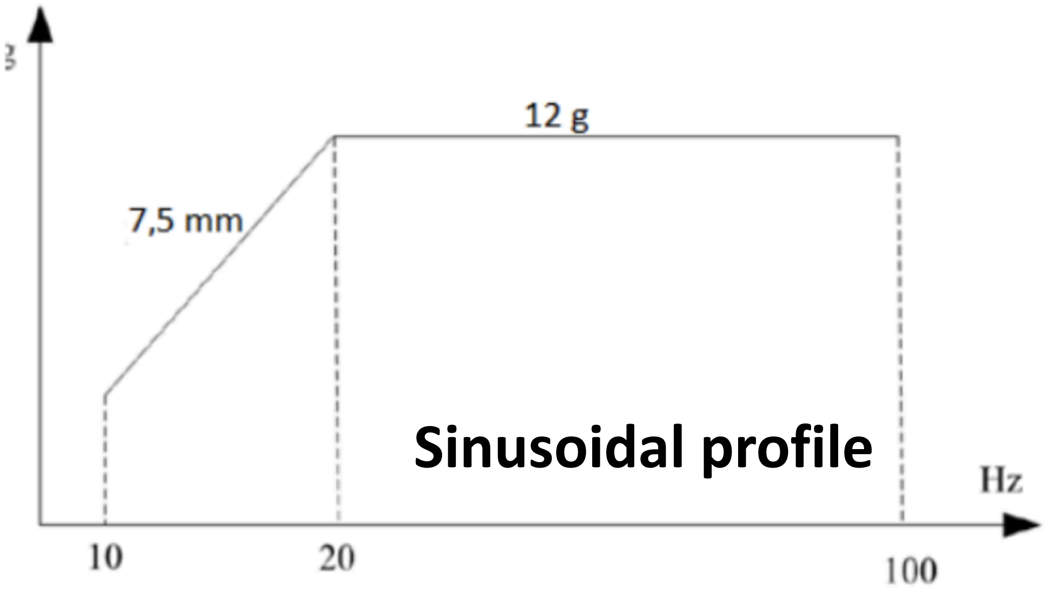

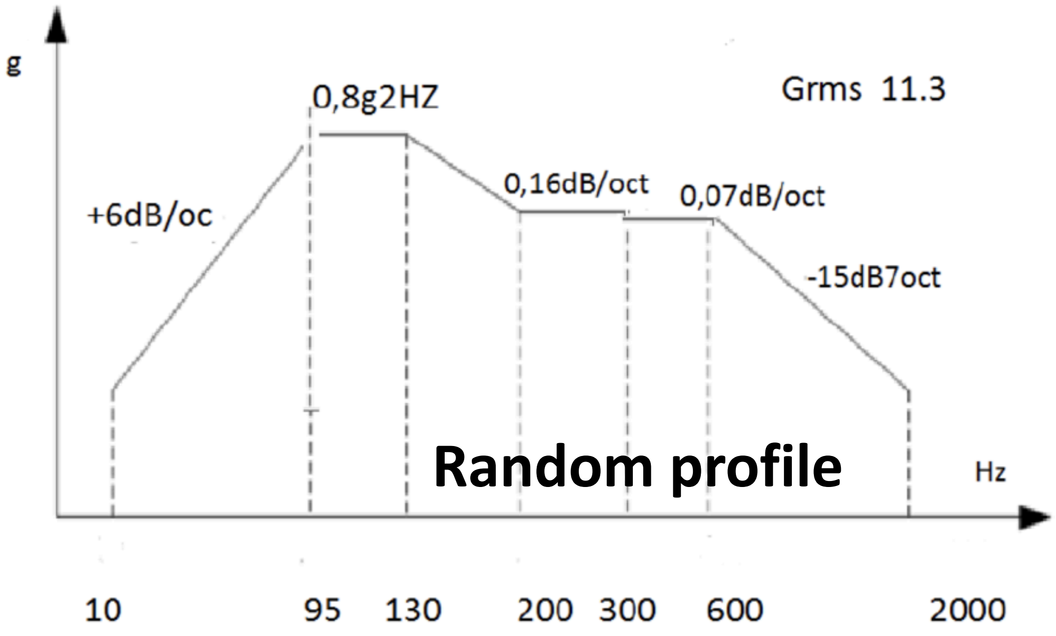

- Vibration profiles given by Chinese Space Agency and is intended to simulate the vibration profile of the launch
- Test has been carried out at SERMS s.r.l. in Terni, Italy
- The stress must be applied on the three axes of the DUT
- Accelerometers are located on the DUT and on the fixture that ensure it to the machine.
- **Test has been successfully carried out along all the three axes of the DUT**

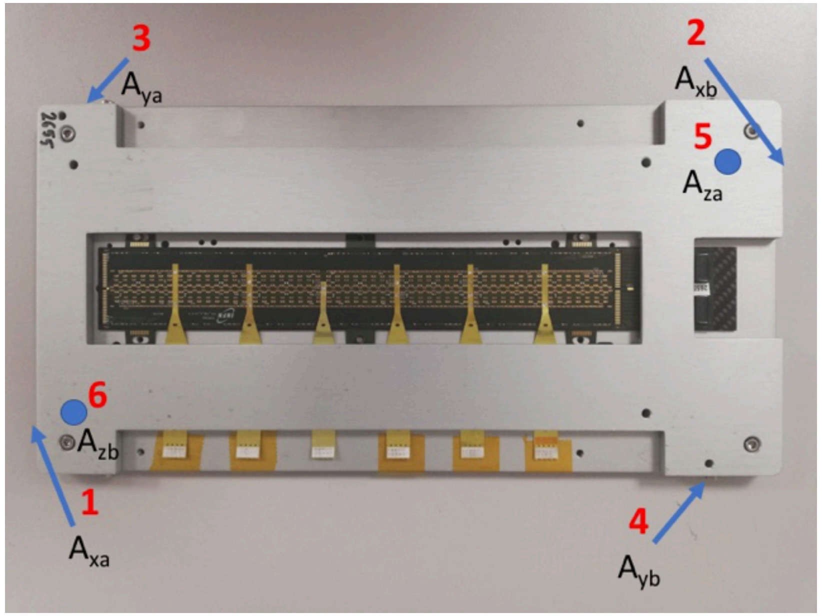

Roberto Iuppa

Space compliance tests: thermal-vacuum test

- Thermo-vacuum cycles simulate the conditions after the launch
- Parameters of the test are reported on the table
- The dwell time has been reduced to two hours because of the small dimensions of DUT
- During the cycles, different stress levels have been applied to the DUT
- Performances have been monitored at low and high temperatures
- **Test has been successfully carried out. The DUT performance was stable during and after the thermal cycles.**

Parameter	Test conditions
Pressure [Pa]	$<6.66x10^{-3}$
Hot temperature [ºC]	+50
Cold temperature [ºC]	-30
Start cycle	Hot (for outgassing)
Number of cycles	6,5
Temperature rate of change [ºC/min]	≥1
Dwell time [hr]	≥4

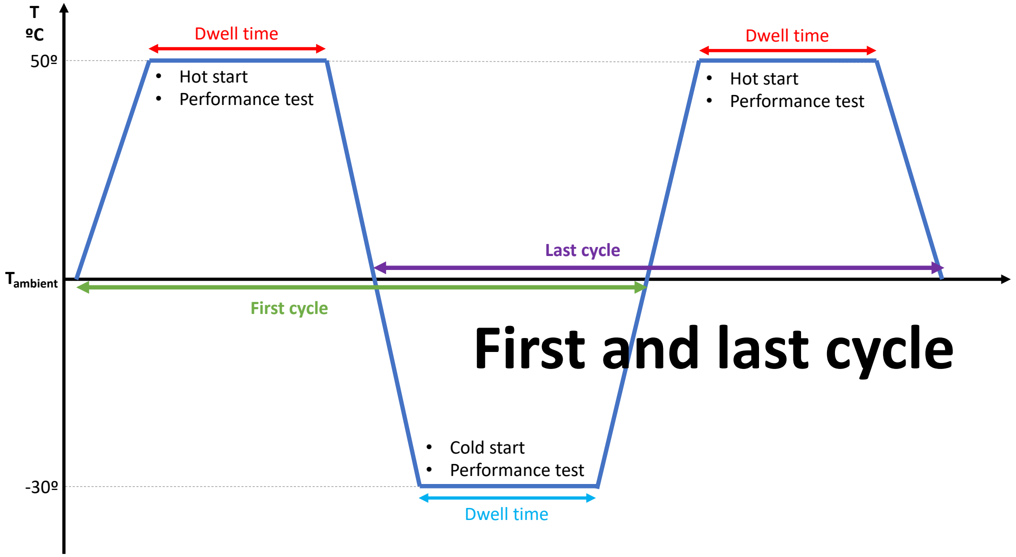

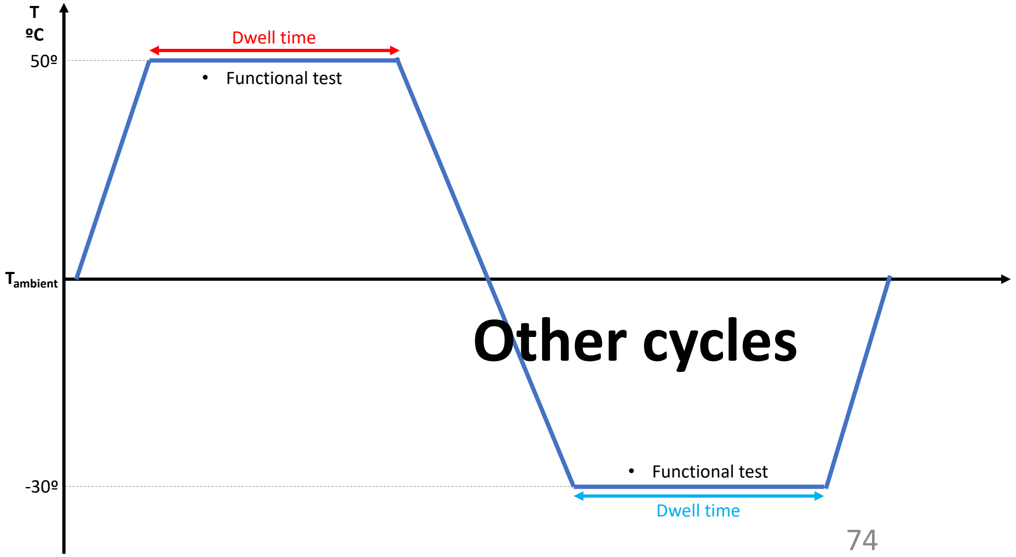

It survived…

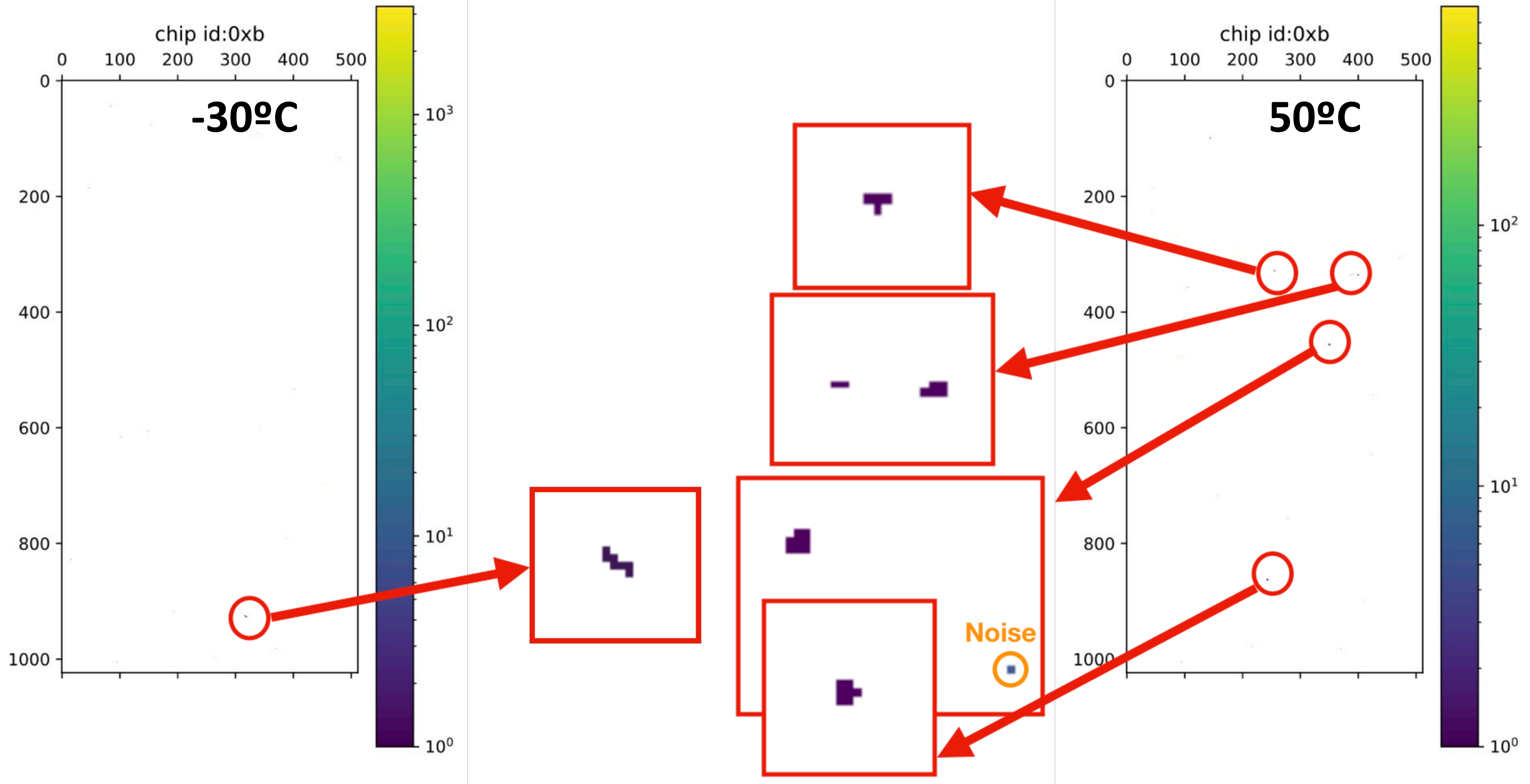

Roberto Iuppa

The LIMADOU Experiment on the CSES Satellite


JUST START